

Human immune dysregulation caused by genetic defects in cellular signaling pathways

Doctoral Thesis at the Medical University of Vienna for obtaining the academic
degree

Doctor of Philosophy

Submitted by

Marini Thian, BSc (Hons)

Supervisor:

Assoc. Prof. Priv.-Doz. Dr. Kaan Boztug

Scientific Director, Children's Cancer Research Institute/ St. Anna
Kinderkrebsforschung

Director, Ludwig Boltzmann Institute for Rare and Undiagnosed Diseases

Director, CeRUD Vienna Center for Rare und Undiagnosed Diseases

Adjunct PI, CeMM Research Center for Molecular Medicine, Austrian Academy of
Sciences

Associate Professor of Pediatrics and Adolescent Medicine, Medical University of
Vienna

Consultant in Pediatric Hematology, Oncology and Immunology, St. Anna Children's
Hospital Vienna

Vienna, 02/2021

Declaration

This thesis is written in a cumulative manner. The work accomplished in this thesis was performed in different laboratories or academic institutions in a collaborative effort. All contributions are listed below.

Chapter 3.1. was published by Ido Somekh, Marini Thian et al. 2019 Blood. The author of this thesis designed, performed and analyzed all experiments together with Ido Somekh for all patients except the TCR repertoire analysis, which was performed by Yu Nee Lee. The author of this manuscript also generated CD137 protein and performed rescue experiments with the help of David Medgyesi and Artem Kalinichenko. Additionally, the author of this thesis performed and analyzed cytotoxic T-cell assay in all patients. Nesrin Gülez, Tali Stauber, Ferah Genel, Ekrem Unal, Ginette Schiby, Jeffrey M. Jacobson, Erdener Özer, Ömer Akcal, Türkan Patiroglu, Musa Karakukcu, Alper Ozcan, Claudia Milena Trujillo-Vargas and José Luis Franco provided patient samples and interpreted clinical, pathology and/or imaging data. Atar Lev and Amos J. Simon performed and analyzed immune and genetic experiments on Patient 2. Meino Rohlf's conducted and analyzed NGS of Patients 1 and 2. Jasmin Dmytrus conducted and analyzed NGS of Patient 3. Catalina Martinez-Jaramillo, Ivan K. Chinn and Jordan S. Orange conducted and analyzed NGS of Patient 4. Raffaele Conca conducted immunophenotyping for Patients 1, 2 and 4. The author of this thesis and Tala Shahin performed immunophenotyping for Patient 3. Alejandro Gallón Duque, Eliana Appella and Megumi Tatematsu provided technical and experimental help. David Medgyesi, Thomas Magg, Michael J. Kraakman and Fabian Hauck helped supervise the study and gave intellectual input. Raz Somech, Christoph Klein and Kaan Boztug conceptualized, initiated and supervised the study. The author of this thesis, along with Ido Somekh, Raz Somech, Christoph Klein and Kaan Boztug wrote the manuscript which was reviewed and approved by all authors.

Chapter 3.2. was published by Marini Thian et al. 2020 Haematologica. The author of this thesis conceptualized, designed and performed most experiments, analyzed data, and wrote the manuscript. Birgit Hoeger performed and analyzed neutrophil assays and edited the manuscript. The author of this thesis performed macrophage morphology assays with Anton Kamnev and Michael Caldera conducted macrophage image analysis. Fiona Poyer, Caroline Hutter and Andishe Attarbaschi took care of the

patient, provided patient samples and interpreted clinical data. Sevgi Köstel Bal and Jakob Huemer provided experimental help. Raúl Jiménez-Heredia conducted and analyzed NGS data, performed variant filtering, Sanger validation and identified *PIK3CG* mutations in the patient. Winfried F. Pickl performed routine diagnostic immunophenotyping analysis. Miriam Groß established and performed initial NK-cell degranulation assays. Stephan Ehl, Carrie L. Lucas, Jörg Menche, and Loïc Dupré gave important intellectual input. Kaan Boztug supervised the study, reviewed clinical and experimental data, and finalized the manuscript. All authors reviewed and approved the manuscript.

All chapters of the thesis were written by the author. Dr. Kaan Boztug provided input to the writing of the thesis.

The author of this thesis was supported by the Cell Communication in Health and Disease program (CCHD, Medical University of Vienna), and a DOC doctoral fellowship of the Austrian Academy of Sciences (ÖAW 25225).

Reprint permissions for all figures and manuscripts were obtained.

Table of Contents

Declaration	i
List of Figures	v
Abstract	vi
Deutschsprachige Zusammenfassung	vii
Publications arising from this thesis.....	ix
List of Abbreviations	x
Acknowledgements	xiii
1. Introduction	1
1.1. Human innate immunity.....	1
1.2. Human adaptive immunity	3
1.2.1. Immunological diversity and development	3
1.2.2. Cellular immunity	5
1.2.3. Humoral immunity	8
1.2.4. Immunological memory.....	11
1.3. Human immune cellular signaling pathways.....	12
1.3.1. T-cell costimulation	12
1.3.2. PI3K/AKT pathway.....	14
1.3.3. NF- κ B pathways.....	16
1.4. Human inborn errors of immunity	17
1.4.1. Combined immunodeficiency.....	17
1.4.2. EBV-driven diseases.....	18
1.4.3. Hemophagocytic lymphohistiocytosis	20
1.4.4. Autoinflammatory syndromes.....	21
2. Aims of thesis.....	23
3. Results	24
3.1. CD137 deficiency causes immune dysregulation with predisposition to lymphomagenesis	24
3.2. Germline biallelic <i>PIK3CG</i> mutations in a multifaceted immunodeficiency with immune dysregulation.....	65
4. Discussion.....	86
4.1. Human CD137 deficiency and impaired EBV immunity.....	86
4.1.1. The role of CD137 in immunity.....	86
4.1.2. Human CD137 deficiency	88
4.1.3. Defective EBV immunity in CD137-deficient patients.....	90

4.2. Human PI3K γ deficiency and immune dysregulation.....	91
4.2.1. The biology of PI3K γ	91
4.2.2. Human <i>PIK3CG</i> mutations.....	92
4.2.3. Immune dysregulation in PI3K γ -deficient patients	93
5. Conclusion and Outlook.....	95
References	96
Curriculum Vitae	102

List of Figures

Figure 1. B cell development

Figure 2. T cell receptor signaling pathways downstream of CD28 family receptors

Figure 3. Relationship of T_{FH} cells and B cell affinity maturation

Figure 4. Costimulatory molecule interactions between T cells and antigen presenting cells

Abstract

A plethora of cellular signaling pathways plays crucial roles in human immune cell function. Studies on different cellular signaling components of the immune system have been widely explored in animal models, however, their roles in humans remain to be clarified. Human inborn errors of immunity (IEIs) represent unique models to unravel precise genotype to phenotype relationship and molecular mechanisms underlying important unknown human biology, which may substantially improve patient diagnostics and enable personalized medicine. The aim of this thesis was to attain mechanistic understanding of human immune homeostasis by studying novel human IEIs affecting cellular signaling pathways using whole exome sequencing in a cohort of patients with autosomal recessive, monogenic forms of immune diseases presenting with immune dysregulation. Systematically, we identified and investigated two novel monogenic human IEIs caused by biallelic loss of function mutations in *TNFRSF9* or *PIK3CG*, respectively.

Genetic characterization of four unrelated patients with defects in immunity against EBV infection and EBV-driven disorders, revealed a novel monogenic human IEI caused by mutations in *TNFRSF9* encoding for CD137 or 4-1BB. We unraveled that CD137 plays a crucial role in human immunity against EBV and its associated diseases, especially in T-cell activation, proliferation, and cytotoxicity against EBV. Moreover, we uncovered the previously unknown direct role of CD137 in human B cell function. In the second publication, we identified the second patient with novel germline biallelic *PIK3CG* mutations presented with systemic autoinflammation with hemophagocytic lymphohistiocytosis (HLH)-like phenotype. We demonstrated impaired PI3K/AKT signaling and therefore activation and proliferation in patient T cells. Furthermore, human PI3K γ plays an important role in myeloid cell function such as phagocytosis.

Collectively, the work in this thesis reveals previously unknown pivotal roles of human immune signaling components in regulating homeostasis of the immune system, and therefore open new therapeutic avenues for the treatment of patients with rare immunological diseases.

Deutschsprachige Zusammenfassung

Es existiert eine Vielzahl von zellulären Signalwegen, die für das Funktionieren menschlicher Immunzellen unerlässlich sind. Die verschiedenen Bestandteile dieser Signalwege wurden ausgiebig in Tiermodellen untersucht, ihre Rolle im Menschen ist jedoch oft unklar. Angeborene Immunitätsfehler beim Menschen (Human inborn errors of immunity (IEIs)) sind einzigartige Modelle die es uns ermöglichen, klare Rückschlüsse vom Genotyp auf den Phänotyp zu ziehen und die molekularen Mechanismen dieser Signalkomponenten auch im Menschen aufzuklären. Dadurch entsteht die Möglichkeit die Diagnostik von Patienten zu verbessern, sowie personalisierte Behandlungen/Therapieansätze zu ermöglichen. Das Ziel dieser Doktorarbeit war es, durch die Erforschung von IEIs, welche die zellulären Signalwege beeinträchtigen, ein besseres mechanisches Verständnis für die menschliche Immunhomöostase zu erlangen. Whole Exome Sequenzierung (WES) von Patienten mit Immunsstörungen, aufgrund von autosomal rezessiven monogenetischen Immunerkrankungen, ermöglichte uns die Identifizierung von neuartigen monogenetischen menschlichen IEI. Durch systematische Aufarbeitung gelang uns die Erstbeschreibung von zwei neuen monogenetischen Immunerkrankungen, ausgelöst durch biallelische Mutationen mit Funktionsverlust in den jeweiligen Genen *TNFRSF9* bzw. *PIK3CG*.

Die genetische Charakterisierung von vier nicht miteinander verwandten Patienten mit Störungen der Immunabwehr gegenüber EBV Infektionen und damit verbundenen Erkrankungen, enthüllte einen neuen monogenetischen humanen IEI verursacht durch Mutationen in dem für CD137 oder 4-1BB kodierenden Gen *TNFRSF9*. Wir konnten nachweisen, dass CD137 durch T-Zell Aktivierung, Proliferation und Zytotoxizität eine unverzichtbare Rolle für die humane Immunabwehr gegen EBV und damit einhergehende Begleiterkrankungen spielt. Darüber hinaus zeigten wir eine bisher unbekannte direkte Funktion von CD137 in menschlichen B Zellen. In einer zweiten Publikation konnten wir den erst zweiten Patienten mit einer neuen biallelischen Keimbahnmutation in *PIK3CG* identifizieren, welche sich in Form von systemischer Autoinflammation mit Hämophagozytisch Lymphohistiozytose ähnlichem Phänotyp darstellt. Als Mechanismus konnten wir hier eine Beeinträchtigung des PI3K/AKT Signalweges feststellen und die dadurch verursachte Störung der Aktivierung und Proliferation der T Zellen des Patienten nachweisen. Außerdem konnten wir zeigen

welche wichtige Rolle PI3K γ im Menschen in myeloiden Zellfunktionen, wie beispielsweise Phagozytose, spielt.

Zusammenfassend befasst sich diese Doktorarbeit mit der Erstbeschreibung der Funktion von verschiedenen zellulären Signalkomponenten und ihrer zentralen Rolle für die Regulierung der Homöostase des menschlichen Immunsystems. Dadurch eröffnen sich neue Wege für die Therapie von Menschen mit seltenen Erkrankungen des Immunsystems.

Publications arising from this thesis

Thian M, Hoeger B, Kamnev A, Poyer F, Bal SK, Caldera M, Jiménez-Heredia R, Huemer J, Pickl WF, Groß M, Ehl S, Lucas CL, Menche J, Hutter C, Attarbaschi A, Dupré L, Boztug K. (2020) Germline biallelic *PIK3CG* mutations in a multifaceted immunodeficiency with immune dysregulation. *Haematologica*. 105(10):e488-492. doi:10.3324/haematol.2019.231399.

Somekh I*, **Thian M***, Medgyesi D, Gülez N, Magg T, Duque AG, Stauber T, Lev A, Genel F, Unal E, Simon AJ, Lee YN, Kalinichenko A, Dmytrus J, Kraakman MJ, Schiby G, Rohlf M, Jacobson JM, Özer E, Akcal Ö, Conca R, Patiroglu T, Karakukcu M, Ozcan A, Shahin T, Appella E, Tatematsu M, Martinez-Jaramillo C, Chinn IK, Orange JS, Trujillo-Vargas CM, Franco JL, Hauck F, Somech R#, Klein C#, Boztug K#. (2019) CD137 deficiency causes immune dysregulation with predisposition to lymphomagenesis. *Blood*. **134(18)**:1510-1516. doi:10.1182/blood.2019000644.

* indicates shared first authorship

indicates shared senior authorship

List of Abbreviations

AIM2	Absent in melanoma 2
AMP	Antimicrobial peptide
APC	Antigen-presenting cell
AP1	Activator protein 1
AP-MS	Affinity purification mass spectrometry
BCR	B cell receptor
CAR	Chimeric antigen receptor
CARD	Caspase recruitment domain
CID	Combined immunodeficiency
CLP	Common lymphocyte progenitor
C _H	Heavy-chain constant
CTL	Cytotoxic T lymphocyte
CRD	Cysteine-rich domain
CSR	Class switch recombination
DAMP	Damage-associated molecular patterns
DC	Dendritic cell
DN	Double-negative
DP	Double-positive
DNA	Deoxyribonucleic acid
EBV	Epstein-Barr virus
FDA	Food and Drug Administration
FHL	Familial hemophagocytic lymphohistiocytosis
FMF	Familial Mediterranean fever
GC	Germinal center
GM-CSF	Granulocyte-macrophage colony-stimulating factor
GOF	Gain-of-function
GPCR	G-protein coupled receptor
HLH	Hemophagocytic lymphohistiocytosis
HSCT	Hematopoietic stem cell transplantation

HSV	Herpes simplex virus
IEI	Inborn errors of immunity
IFN	Interferon
Ig	Immunoglobulin
IKK	I κ B kinase
IL	Interleukin
IPEX	Immune dysregulation, polyendocrinopathy, enteropathy, X-linked
IRF	Interferon-regulatory factor
LCL	Lymphoblastoid cell line
LPS	Lipopolysaccharide
mAb	Monoclonal antibody
MHC	Major histocompatibility complex
MS	Multiple sclerosis
mTORC2	Mechanistic target of rapamycin complex-2
NEMO	NF- κ B essential modulator
NF- κ B	Nuclear factor- κ B
NK	Natural killer
NLR	Nucleotide-binding oligomerization domain, leucine-rich repeat containing receptor
PAMP	Pathogen-associated molecular pattern
PDK1	Phosphoinositide-dependent kinase-1
PID	Primary immunodeficiency
PIP ₂	Phosphatidylinositol-4,5-bisphosphate
PIP ₃	Phosphatidylinositol-3,4,5-trisphosphate
PI3K	Phosphatidylinositol-3-kinase
PRR	Pattern recognition receptor
PYD	Pyrin domain
RA	Rheumatoid arthritis
RAG	Recombination-activating gene
RBD	Ras binding domain
RNA	Ribonucleic acid

ROS	Reactive oxygen species
RTK	Receptor tyrosine kinase
SCID	Severe combined immunodeficiency
SHM	Somatic hypermutation
SLE	Systemic lupus erythematosus
SP	Single-positive
TAM	Tumor-associated macrophage
TCR	T cell receptor
T _{CM}	Central-memory T cell
T _{EM}	Effector-memory T cell
T _{FH}	Follicular helper T cell
T _H	Helper T cell
THD	TNF homology domain
TI	Thymus-independent
Treg	Regulatory T cell
TLR	Toll-like receptor
TME	Tumor microenvironment
TNF	Tumor necrosis factor
TNFRSF	Tumor necrosis factor receptor superfamily
TNFSF	Tumor necrosis factor superfamily
TRAF	TNF-receptor associated factor
TRAPS	TNF receptor–associated periodic syndrome
T _{SCM}	Stem-cell memory T cell
XLP1	X-linked lymphoproliferative disorder type 1
WES	Whole exome sequencing

Acknowledgements

I would like to express my deepest gratitude to my PhD supervisor, Kaan Boztug for the privilege of joining his team and working under his guidance for my PhD studies.

I am thankful to my thesis committee members Christoph J. Binder and Wilfried Ellmeier for their helpful advice.

I am grateful to be part of the international vibrant environment of CeMM, LBI-RUD and CCRI, which are conducive for fostering collaborations and friendships.

I am thankful for CCHD program at the Medical University of Vienna and the Austrian Academy of Sciences (ÖAW) for the support and funding throughout my PhD studies.

I would also like to acknowledge all the patients and their families and collaborators.

Thank you Ido for being part of my PhD journey in our collaborative CD137 story. It has been a pleasure working together.

I am happy to be surrounded by kind and friendly colleagues who made working environment an enjoyable one at the Boztug lab. I am especially grateful to David Medgyesi, Birgit Höger and Irinka Castanon who always believe in me. Special thanks to Bernhard and Johannes for helping me to translate the abstract of this thesis to German! I am grateful to Rico, Artem, and Mike for their help in one way or another. Thank you Wojtek for always making sure that our needs in the lab are met! A shout-out to the G-team: Raúl, Ana, Jasmin and Anna; as well as the TAs.

Special mention to the 2016 PhD batch whom I started together with, every single one of you, thank you for the wonderful journey together! I will miss you guys and the sweet memories we shared! Your presence made the whole PhD experience so much better!

I am thankful to my husband, Ben, for his unfailing love and support, always being there for me throughout my PhD studies and beyond.

I thank my family and family-in-law for believing in me and supporting me in my pursuit of knowledge. To my mum and dad, this is dedicated especially for you. Nothing could describe how much you both mean to me.

To Angie, Margaret and Sharon, thank you for being so supportive, always praying for me. To Cindy, Wei Yi and Myi Mi, thanks for the lovely friendships and the tours we

had together! To Queby, Precious, Andrea, the Good Deposit ladies, and TTO ladies, thanks for walking alongside together and cheering me on!

Finally, all these will not be possible without my Lord and Saviour Jesus Christ, who always stands by my side guiding me all the way into His marvellous light. To Him be all glory and honour forever. Amen!

1. Introduction

The human immune system comprises of a group of distinct cell types of well-defined functions, working together to protect the body from harmful effects of pathogens and altered self-structures (Murphy, 2012). Two interdependent arms of immunity have emerged throughout evolution: the innate and the adaptive immune responses. To effectively defend the body against threats and diseases, the immune system needs to achieve four main functions: immunological recognition, immune effector functions, immune regulation and immunological memory (Murphy, 2012).

1.1. Human innate immunity

Widely considered as the first lines of defense, the innate immune system provides rapid initial immune responses against most invading microorganisms (Murphy, 2012). The human innate immune system encompasses all tissues, particularly barrier surfaces such as the skin or the mucosal surfaces of the respiratory and gastrointestinal tract (Gasteiger et al, 2017). Innate immune responses can be mediated through cell-dependent mechanisms such as phagocytosis or through secreted factors, including antimicrobial peptides (AMPs) (Bevins & Salzman, 2011).

Immunological recognition of the innate immune system is highly conserved across species and is achieved using germline-encoded pattern recognition receptors (PRRs) such as Toll-like receptors (TLRs). These receptors are crucial to sense and bind to pathogen-associated molecular patterns (PAMPs) or damage-associated molecular patterns (DAMPs) (Takeuchi & Akira, 2010). Human innate immune cells express several different TLRs which recognize distinct PAMPs/DAMPs. TLR-1, TLR-2 and TLR-6 recognize lipoproteins from Gram-negative bacteria. TLR-4 binds to bacterial lipopolysaccharide (LPS) while TLR-5 recognizes flagellin. TLR-3, TLR-7 and TLR-9 are endosomal receptors involved in mainly recognizing viruses. TLR-3 binds to double-stranded ribonucleic acid (RNA), whereas TLR-7 recognizes single-stranded RNA. TLR-9 recognizes unmethylated CpG deoxyribonucleic acid (DNA) of bacteria and viruses (Murphy, 2012).

Upon microbial invasion, pathogens are usually recognized by PRRs of the resident phagocytic cells such as macrophages or dendritic cells, which trigger a downstream signaling cascade to induce the secretion of proinflammatory cytokines and

chemokines to recruit other innate immune cells, such as monocytes and neutrophils to the infected site through chemokine gradients. An inflammatory response is therefore triggered (Gasteiger et al, 2017).

Inflammatory responses are characterized by heat, redness, pain and swelling at the infected site. There are three essential roles of inflammation in fighting infection. Firstly, additional effector cells and molecules are recruited to increase the destruction of invading pathogens at the site of infection. Secondly, to prevent the spread of infection by inducing local blood clotting and thus, a physical barrier. Thirdly, to promote tissue repair of the infected site (Murphy, 2012).

Neutrophils are the earliest and most numerous innate immune cells recruited, followed by monocytes and dendritic cells (DCs). The initial response of neutrophils to microbial exposure is engulfment through phagocytosis, followed by the release of different types of antimicrobial granules, and resulting in respiratory or oxidative burst to kill the engulfed pathogen (Murphy, 2012; Häger et al, 2010). However, neutrophils are short-lived, and undergo phagocytosis-induced cell death after they have achieved a round of phagocytosis (Gasteiger et al, 2017; Murphy, 2012).

Monocytes are key players in inflammation while tissue-resident macrophages are important players for the resolution of inflammation, tissue development and homeostasis. Monocytes can differentiate into monocyte-derive macrophages or dendritic cells in the tissues, depending on the precise signals that they receive from the surroundings (Coillard & Segura, 2019). These cells are major producers of pro-inflammatory cytokines such as tumor necrosis factor- α (TNF- α), interleukin-6 (IL-6) and IL-1 β (Coillard & Segura, 2019).

During virus infection, type I interferons (IFN- α and IFN- β) are produced and in turn, activate natural killer (NK) cells. Activated macrophages also secrete IL-12 and IL-18 to stimulate NK cells to produce IFN- γ . NK cells recognize and kill their target cells by releasing cytotoxic granules containing granzyme and perforin. Activated NK cells increase their killing activity and serve to control virus infections while adaptive immunity is generating antigen-specific immune responses to clear the infection (Murphy, 2012).

1.2. Human adaptive immunity

An adaptive immune response is triggered when innate immune responses are overwhelmed. To effectively fight pathogens and defend our body, the adaptive immune system has evolved to recognize a myriad of antigens due to their diverse antigen receptors (Murphy, 2012).

1.2.1. Immunological diversity and development

In adaptive immunity, antigen can be recognized by two distinct molecules: the immunoglobulins on the B cells and the antigen-specific receptors on the T cells (Murphy, 2012). The diversity of B- and T-cell antigen receptors (BCR and TCR) enable the body to elicit immune responses against a plethora of pathogens encountered during a lifetime. The genes that encode these antigen receptors exist in a non-functional state in the germline, with the 5' portion of each gene (which encodes the antigen binding domain) organized as arrays of variable (V), diversity (D; only present in immunoglobulin heavy-chain in B cells and TCR β - and γ -chains) and joining (J) gene segments (Schatz & Ji, 2011). Assembly of these genes by V(D)J recombination through expression of recombination-activating genes (RAG1 and RAG2) generates a diversity of antigen receptors and is the fundamental process of how early lymphocyte development is established (Schatz & Ji, 2011; Nemazee, 2017).

Lymphocytes derive from common lymphocyte progenitors (CLPs) which are differentiated from multipotent hematopoietic stem cells in the bone marrow. Immature B cells are developed from CLP in the bone marrow and migrate to peripheral lymphoid tissues, while T-cell progenitors emigrate from the bone marrow to undergo maturation in the thymus (Murphy, 2012).

CLP give rise to early pro-B cell where heavy (H)-chain D to J gene segments are rearranged and subsequently becomes late pro-B cell when both alleles had undergone D to J_H rearrangements. Late pro-B cell develops into large pre-B cell by rearranging V_H to DJ_H gene segments to generate intact μ H-chains (Nemazee, 2017). The diversity of the BCR repertoire is enhanced at this stage by the enzyme terminal deoxynucleotidyl transferase (TdT) which adds non-templated nucleotides at the joints between gene segments (Murphy, 2012). A functional heavy chain is tested for its successful production in the absence of light (L)-chain using a surrogate. Signaling from the pre-B-cell receptor promotes H-chain allelic exclusion and inhibits further H-chain rearrangement. Small pre-B cells are achieved by rearranging L-chain (κ or λ) V

to J gene segments to produce intact light chain which results in the entry to immature B cell stage (Figure 1) by expressing intact cell-surface immunoglobulin M (IgM) (Nemazee, 2017).

V(D)J recombination is intrinsically random and error-prone, generating diversity, but often assembling genes that are non-productive or that encode potentially autoreactive antibodies (Nemazee, 2017). Developing lymphocytes with receptors that interact weakly with self-antigens receive survival signal, resulting in positive selection (Figure 1). Negative selection occurs when receptors on the lymphocytes react strongly to self-antigens and are therefore eliminated to ensure central tolerance. There are four possible fates for self-reactive lymphocytes: anergy, receptor editing, clonal deletion and a state of immunological ignorance (Murphy, 2012). Immature B cells which undergo selection migrate to the periphery for later developmental stages (Nemazee, 2017).

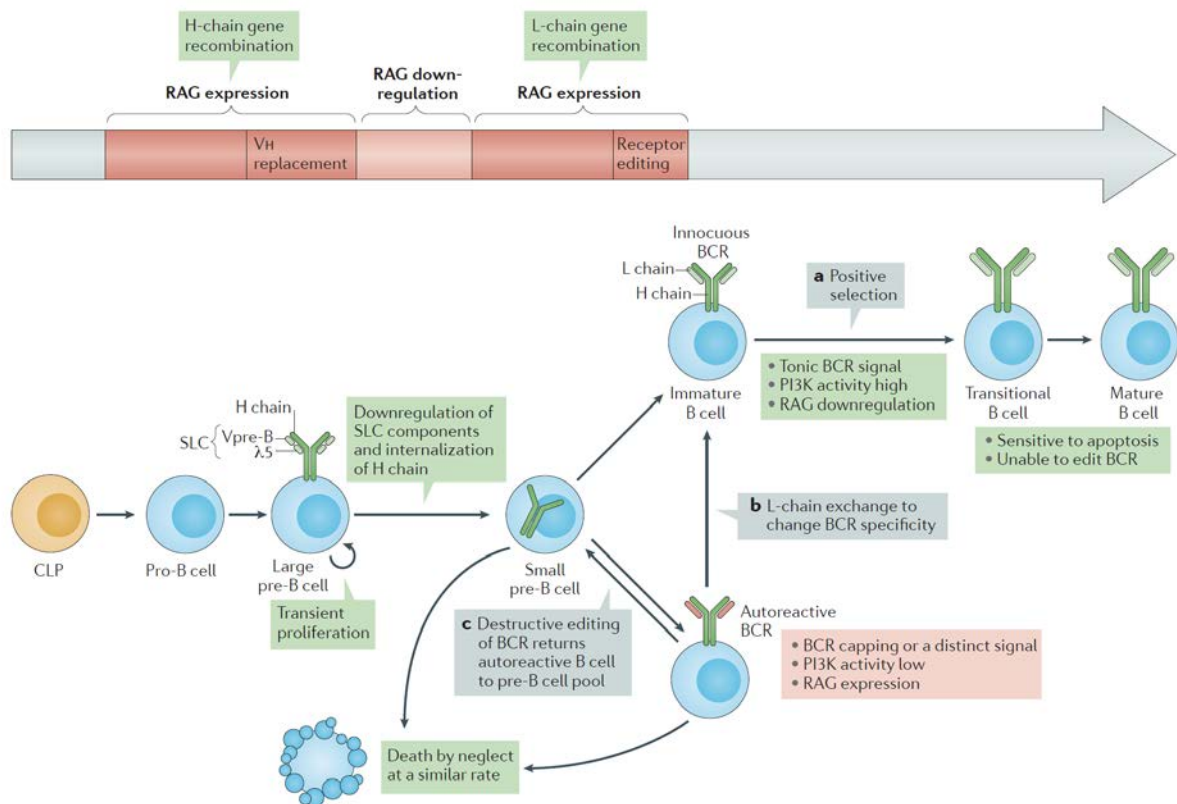


Figure 1. B cell development (Adapted from Nemazee 2017). SLC: Surrogate light-chain.

In the thymus, CLP receives the Notch signal from stromal cells to commit to the T-cell lineage rather than B-cell lineage. T-cell development resembles that of B cells in many ways but there are also some additional features, such as the generation of two distinct lineages of T cells, the $\gamma:\delta$ and the $\alpha:\beta$ lineages, which express different antigen-receptor genes (Murphy, 2012).

Double-negative (DN) thymocytes lacking CD4 and CD8 coreceptors undergo TCR V(D)J rearrangement, giving rise to CD4⁺CD8⁺ double-positive (DP) thymocytes. DP cells undergo positive and negative selection that depends on their TCR interaction with self-peptide:self-major histocompatibility complex (MHC) complexes to generate CD4⁺ or CD8⁺ single-positive (SP) thymocytes which eventually emerge into the periphery as naïve T cells (Kumar et al, 2018).

1.2.2. Cellular immunity

Cellular immunity is mediated by T cells which are developed in the thymus and emigrate to the periphery via the bloodstream. Mature recirculating T cells which have not encountered their specific antigens are naïve T cells. DCs constantly take up and process antigens from surrounding environment and travel to lymphoid tissues where they present their antigens to naïve T cells. Naïve T cells are primed when they encounter their specific antigen via peptide-MHC on the surface of antigen-presenting cells (APCs). Generally, CD8⁺ T cells recognize peptides presented by MHC class I molecules while CD4⁺ T cells by MHC class II molecules (Murphy, 2012).

Three signals are involved in activating naïve T cells by the same APC: Firstly, the engagement of TCR with its specific peptide-MHC. A second costimulatory signal is required to promote T cell survival and expansion. The third signal is needed to differentiate T cells into different effector subsets (Hwang et al, 2020; Murphy, 2012). Multiple signaling cascades can be triggered upon activation of naïve T cells (Figure 2) and we will discuss this further in chapter 1.3.

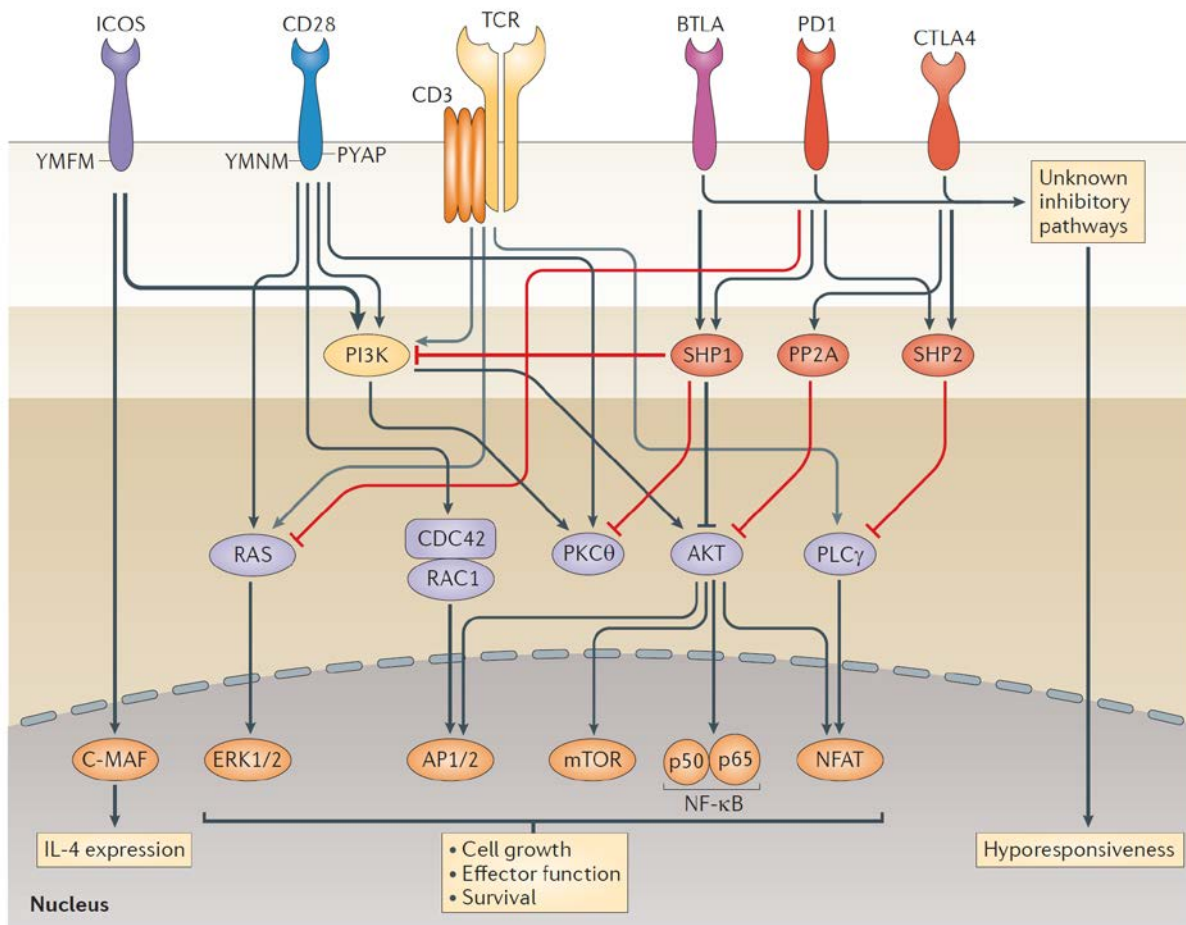


Figure 2. T cell receptor signaling pathways downstream of CD28 family receptors (Adapted from Chen & Flies, 2013). AP: activator protein; mTOR: mammalian target of rapamycin; NF- κ B: nuclear factor- κ B; NFAT: nuclear factor of activated T cells; PKC θ : protein kinase C θ ; PLC γ : phospholipase C γ ; ICOS: inducible T cell co-stimulator; PI3K: phosphatidylinositol 3-kinase; IL-4: interleukin-4; BTLA: B and T lymphocyte attenuator; PD1: programmed cell death 1; CTLA4: cytotoxic T lymphocyte antigen 4; SHP: SH2 domain-containing tyrosine phosphatase; PP2A: protein phosphatase 2A; ERK: extracellular signal-regulated kinase.

Upon antigen recognition, naïve CD8⁺ T cells differentiate into cytotoxic effector T lymphocytes (CTLs) to kill infected target cells by releasing cytotoxic granules containing perforin and granzymes. CD8⁺ T cells can be activated by DCs to produce IL-2 required for proliferation and differentiation. Additionally, CD8⁺ T-cell memory require effector CD4⁺ T cell help to provide CD40L and IL-2 to DC which in turn, upregulates expressions of B7 and 4-1BBL (CD137L) on the DC to be delivered to CD8⁺ T cells. CTLs are crucial for defense against viruses and intracellular pathogens (Murphy, 2012). By contrast, CD4⁺ T cells differentiate into distinct effector T helper

(T_H) subsets with different immunological functions. Currently, these subsets are T_H1, T_H2, T_H9, T_H17, T_H22, T follicular helper cells (T_{FH}) and regulatory T cells (Tregs) (Hirahara & Nakayama, 2016).

T_H1 cells express the transcription factor T-bet and are known to produce IFN- γ , IL-2, TNF, lymphotoxin and granulocyte-macrophage colony-stimulating factor (GM-CSF). T_H1 cells are important for immunity against intracellular pathogens. However, it has also been associated with pathology in autoinflammatory/autoimmune diseases such as autoimmune type 1 diabetes, multiple sclerosis (MS) and rheumatoid arthritis (RA) (Raphael et al, 2015).

T_H2 cells express the transcription factor GATA-3 and are known for their role against extracellular pathogens such as helminth and parasites. T_H2 cells produce IL-4, IL-5 and IL-13 and have been shown to play key role in allergies and atopic diseases (Raphael et al, 2015).

The master regulator of the T_H17 cell lineage is ROR γ t, however, other factors such as IRF4 and BATF are also required (Stockinger & Omenetti, 2017). Due to the relative instability nature of T_H17 cells, they show a significant degree of plasticity in their function and phenotype towards environmental signals. T_H17 cells produce IL-17, IL-21, IL-22 and play a role in extracellular bacterial and fungal defenses. However, the pathogenic role of T_H17 in various inflammatory diseases is well documented (Stockinger & Omenetti, 2017; Geginat et al, 2014).

The lineage-defining transcription factor for T_{FH} differentiation is BCL6. T_{FH} differentiation requires DC priming during early stage and B cells for later stage to reach full maturation in the germinal centers (GCs). Reciprocally, T_{FH} cells stay resident in secondary lymphoid organs to help B cells in their developmental stages (Crotty, 2019). These feedback loops are central aspects of proper regulation of humoral immunity, which we will discuss in chapter 1.2.3. Generally, a decrease in T_{FH} cells have been associated with humoral immunodeficiency while an increase proportion of these cells has been associated with autoimmunity (Tangye et al, 2013).

FOXP3 is the master regulator of Tregs, important for their development and function. Tregs are important for immune tolerance and homeostasis (Shevryev & Tereshchenko, 2020). Mechanisms of Treg immune suppression include the secretion of anti-inflammatory cytokines such as IL-10 and transforming growth factor- β (TGF-

β), cytokine deprivation and inhibitory receptor expression (Raphael et al, 2015). Mutations in *FOXP3* have been described in humans to result in immune dysregulation, polyendocrinopathy, enteropathy, X-linked (IPEX), which is a rare and devastating autoimmune syndrome (Geginat et al, 2014).

1.2.3. Humoral immunity

Humoral immunity is mediated by B cells which are developed in the bone marrow and migrate to peripheral organs such as lymph nodes where they can be activated by antigens. The humoral immune response is initiated when B cells receive signals from T_{FH} cells during thymus-dependent antigen recognition. T_{FH} provides CD40L, IL-21 and/or IL-4 for B cell to undergo proliferation to form GCs. Somatic hypermutation (SHM) happens in the GC to allow affinity maturation (Figure 3), which selects for the survival of mutated B cells with high affinity for the antigen (Crotty, 2019).

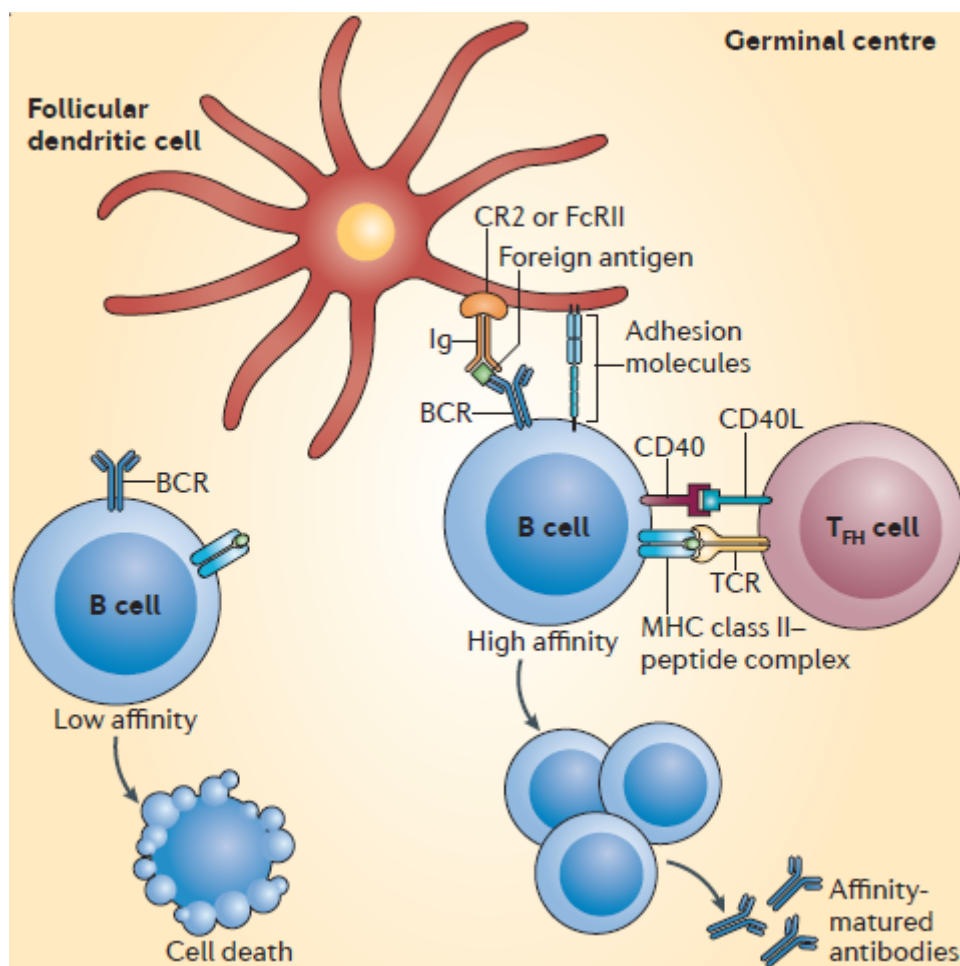


Figure 3. Relationship of T_{FH} cells and B cell affinity maturation (Adapted from Tangye et al, 2013). CR2: complement receptor 2; FcRII: low affinity Fc receptor for immunoglobulin.

GC B cells also undergo class switch recombination (CSR). The classes of immunoglobulins are defined by their heavy-chain constant (C_H) regions, with the different isotypes being encoded by different C_H genes (Xu et al, 2012). CSR is the process whereby a C_H gene can be changed at the DNA level with another downstream C_H gene, for example from C_μ for IgM with C_γ , C_ϵ or C_α for IgG, IgE or IgA respectively. This allows the alteration of antibody isotypes to elicit different immune responses at different locations in the organism while retaining their antigen-specificity (Xu et al, 2012).

The immunoglobulin classes have distinct tissue distribution and potency against different types of pathogens. Although naïve B cells express only IgM and IgD on their cell-surface, CSR can take place over the course of an immune response, depending on the signals or cytokines received. IgM is the first antibody secreted by activated B cells because it is expressed without CSR and have undergone little SHM. These early IgM antibodies are also called natural antibodies with low affinity and tend to be polyreactive but allow B cells to respond quickly to variety of antigens (Murphy, 2012). IgM can form multimers which have high avidity for antigens with repetitive motifs and function by opsonizing antigen for destruction and result in the activation of classical complement pathway (Xu et al, 2012; Schroeder & Cavacini, 2010). The process of SHM and CSR requires activation-induced cytidine deaminase (AID) (Schroeder & Cavacini, 2010). In individuals with AID deficiency resulted in the autosomal recessive form of the Hyper-IgM syndrome (Revy et al, 2000).

IgG exists as a monomer and is the most abundant isotype and there are 4 subclasses in humans and were ordered based on their serum levels in the blood: IgG1, IgG2, IgG3 and IgG4. These subclasses exhibit distinct functional capacities. All IgG subclasses except IgG4 can efficiently opsonize pathogens for phagocytosis and activate classical complement pathway. IgG1 and IgG3 can bind to all three classes of Fc γ R but IgG4 can only bind Fc γ RII and III, while IgG2 only binds to Fc γ RII. Different IgG subclasses also contribute distinctly to neutralization of toxins and viruses (Schroeder & Cavacini, 2010).

IgA is the predominant class of antibody in the mucosal surfaces and in secretions. Generally, IgA in the serum exists as a monomer with predominantly IgA1 subclass while in the mucosal sites, IgA forms dimer, which is mainly IgA2 subclass (Murphy, 2012). IgA is secreted in breast milk and transferred from mothers to neonates to

provide protection against pathogens. Additionally, IgA is crucial in protecting mucosal surfaces by neutralizing toxins and viruses. IgA receptor is also expressed on neutrophils which may allow its activation by antibody-dependent cellular cytotoxicity (ADCC) at mucosal sites (Schroeder & Cavacini, 2010).

IgE is present at low levels in the serum with the shortest half-life but an extremely potent immunoglobulin which binds Fc ϵ RI on mast cells, basophils, eosinophils and Langerhans cells with very high affinity. Upon crosslinking of antigen with IgE-bound Fc ϵ RI on mast cells, a signaling cascade results in degranulation of chemical mediators of immune response. IgE is important for defense against parasitic worms but has also been associated with allergies and hypersensitivity (Murphy, 2012; Schroeder & Cavacini, 2010).

Most humoral responses are dependent on T cell help, however, in the absence of T cell help, naïve B cells can be stimulated through thymus-independent (TI) antigen recognition. There are two classes of TI antigens: TI-1 antigens such as bacterial LPS, which can activate TLRs expressed by B cells, and TI-2 antigens such as bacterial capsular polysaccharides which have highly repetitive structures (Murphy, 2012).

1.2.4. Immunological memory

Immunological memory is one of the most important consequences of the adaptive immunity. It is the ability to store and recall information on previously encountered pathogens. Memory immune cells are long-lived, antigen-specific which can respond more rapidly and effectively to repeated encounters with a specific antigen. Immunological memory is the basis of an effective vaccine. Memory responses are also known as secondary immune responses (Ratajczak et al, 2018).

Primary humoral response in naïve B cells is characterized by an initial production of IgM, followed by IgG from CSR, while secondary humoral response in memory B cells is characterized by the generation of low IgM, but large quantities of IgG antibodies with some IgA and IgE. Antibodies generated by the secondary humoral response have higher affinity due to SHM compared to the primary response (Murphy, 2012).

Memory T cells are long-lived and represent a major circulating population in human blood which are subdivided into central-memory (T_{CM}), effector-memory (T_{EM}), and stem-cell memory (T_{SCM}) T cells. Functionally, both T_{CM} and T_{EM} cells are able to produce IL-2 and effector cytokines upon stimulation; however, T_{CM} cells show lymphoid homing profiles ($CCR7^+$) and a high proliferative capacity, while T_{EM} cells generate more effector cytokines. T_{SCM} cells show high self-renewal and proliferative capacities with no effector function (Kumar et al, 2018).

1.3. Human immune cellular signaling pathways

A plethora of cellular signaling pathways plays crucial roles in human immune cell function. Many of these signaling pathways control important cellular processes and regulate transcription factors that switch on a fine-tuned, response-appropriate gene expression program involved in cell growth, survival, proliferation, differentiation and inflammation.

1.3.1. T-cell costimulation

Cell-surface receptors function to sense their environment and to transmit information along intracellular signaling pathways to the nucleus, in order to alter gene expression and therefore protein synthesis to react to threats that would endanger the organisms (Murphy, 2012). TCR recognizes and binds antigen in the form of peptide-MHC complexes expressed by APCs such as DCs. However, signaling from TCR itself is insufficient to activate a naïve T cell. Costimulatory receptors play fundamental roles in achieving full activation and fine-tuning the signaling output of the antigen receptors (Croft, 2003).

Many costimulatory receptors have been described so far and they are mostly members of the immunoglobulin superfamily (IgSF) and tumor necrosis factor receptor superfamily (TNFRSF) (Croft, 2003; Chen & Flies, 2013). The CD28 and B7 families are the best-characterized IgSF receptors. Studies demonstrated the function of CD28 receptor as a costimulatory molecule for T cell activation with B7 family members, CD80 and CD86 expressed on APCs as its ligands (Sharpe, 2009). A variety of CD28 receptor family members mainly bind to B7 family members (Chen & Flies, 2013).

TNF receptor (TNFR) family members are usually expressed by T cells and their respective TNF-family ligands are expressed by APCs (Croft, 2003). TNF family molecules are active mainly in trimeric form, either on the cell surface or soluble after extracellular cleavage (Croft et al, 2012). TNFRs share conserved extracellular cysteine-rich domains (CRDs) whereas their ligands share a conserved extracellular TNF homology domain (THD) (Chen & Flies, 2013). Members of TNFRSF function primarily in T-cell costimulation such as TNFRSF4 (OX40), TNFRSF7 (CD27), TNFRSF8 (CD30) and TNFRSF9 (CD137 or 4-1BB). However, several members of TNFRSF are also involved in various cellular processes other than costimulation (Chen & Flies, 2013).

Studies show that TNFSF ligand–receptor signaling pathways are highly active in autoinflammatory and autoimmune disease. Therapeutic approaches targeting several members of TNFRSF are currently considered for intervention in autoimmunity and cancer (Croft et al, 2013). Furthermore, several studies showed that genetic mutations in TNFSF or TNFRSF result in immunological diseases in humans (Tangye & Latour, 2020).

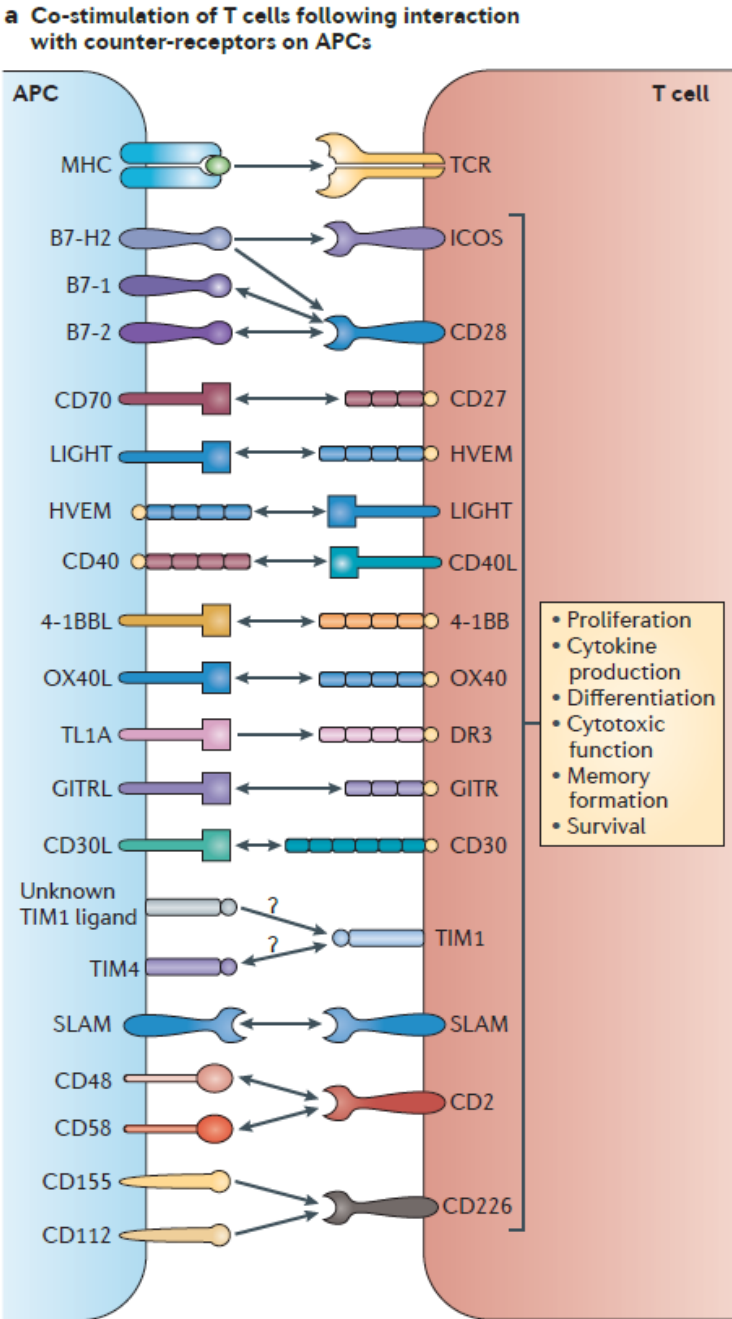


Figure 4. Costimulatory molecule interactions between T cells and antigen presenting cells (Adapted from Chen & Flies, 2013). Some costimulatory molecule interactions are bidirectional, indicated by arrowheads on both ends.

1.3.2. PI3K/AKT pathway

The PI3K/AKT signaling axis is one of the critical molecular pathways in humans, regulating crucial cellular processes including cell proliferation, growth, survival, and metabolic adaptation (Fruman et al, 2017). Accordingly, it is also one of the most dysregulated pathways in cancer (Janku et al, 2018).

Phosphatidylinositol-3-kinases (PI3Ks) represent key signaling hubs that integrate signals derived from plasma membrane receptors to act on lipid second messenger molecules for signal propagation, driving cell activation, cell polarization and morphological adaptations (Koyasu, 2003; Fruman et al, 2017).

PI3Ks are evolutionarily conserved and are divided into three classes of enzymes in humans, according to their molecular structure, substrate specificities and regulation (Rommel et al, 2007). Class I PI3Ks consist of class IA (PI3K α , β , and δ isoforms) and class IB (PI3K γ isoform). There are three class II PI3Ks (PI3K-C2 α , C2 β , and C2 γ isoforms) and a single class III PI3K (hVPS34) (Hawkins & Stephens, 2015; Fruman et al, 2017).

Class I PI3Ks are the best described among classes of PI3Ks. All four class I PI3Ks are heterodimers composed of a catalytic subunit of p110 (α , β , δ , and γ) and a tightly-bound regulatory subunit that controls their expression, activation and subcellular localization (Rommel et al, 2007). Class IA PI3Ks consist of one of five homologous regulatory subunits (p85 α /p55 α /p50 α , p85 β or p55 γ) associated to a single (p110 α , p110 β , or p110 δ) catalytic subunit to form five potential heterodimers for each catalytic subunit, known as PI3K α , PI3K β or PI3K δ , respectively. Contrarily, class IB PI3Ks contain one of two homologous subunits (p101 or p84) which bind to a single p110 γ catalytic subunit to form two potential heterodimers, p101/p110 γ or p84/p110 γ , also known as PI3K γ (Hawkins & Stephens, 2015).

Multiple upstream signaling events can activate different class I PI3K isoforms. Studies showed that Ras-related GTPases can bind and activate p110 α , p110 δ , and p110 γ through its Ras binding domain (RBD). On the other hand, the RBD of p110 β is selective for Rac/CDC42 (Fruman et al, 2017). Receptor tyrosine kinases (RTKs) and G-protein coupled receptors (GPCRs) can also activate class I PI3Ks, however, further studies on the coupling of each isoform and their cellular context need to be clarified (Fruman et al, 2017).

PI3K α and PI3K β are ubiquitously expressed in humans while PI3K δ and PI3K γ are primarily expressed in immune cells (Fruman et al, 2017). Class I PI3Ks catalyze the phosphorylation of phosphatidylinositol-4,5-bisphosphate (PIP₂) to generate the second messenger, phosphatidylinositol-3,4,5-trisphosphate (PIP₃) (Rommel et al, 2007). The generation of PIP₃ results in the recruitment of specific proteins such as phosphoinositide-dependent kinase-1 (PDK1) and AKT to membrane-signaling complexes (Manning & Toker, 2017).

The activation and phosphorylation of AKT is the hallmark effector downstream of class I PI3K activation. PDK1 phosphorylates AKT at Thr308 residue, while mechanistic target of rapamycin (mTOR) complex-2 (mTORC2) phosphorylates AKT at Ser473 residue, which stabilizes T308 phosphorylation and provides maximal activation (Manning & Toker, 2017). Activated AKT in turn, phosphorylates a multitude of downstream substrates involved in cell survival, proliferation, metabolism, and motility (Manning & Toker, 2017).

The PI3K/AKT pathway plays a diverse role in both myeloid and lymphoid cell lineages of the immune system. While all four class I PI3K isoforms are expressed in immune cells, PI3K δ and PI3K γ are the primary sources of PIP₃ production following activation in these cells (Fruman et al, 2017).

Given that most human cancers resulted from genomic alterations that aberrantly activate PI3K/AKT signaling pathway, investigations targeting components of this pathway have been initiated in clinical trials (Janku et al, 2018). This resulted in the development of over 40 different inhibitors, however, only a few have been approved for clinical use in the treatment of cancer patients, such as PI3K inhibitors idelalisib and copanlisib (Janku et al, 2018).

1.3.3. NF- κ B pathways

The nuclear factor (NF- κ B) transcription factor family members are central regulators of cellular processes by controlling the development, survival, activation and differentiation of cells of the innate and adaptive immune system. The NF- κ B family comprises of five members that share a Rel homology domain for DNA binding and dimerization: RelA (p65), RelB, c-Rel, p50 (NF- κ B1) and p52 (NF- κ B2). NF- κ B exists as a latent transcription factor in the cytoplasm, which can be activated through various extracellular stimuli (Hayden & Ghosh, 2012).

Generally, two distinct NF- κ B-activating pathways are distinguished. The canonical NF- κ B pathway is dependent on I κ B kinase (IKK)- β and NF- κ B essential modulator (NEMO), and is triggered by TNFR, PRR, as well as TCR and BCR (Liu et al, 2017). A central event of this pathway is the phosphorylation of I κ B α and its subsequent degradation, leading to the nuclear translocation of p65/p50 NF- κ B1 heterodimers. Moreover, phosphorylation of p65 at Ser536 is required to enhance its transactivation potential (Sakurai et al, 1999). The noncanonical pathway is activated by a specific set of TNFRs (such as CD40, LT β R, BAFFR and RANK) and relies on the phosphorylation of the NF- κ B2 precursor p100 by IKK α and the NF- κ B inducing kinase (NIK) and its subsequent proteolytic processing to p52 (Sun, 2012). Importantly, IKK α , IKK β and NEMO are capable of mediating crosstalk with other signaling pathways such as MAPK, IRF and p53 pathways (Oeckinghaus et al, 2011).

The activity of NF- κ B1 is transient, peaking by 30 minutes after induction and leading to the rapid resynthesis of I κ B α encoded by the NFKBIA gene (Smale, 2011), which is a target of NF- κ B1 signaling. Newly synthesized I κ B α translocates into the nucleus and binds to DNA-bound NF- κ B dimers, resulting in nuclear export of the complex and thereby creating a negative feedback loop that is essential for the resolution (Figure 1) of NF- κ B1 activity. Aberrant NF- κ B function may cause severe diseases such as immunodeficiency, autoinflammation and cancer, therefore, proper regulation of these pathways is crucial to maintain homeostasis (Ruland, 2011).

To date, a number of human genetic disorders involving mutations in the regulation and function of NF- κ B components have been described with diverse clinical manifestations and phenotypes, illustrating non-redundancy of these regulatory components of NF- κ B signaling and fundamentally contributed to our current understanding of the NF- κ B signaling pathways (Zhang et al, 2017).

1.4. Human inborn errors of immunity

Human inborn errors of immunity (IEI) or primary immunodeficiencies (PID) refers to a heterogeneous group of inherited human diseases that affect the development and/or function of immune system (McCusker & Warrington, 2011). Patients often suffered from recurrent infections, autoinflammation, autoimmunity and/or malignancy (Tangye et al, 2020). These disorders are caused by monogenic germline mutations and are usually rare, affecting approximately 1 in 10,000 to 1 in 50,000 births. However, their collective prevalence is approximately 1 in 1,000-5,000 births (Tangye et al, 2020).

Monogenic diseases such as human IEI provide opportunities to unravel precise genotype to phenotype relationship. They represent unique models to identify and characterize molecular mechanisms underlying important unknown human biology, which may substantially improve patient diagnostics and enable targeted therapy (Tangye et al, 2020). Advancements in genetics, such as whole-exome sequencing (WES) in human monogenic diseases, has helped to identify new genes involved in the immune system. To date, 430 known genetic defects were identified as causing human IEI (Tangye et al, 2020).

1.4.1. Combined immunodeficiency

Combined immunodeficiencies (CID) are a group of heterogeneous inherited monogenic immunological diseases affecting T- and B-lymphocytes with respect to their development and effector function in immune-regulation. Impaired adaptive immunity in affected patients may cause early-onset elevated susceptibility to infections, autoimmune manifestations and cancer (Akar et al, 2016).

The most frequent forms of CID are with genetic disorders affecting T cells, in terms of absolute numbers, development and/or function, which in turn could also lead to B-cell defects (McCusker & Warrington, 2011; Akar et al, 2016). Defects in TCR signaling components such as LCK, ZAP70, as well as defects in components involved in actin cytoskeleton remodeling such as DOCK8, DOCK2, have been reported to cause CID (Fischer et al, 2015).

In severe forms of CID, also known as severe combined immunodeficiency (SCID), there is a deficiency of functional T cells which can be additionally categorized into whether there is an absence or presence of B and/or NK cells (T⁻ B⁺ NK⁺, T⁻ B⁻ NK⁺, T⁻ B⁺ NK⁻, or T⁻ B⁻ NK⁻) (McCusker & Warrington, 2011; Akar et al, 2016). SCID

subtypes can also be distinguished by genetic mutations and patterns of inheritance: autosomal recessive or X-linked (Fischer et al, 2015). To date, there are 18 known genetic mutations identified to cause SCID (Tangye et al, 2020). X-linked SCID has a constant incidence worldwide, as novel mutations in *IL2RG*, the gene causing this subtype, occur sporadically at a stable rate. Autosomal recessive SCID (AR-SCID) occurs less frequently than X-linked SCID because a mutant allele must be inherited from both seemingly health carrier parents (Fischer et al, 2015). However, consanguineous marriages and geographically isolated populations can result in higher incidence of AR-SCID. Moreover, some forms of SCIDs occur at a higher rate in some populations with specific founder mutations, such as Artemis (encoded by *DCLRE1C*)-deficient SCID affects 1 in 2,000 Native American (Navajo) births (Fischer et al, 2015).

Since SCIDs and CIDs are life-threatening conditions, early diagnosis is of paramount importance. Several newborn-screening programs have been established and immensely enhanced survival rate because hematopoietic stem cell transplantation (HSCT) and gene therapy can be performed early in life (Fischer et al, 2015).

1.4.2. EBV-driven diseases

Epstein-Barr virus (EBV) is one of the most prevalent viruses that infect humans (>90%), however, it maintains lifelong viral latency in most individuals and therefore, many are asymptomatic (Taylor et al, 2015; Long et al, 2019). Most of the time, EBV infection occurs in your children with almost no symptoms. However, if infection happens later in life at adolescent, some may develop acute infectious mononucleosis, which is characterized by fatigue, fever, sore throat and lymphadenopathy. Usually, the acute symptoms of infectious mononucleosis resolve by themselves without significant medical attention (Long et al, 2019).

Initially, orally transmitted EBV infects and replicates in epithelial cells and B cells in the oropharynx (Long et al, 2019). During lytic infection, high levels of virus shedding in the throat and the infection starts to spread through growth-transforming (latency) infection of B cells in oropharyngeal lymphoid organs and appearance of infected B cells in the peripheral blood (Taylor et al, 2015; Long et al, 2019). There will then be a downregulation of the growth-transforming program in some infected B cells and enter the memory B cell pool. At this stage, lifelong viral latency is achieved in these memory B cell pool. These cells circulate between oropharyngeal lymphoid organs and blood.

Intermittently, lytic cycle can be triggered to shed low level of virus shedding into the throat, releasing infectious virus for oral transmission to new hosts (Taylor et al, 2015; Long et al, 2019).

EBV is capable of transforming B cells into immortalized lymphoblastoid cell lines (LCLs) in vitro, due to its strong growth transforming capacity. In individuals with impaired immunity or children with IEI, EBV infection may result in life-threatening diseases such as severe infectious mononucleosis, hemophagocytic lymphohistiocytosis (HLH), lymphoproliferation and malignant lymphomas (Tangye & Latour, 2020). Majority of people do not suffer any ill-effects of EBV infection due to robust anti-viral immune responses in healthy individuals and ongoing immune surveillance to maintain lifelong control of host immune homeostasis and prevent the development of malignancies (Tangye & Latour, 2020; Long et al, 2019).

Both the innate and adaptive immune systems work together to regulate host response to EBV infection. During EBV infection, NK cells have been shown to limit B-cell transformation mediated by viral particles in vitro by secreting IFN- γ (Taylor et al, 2015). Subsequently, EBV-specific T cells are activated and undergo expansion. Over time, EBV-specific T cell responses diminish to values typical of lifelong virus carriage (Long et al, 2019).

To date, a number of inherited monogenic mutations have been identified in humans to cause immune dysregulation with EBV viremia and/or EBV-associated diseases. Studies of these patients shed light into the biology of EBV and immune responses against EBV in humans (Tangye & Latour, 2020).

X-linked lymphoproliferative disorder type 1 (XLP1) is caused by mutations in *SH2D1A* and was the first reported immunodeficiency disorder associated to EBV infection. Remarkably, these patients showed intact immunity against other childhood viruses such as herpes simplex virus (HSV). Patients with XLP1 suffer from EBV-induced HLH (see chapter 1.4.3.), B cell lymphoma and dysgammaglobulinemia (Tangye & Latour, 2020).

Mutations in several distinct components of TCR-induced signaling pathways result in immunodeficiency with predisposition to severe EBV-driven diseases, including *ITK*, *MAGT1*, *CTPS1* and *RASGRP1* (Tangye & Latour, 2020). Furthermore, EBV-associated immunodeficiency has been identified in patients with mutations in T cell

costimulatory molecules which play crucial roles in initiating EBV-specific CD8⁺ T cell responses such as *CD27*, *CD70* and *TNFRSF9* (Tangye & Latour, 2020).

1.4.3. Hemophagocytic lymphohistiocytosis

Hemophagocytic lymphohistiocytosis (HLH) is an uncontrolled hyperinflammatory syndrome, which is potentially life-threatening (Sieni et al, 2014; Al-Samkari & Berliner, 2018). The inability to control immune response, resulting in the massive secretion of inflammatory cytokines and macrophage activation, leads to systemic inflammatory signs and symptoms (Al-Samkari & Berliner, 2018).

There are two types of HLH: primary or familial (known as familial hemophagocytic lymphohistiocytosis (FHL)), and secondary HLH. FHL occurs due to an inherited genetic defect in specific genes that cause immune dysfunction (Al-Samkari & Berliner, 2018). To date, FHL syndromes are classified into FHL1 to FHL5, which are defined by mutations in the following genes: *PRF1* in FHL2, *UNC13D* in FHL3, *STX11* in FHL4, and *STXBP2* in FHL5 (Sieni et al, 2014). These genes are essential for NK- and T-cell cytotoxicity, and mutations in genes that disrupt crucial cytotoxicity pathways such as granule release or the pore forming machinery are likely to result in HLH. The genetic mutation responsible for the development of FHL1 is not yet known, however, has been shown to reside on chromosome 9p21.3-q22 (George, 2014; Al-Samkari & Berliner, 2018).

In healthy individuals, cytotoxic T cells and NK cells respond to pathogens by releasing cytolytic granules such as perforin (encoded by *PRF1*) and granzymes to the target cell. These granules need to be properly trafficked and undergo exocytosis into the immunological synapse to be delivered to the target cell. Disruption in any of these processes caused by genetic mutations predisposes to the development of FHL (Al-Samkari & Berliner, 2018). Apart from FHL, immune disorders associated with HLH includes Griscelli syndrome type 2 (mutations in *RAB27A*), Chediak–Higashi syndrome (mutations in *LYST*), Hermansky–Pudlak type 2 (mutations in *AP3B1*), X-linked lymphoproliferative disorder type 1 (mutations in *SH2D1A*) and type 2 (mutations in *BIRC4*) (Sieni et al, 2014; George, 2014).

Most patients with FHL have persistent fever, which does not respond to antibiotic therapy. Hepatosplenomegaly can usually be detected by physical examination. Patients often suffer from cytopenias affecting at least two lineages in peripheral blood.

Hemophagocytosis by activated macrophages in the bone marrow aspirates can also be seen. Low or absent NK-cell activity is also one of the hallmarks of HLH. Characteristic clinical biomarkers such as elevated ferritin, triglycerides, soluble CD25 and low fibrinogen level, are helpful diagnostic criteria for HLH (Sieni et al, 2014; George, 2014). The official diagnosis of HLH, established by the Histiocyte Society, is either based on a molecular diagnosis consistent with HLH or fulfilling five out of nine criteria listed above (Sieni et al, 2014; George, 2014). Nevertheless, diagnosing HLH is still a challenge for pediatricians, especially because the criteria are not exclusive to HLH manifestation (Sieni et al, 2014).

Gene expression analysis of mononuclear cells and serum cytokines from patients with HLH has demonstrated increased expression and level of IL-1 β , IL-2, IL-6, IL-8, IL-18, TNF- α and IFN- γ (George 2014; Al-Samkari & Berliner, 2018). Higher measured cytokine levels have been correlated with poorer outcomes, therefore, cytokine levels and gene expression profiling may be useful in predicting the risk of relapse and response to treatment, along with the clinical diagnosis of HLH (George, 2014). Generally, treatment of HLH aims at reversing harmful effects of uncontrolled immune response. The acute therapy includes immune-suppressive and modulatory agents such as corticosteroids, to suppress the hyperinflammatory state and the immune dysregulation that leads to life-threatening organ failure. Without treatment, FHL is nearly fatal (George, 2014; Al-Samkari & Berliner, 2018).

1.4.4. Autoinflammatory syndromes

Autoinflammatory syndromes are a group of disorders characterized by an exaggerated innate immune response resulting in episodes of spontaneous systemic inflammation which affect multiple organ systems. Autoinflammatory disorders are mainly driven by dysregulated innate immunity such as myeloid cells whereas autoimmune diseases by dysregulated adaptive immunity (Havnaer & Han, 2019). Although autoinflammatory disorders and autoimmune diseases usually comprise distinct clinical entities, an increasing understanding of these two syndromes led to the discussion if they should be categorized as a spectrum of a single group of disorders since inappropriate innate immune response may be required to initiate aberrant adaptive immunity in autoimmune diseases (Krainer et al, 2020).

Activation of the innate immunity through PRRs by sensing PAMPs or DAMPs are crucial to initiate downstream signaling pathways mainly via NF- κ B, interferon-

regulatory factors (IRFs) and activator protein 1 (AP1), which regulate inflammation and the production of proinflammatory cytokines to provide first line of defense against pathogens (Takeuchi & Akira, 2010).

Intracellular PRRs such as nucleotide-binding oligomerization domain, leucine-rich repeat containing receptors (NLRs), absent in melanoma 2 (AIM2) and pyrin are part of multiprotein scaffolds called inflammasomes. An inflammasome is made up of an adaptor molecule known as ASC (apoptosis related speck-like protein containing caspase activation and recruitment domains), a pyrin domain (PYD) and a caspase recruitment domain (CARD). Inflammasomes are crucial to activate caspase-1 for the generation of active IL-1 β and IL-18, as well as the induction of pyroptosis (Broz & Dixit, 2016; Krainer et al, 2020).

IL-1 β is a potent proinflammatory cytokine, known to be released not only by immune cells but also non-immune cells such as keratinocytes. Once released, IL-1 β activates NF- κ B signaling via IL-1RI to promote NF- κ B-dependent target genes such as NLRP3, IL-6, TNF- α leading to a robust inflammatory response. However, an aberrant immune response involving these signaling pathways may result in autoinflammatory syndromes (Havner & Han, 2019; Krainer et al, 2020).

Systemic autoinflammatory diseases can be categorized as monogenic or multifactorial. The former refers to inherited disease caused by a mutation in a single gene whereas the latter refers to complex disease associated to a combination of genetic mutations or external influences with unclear etiology (Havner & Han, 2019; Krainer et al, 2020).

Monogenic autoinflammatory diseases can be further subdivided into inflammasomopathies or IL-1 β -activation syndromes such as mutations in *MEFV* encoding pyrin, result in familial Mediterranean fever (FMF); protein-folding disorders in which gain-of-function (GOF) mutations in *TNFRSF1A* cause TNF receptor-associated periodic syndrome (TRAPS); and NF- κ B-activation disorders whereby GOF mutations in *NOD2* result in Blau syndrome (Havner & Han, 2019).

2. Aims of thesis

This thesis aims to elucidate the molecular mechanisms of human immune dysregulation through the study of patients with monogenic defects in immune cellular signaling pathways.

To achieve this aim, we performed WES on selected patients presenting with early-onset immune dysregulation to identify novel monogenic mutations involving components of immune signaling pathways resulting in primary immunodeficiency/ inborn errors of immunity. Functional studies including various cellular, immunological, molecular and biochemical assays were performed to dissect genotype-phenotype relationships and characterize inheritance pattern and molecular cause of previously unknown primary immunodeficiencies. We also comprehensively studied the role of specific human immune signaling components by proving causality in primary patient materials as well as generating genetic knockout of these components in an independent cellular system. As a result, therapeutic opportunities can be proposed to improve patient clinical outcomes and treatments.

3. Results

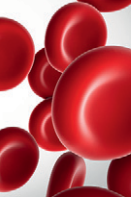
3.1. CD137 deficiency causes immune dysregulation with predisposition to lymphomagenesis

Ido Somekh^{1,2*}, **Marini Thian**^{3-6*}, David Medgyesi^{4,5§}, Nesrin Gülez⁷, Thomas Magg¹, Alejandro Gallón Duque^{1,8}, Tali Stauber^{9,10}, Atar Lev^{9,10}, Ferah Genel⁷, Ekrem Unal^{11,12}, Amos J. Simon^{9,10,13}, Yu Nee Lee^{9,10}, Artem Kalinichenko³⁻⁵, Jasmin Dmytrus³⁻⁵, Michael J. Kraakman³⁻⁵, Ginette Schiby¹⁴, Meino Rohlf¹, Jeffrey M. Jacobson¹⁵, Erdener Özer¹⁶, Ömer Akcal⁷, Raffaele Conca¹, Türkan Patiroglu¹¹, Musa Karakukcu¹¹, Alper Ozcan¹¹, Tala Shahin³⁻⁵, Eliana Appella^{1,17}, Megumi Tatematsu¹, Catalina Martinez-Jaramillo⁸, Ivan K. Chinn^{18,19}, Jordan S. Orange^{18,20}, Claudia Milena Trujillo-Vargas⁸, José Luis Franco⁸, Fabian Hauck¹, Raz Somech^{9,10#}, Christoph Klein^{1#}, and Kaan Boztug^{3-6,21#}

¹Dr. von Hauner Children's Hospital, University Hospital, Ludwig Maximilian University, Munich, Germany; ²Schneider Children's Medical Center of Israel, Department of Pediatric Hematology Oncology, Petah Tikva, Sackler Faculty of Medicine, Tel Aviv University, Israel; ³St. Anna Children's Cancer Research Institute (CCRI); ⁴Ludwig Boltzmann Institute for Rare and Undiagnosed Diseases, Vienna, Austria; ⁵CeMM Research Center for Molecular Medicine of the Austrian Academy of Sciences, Vienna, Austria; ⁶Department of Pediatrics and Adolescent Medicine, Medical University of Vienna, Vienna, Austria; ⁷S.B.U. Dr.Behçet Uz Children's Education And Research Hospital Division of Pediatric Immunology and Allergy, Izmir, Turkey; ⁸Group of Primary Immunodeficiencies, School of Medicine, University of Antioquia UdeA, Medellín, Colombia; ⁹Pediatric Department A and Immunology Service, Jeffrey Modell Foundation Center, Edmond and Lily Safra Children's Hospital, Sheba Medical Center, Tel Hashomer, Sackler Faculty of Medicine, Tel Aviv University, Israel; ¹⁰The Wohl Institute for Translational Medicine, Sheba Medical Center, Tel Hashomer; ¹¹Erciyes University, Faculty of Medicine, Department of Pediatrics, Division of Pediatric Hematology Oncology & HSCT Unit, Melikgazi, Kayseri, Turkey; ¹²Molecular Biology and Genetic Department, Gevher Nesibe Genom and Stem Cell Institution, Genome and Stem Cell Center (GENKOK), Erciyes University, Melikgazi, Kayseri, Turkey; ¹³Haematology lab, Sheba Medical Center, Tel Hashomer, Sackler Faculty of Medicine, Tel Aviv University, Israel; ¹⁴Department of Pathology, Sheba Medical Center, Tel Hashomer, Sackler Faculty of Medicine, Tel Aviv University, Israel; ¹⁵Radiology Department, Sheba Medical Center, Tel Hashomer, Sackler Faculty of Medicine, Tel Aviv University, Israel; ¹⁶Department of Pathology, Dokuz Eylul University School of Medicine, Izmir, Turkey; ¹⁷Ricardo Gutiérrez Children's Hospital, Buenos Aires, Argentina; ¹⁸Center for Human Immunobiology, Texas Children's Hospital, Houston, TX, United States; ¹⁹Department of Pediatrics, Baylor College of Medicine, Houston, TX, United States; ²⁰Department of Pediatrics, Vagelos College of Physicians and Surgeons, Columbia University, New York, NY, United States; ²¹St. Anna Children's Hospital, Department of Pediatrics and Adolescent Medicine, Medical University of Vienna, Vienna, Austria; §Current Address: Becton Dickinson Life Sciences, 2851 Kornye, Hungary.

*These authors contributed equally

#These authors contributed equally



IMMUNOBIOLOGY AND IMMUNOTHERAPY

CD137 deficiency causes immune dysregulation with predisposition to lymphomagenesis

Ido Somekh,^{1,2,*} Marini Thian,^{3-6,*} David Medgyesi,^{4,5} Nesrin Gülez,⁷ Thomas Magg,¹ Alejandro Gallón Duque,^{1,8} Tali Stauber,^{9,10} Atar Lev,^{9,10} Ferah Genel,⁷ Ekrem Unal,^{11,12} Amos J. Simon,^{9,10,13} Yu Nee Lee,^{9,10} Artem Kalinichenko,³⁻⁵ Jasmin Dmytrus,³⁻⁵ Michael J. Kraakman,³⁻⁵ Ginette Schiby,¹⁴ Meino Rohlfis,¹ Jeffrey M. Jacobson,¹⁵ Erdener Özer,¹⁶ Ömer Akcal,⁷ Raffaele Conca,¹ Türkan Patiroglu,¹¹ Musa Karakukcu,¹¹ Alper Ozcan,¹¹ Tala Shahin,³⁻⁵ Eliana Appella,^{1,17} Megumi Tatematsu,¹ Catalina Martinez-Jaramillo,⁸ Ivan K. Chinn,^{18,19} Jordan S. Orange,^{18,20} Claudia Milena Trujillo-Vargas,⁸ José Luis Franco,⁸ Fabian Hauck,¹ Raz Somech,^{9,10,†} Christoph Klein,^{1,†} and Kaan Boztug^{3-6,21,†}

¹Dr. von Hauner Children's Hospital, University Hospital, Ludwig Maximilian University of Munich, Munich, Germany; ²Department of Pediatric Hematology Oncology, Schneider Children's Medical Center of Israel, Petah Tikva, Sackler Faculty of Medicine, Tel Aviv University, Tel Aviv, Israel; ³St. Anna Children's Cancer Research Institute (CCRI), Vienna, Austria; ⁴Ludwig Boltzmann Institute for Rare and Undiagnosed Diseases, Vienna, Austria; ⁵CeMM Research Center for Molecular Medicine of the Austrian Academy of Sciences, Vienna, Austria; ⁶Department of Pediatrics and Adolescent Medicine, Medical University of Vienna, Vienna, Austria; ⁷Division of Pediatric Immunology and Allergy, S.B.Ü. Dr. Behçet Uz Children's Education And Research Hospital, Izmir, Turkey; ⁸Group of Primary Immunodeficiencies, School of Medicine, University of Antioquia (UdeA), Medellín, Colombia; ⁹Pediatric Department A and Immunology Service, Jeffrey Modell Foundation Center, Edmond and Lily Safra Children's Hospital, Sheba Medical Center, Tel HaShomer, Sackler Faculty of Medicine, Tel Aviv University, Israel; ¹⁰The Wohl Institute for Translational Medicine, Sheba Medical Center, Tel HaShomer, Israel; ¹¹Department of Pediatrics, Division of Pediatric Hematology Oncology and HSCT Unit, Erciyes University, Faculty of Medicine, Melikgazi, Kayseri, Turkey; ¹²Molecular Biology and Genetic Department, Gevher Nesibe Genom and Stem Cell Institution, Genome and Stem Cell Center (GENKOK), Erciyes University, Melikgazi, Kayseri, Turkey; ¹³Haematology Laboratory, ¹⁴Department of Pathology, and ¹⁵Radiology Department, Sheba Medical Center, Tel HaShomer, Sackler Faculty of Medicine, Tel Aviv University, Israel; ¹⁶Department of Pathology, School of Medicine, Dokuz Eylül University, Izmir, Turkey; ¹⁷Ricardo Gutiérrez Children's Hospital, Buenos Aires, Argentina; ¹⁸Center for Human Immunobiology, Texas Children's Hospital, Houston, TX; ¹⁹Department of Pediatrics, Baylor College of Medicine, Houston, TX; ²⁰Department of Pediatrics, Vagelos College of Physicians and Surgeons, Columbia University, New York, NY; and ²¹Department of Pediatrics and Adolescent Medicine, St. Anna Children's Hospital, Medical University of Vienna, Vienna, Austria

KEY POINTS

- CD137 deficiency is a novel inborn error of immunity with immune dysregulation and EBV-associated lymphomagenesis.
- Our study highlights the key role of CD137 for immune homeostasis with relevance to immunodeficiency and cancer immunotherapy.

Dysregulated immune responses are essential underlying causes of a plethora of pathologies including cancer, autoimmunity, and immunodeficiency. We here investigated 4 patients from unrelated families presenting with immunodeficiency, autoimmunity, and malignancy. We identified 4 distinct homozygous mutations in *TNFRSF9* encoding the tumor necrosis factor receptor superfamily member CD137/4-1BB, leading to reduced, or loss of, protein expression. Lymphocytic responses crucial for immune surveillance, including activation, proliferation, and differentiation, were impaired. Genetic reconstitution of CD137 reversed these defects. CD137 deficiency is a novel inborn error of human immunity characterized by lymphocytic defects with early-onset Epstein-Barr virus (EBV)-associated lymphoma. Our findings elucidate a functional role and relevance of CD137 in human immune homeostasis and antitumor responses. (*Blood*. 2019;134(18):1510-1516)

Introduction

Antigen receptors and associated signaling machineries function to sense and rapidly react to threats that endanger the organisms such as foreign invaders or altered self-structures. Coreceptors play fundamental roles in regulating and fine-tuning the signal strength of antigen receptors. Defective function of these immune receptors may lead to elevated susceptibility to infections, autoimmune manifestations, and cancer.¹ Epstein-Barr virus (EBV) is one of the most prevalent viruses that infects humans and maintains lifelong latency.^{2,3} In individuals with impaired T-cell immunity, EBV infection may result in lymphoproliferative disease, or malignant lymphomas of T-, B-, or natural killer (NK)-cell origin.³ To date, germline genetic mutations affecting *CD27*, *PRKCD*, *RASGRP1*, *MAGT1*, *SH2D1A*, *ITK*, and others have been identified

to cause immune dysregulation with EBV-associated diseases.² Studies of these patients have provided mechanistic insight into pathways required for robust host immune surveillance against EBV infection and associated lymphomas. Here, we report an inborn deficiency of tumor necrosis factor (TNF) receptor superfamily member 9 (*TNFRSF9*)/CD137/4-1BB with marked immune dysregulation and predisposition to EBV-associated lymphoma.

Study design

Patients

The study was approved by the institutional review boards of the Medical University of Vienna (Vienna, Austria; EK499/2011),

Downloaded from https://ashpublications.org/blood/article-pdf/134/18/1510/504063/blood.bld-2019000644.pdf by MEDIZINISCHE UNIVERSITÄT WIEN user on 31 October 2019

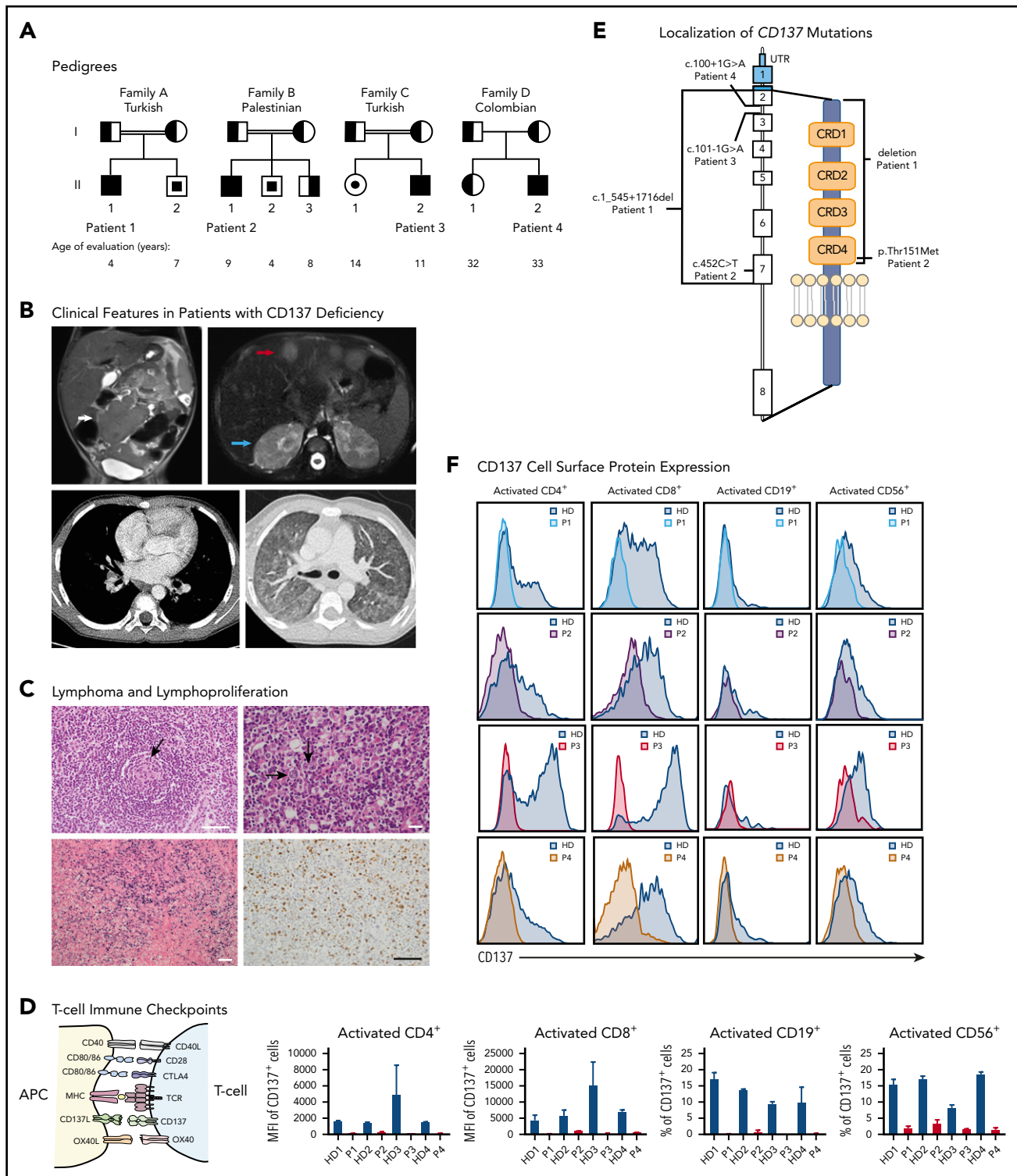


Figure 1. Genetic and clinical presentation of 4 patients with immune dysregulation. (A) Pedigrees showing 4 families with affected individuals (patients) harboring *TNFRSF9* mutations. Solid symbols indicate affected persons who were homozygous for the mutant allele; half-solid symbols, heterozygous persons; center solid symbols, unaffected persons homozygous for the mutant allele; circles, female family members; squares, male family members; double lines, consanguinity. (B) Radiographic features in patients with CD137 deficiency. Top left, Coronal T2-HASTE MR demonstrating a lobulated mass of the small intestine (white arrow) in patient 1 (P1). Top right, axial T2-HASTE STIR MR image of upper abdomen depicting hyperintense multiple metastatic liver nodules (red arrow) and bilateral renal cortical hypointense metastatic nodules (blue arrow) in patient 1. Bottom left, Chest computer tomography (CT) scan indicating right-sided hilar lymph nodes in patient 3 (P3). Bottom right, chest CT scan revealing bilateral ground-glass opacities in patient 2 (P2). (C) Top left, sections of right inguinal lymph node tissue (hematoxylin-and-eosin staining) showing numerous small regressive germinal centers (black arrow) in patient 2 (scale bar, 10 μ m). Bottom right, Ki-67 immunostain in patient 2, positive in 20% to 30% of the cells exhibiting a moderate lymphocyte proliferative activity (scale bar, 10 μ m). Bottom left, in situ hybridization for EBV-encoded small RNAs (EBER) displaying numerous positive cells in blue in patient 3 (scale bar, 200 μ m). Top right, Multinucleated Reed-Sternberg cells (black arrows) typical of Hodgkin lymphoma (scale bar, 20 μ m) in a resection of a submandibular lymph node in patient 3. (D) Schematic illustration displaying the interaction of ligands expressed on antigen-presenting cells (APCs) with their respective receptors on activated T cells, including the interaction

the Ludwig Maximilian University of Munich (Munich, Germany), Sheba Medical Center (Tel HaShomer, Israel), and the Baylor University College of Medicine (Houston, TX). All study participants provided written informed consent. Informed assent was obtained for children.

Experimental methodologies

All methods are detailed in the supplemental Materials and methods (available on the *Blood* Web site).

Results and discussion

Clinical phenotypes

We studied 4 patients from 4 unrelated families, 3 of whom were from consanguineous background (Figure 1A). Patients had early childhood recurrent infections of bacterial and viral origin, and signs of autoimmunity (Figure 1B-C; supplemental Figure 1; supplemental Table 1). Sinopulmonary and herpes virus infections were common. All patients exhibited hepatomegaly, splenomegaly, and/or lymphadenopathy. Signs of autoimmunity, including hemolytic anemia, were present in some patients. We found abnormal immunoglobulin levels in all patients (supplemental Table 2). Patients 1 and 3 developed EBV-related B-cell lymphoma, patient 2 had an autoimmune lymphoproliferative syndrome-like phenotype, and patient 4 was diagnosed as having common variable immune deficiency. Therapeutic regimens included chemotherapy, immunosuppression, antibiotic prophylaxis, and regular immunoglobulin substitution (supplemental Table 1).

Genetic evaluation and loss-of-function mutations in *TNFRSF9*

To elucidate the disease etiology, we performed whole-exome sequencing and identified distinct homozygous variants in *TNFRSF9* encoding the costimulatory immune checkpoint CD137/4-1BB (Figure 1D-E; supplemental Figure 2; supplemental Table 3). Parents were heterozygous carriers in all cases. All *TNFRSF9* variants were absent in gnomAD, and predicted to be deleterious using common prediction algorithms (supplemental Table 4). Patient 1 was homozygous for a large deletion in *TNFRSF9*, and patient 2 harbored a homozygous missense mutation affecting evolutionarily conserved residues (supplemental Figure 3). Patient 3 was homozygous for a *TNFRSF9* mutation disrupting the splice-acceptor site of exon 3, resulting in the skipping of exons 3 and 6. It remains unclear why alternative splice variants are present in this patient, including a smaller fraction of transcripts that has both exon 3 and exon 6 of *TNFRSF9* skipped (supplemental Figure 4). However, it is possible that this specific splice-acceptor site regulates the splicing of nearby exons, as demonstrated by variants in *ERBB4*.⁴ Additional investigations in the splicing effects of this genetic variant were, however, beyond the scope of this study. Patient 4 was homozygous for a mutation in the splice-donor site of exon 2 causing skipping of exon 2 (supplemental Figure 4). All mutations resulted in markedly reduced or abrogated expression of CD137 on activated T, B, and NK cells, indicating a loss-of-function

phenotype (Figure 1F; supplemental Figure 5). However, the loss of CD137 did not affect CD137L protein expression in patients' T cells (supplemental Figure 7D). Recent studies showed that CD137 can be transferred from Hodgkin and Reed-Sternberg cells to neighboring cells by trogocytosis.⁵ We thus investigated the expression of *CD137L* in T cells by reverse transcription polymerase chain reaction and found that *TNFRSF9/CD137L* messenger RNA is expressed intrinsically in T cells (supplemental Figure 7D).

Interestingly, in 3 of the pedigrees, 1 healthy sibling each was also homozygous for the same *TNFRSF9* mutation. Accordingly, they had abrogated or reduced CD137 expression, without overt clinical disease. It is currently unknown whether CD137 deficiency may be aggravated by infections or other extrinsic challenges. Incomplete penetrance is well known for pathogenic immune system mutations,⁶ especially for defects with predominant immune dysregulation, as exemplified by CTLA-4 haploinsufficiency.⁷

Immune-cell phenotypes

Patients had variable lymphocyte abnormalities (supplemental Table 2). All patients had elevated proportions of transitional and immature B cells but markedly reduced memory B cells and plasmablasts. Decreased NK-cell counts were observed in patients 2 and 3. Patients 1, 2, and 3 had reduced follicular helper T cells (T_{FH}) (Figure 2A; supplemental Figure 6).

Functional T-cell defects in CD137-deficient patients

CD137-deficient mice have impaired T-cell survival, proliferation, and cytotoxicity.⁸⁻¹⁰ We thus hypothesized that human CD137 deficiency may also hamper T-cell differentiation and function. Indeed, T-cell proliferation responses to various stimuli were reduced in all patients (Figure 2B). Surprisingly, patients' T cells showed impaired proliferation to anti-CD3 stimulation alone. We hypothesized that CD137L is functionally important and required to elicit a normal cellular response to CD3. By blocking CD137 in healthy donor (HD) peripheral blood mononuclear cells (PBMCs) stimulated with anti-CD3, we showed a dose-dependent reduction in T-cell proliferation (supplemental Figure 7A). Indeed, CD137 receptor/ligand interaction plays a functional role in T cells. Remarkably, the addition of anti-CD28–mediating T-cell receptor (TCR) costimulation restored proliferative functions, and partial compensation was seen upon OX40 costimulation (Figure 2B). We also observed reduced T-cell activation in patients 1 to 3, amenable to correction upon additional CD28 costimulation. Patient 4 had normal T-cell activation (Figure 2C; supplemental Figure 7B), consistent with a milder T-cell proliferation defect (Figure 2B). Collectively, our findings highlight the importance of CD137 in immune homeostasis costimulation and, intriguingly, the lack of CD137 costimulation may be compensated in the presence of other costimulators.

Figure 1 (continued) between CD137L and CD137. (E) Localization of *CD137* mutations in our patients. *CD137* gene and protein domains with the 4 newly identified mutations are indicated. (F) CD137 protein expressions in activated (CD25⁺) CD4⁺ and CD8⁺ T cells, activated (CD86⁺) CD19⁺ B cells, and activated (interleukin 2 [IL-2] stimulated) NK cells (CD56⁺) in patients and healthy donors (HDs) demonstrating complete loss or markedly reduced expression in patients' cells, measured by flow cytometry. All error bars indicate plus or minus standard error of mean (SEM). CRD, cysteine-rich domain; MFI, mean fluorescence intensity; MHC, major histocompatibility complex; P4, patient 4; UTR, untranslated region.

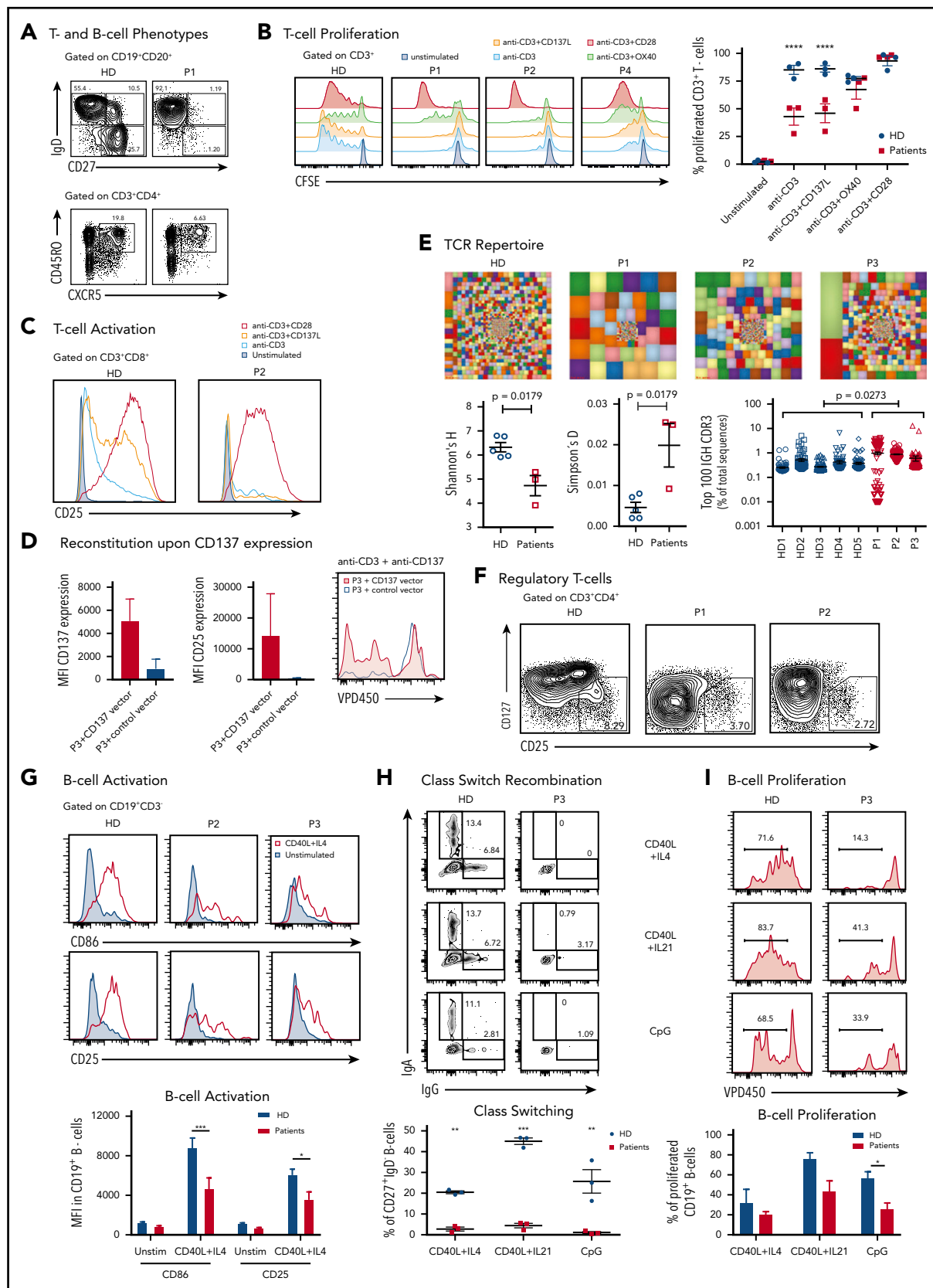


Figure 2. Immunological and functional phenotypes in CD137-deficient patients. (A) T- and B-cell features in our patients: immunophenotyping revealed decreased frequencies of class-switched (CD27⁺ immunoglobulin D-negative [IgD⁻]) B cells and T_{FH} (CD45RO⁺CXCR5⁺) cells in patient 1 (P1) compared with an HD, as measured by flow cytometry. (B) T-cell proliferation with carboxyfluorescein succinimidyl ester (CFSE) fluorescence cell incorporation assay 4 days poststimulation exhibiting reduced CD3⁺ T-cell proliferation in response to anti-CD3 and anti-CD3 in combination with CD137L in patients 1, 2 (P2), and 4 (P4) with partial and complete restoration upon OX40 and CD28

To prove the causative role of lack of CD137 for the observed phenotypes, we performed a gene-rescue experiment in T cells from patient 3. Upon exogenous expression of wild-type CD137, T-cell proliferation and activation defects were restored (Figure 2D; supplemental Figure 7C).

TCR repertoire analysis in patients 1 to 3 showed significant clonal expansion associated with reduced diversity (Figure 2E). CD137 is expressed in regulatory T cells (Tregs) and has been shown to play a role in Treg function, survival, and expansion.^{10,11} We therefore assessed Treg frequencies in PBMCs and observed lower Treg frequencies in our patients (Figure 2F).

In Cd137-deficient mice, NK-cell and cytotoxic T-lymphocyte (CTL) function were diminished. Indeed, EBV-specific CTL cytotoxicity was reduced in patient CTLs compared with HDs (supplemental Figure 8A), suggesting that CD137 deficiency results in susceptibility to EBV and its related lymphomagenesis. However, CTL and NK-cell degranulation, as well as downstream TCR-signaling pathways, were intact in CD137-deficient patients (supplemental Figure 8B-E). This is reminiscent of a study investigating human FERMT3-deficient patients where there was specific cytotoxicity impairment but not general cytotoxicity.¹²

B-cell defects in CD137-deficient patients

CD137 is expressed in activated human B cells,¹³ T_{FH},¹⁰ and follicular dendritic cells.¹⁴ CD137 has been shown to be essential for B-cell function, including activation, affinity maturation, proliferation, and class switch recombination (CSR) through its interaction with CD137L in germinal centers.¹⁴⁻¹⁶ We thus hypothesized that these functions may be impaired in patient B cells. Indeed, CD137 expression was abrogated in B cells from all patients (Figure 1F), and B-cell activation was impaired (Figure 2G). Correspondingly, we mimicked T-cell-dependent and -independent stimulation on patient B cells and found defective CSR, proliferation, and lower frequencies of plasmablasts (Figure 2H-I; supplemental Figure 9). Patients' B cells consistently showed maturation and differentiation defects with a marked reduction in memory B cells, plasmablasts, and CSR (Figure 2A,H; supplemental Figure 9A). In accordance with our data, it has been shown that CD137L signaling is required for proper activation and maturation of B cells and humoral responses.¹⁴ Alternatively, the maturation defects in B cells could also be an indirect effect of the lack of CD137 signaling in T_{FH} cells, resulting in the reduction of these cells and, therefore, the lack of help by these specific T-cell subsets to B cells. However, because CD137 is also expressed on activated B cells (Figure 1F),

although to a smaller extent than in activated T cells, we believe that the lack of CD137 on patient B cells may contribute to their proliferation and survival directly.¹³ Additionally, despite normal T_{FH} cell frequency in patient 4, B-cell development was still impaired (supplemental Figure 6), supporting the notion of a primary B-cell maturation defect. Furthermore, sorted naïve B cells also showed reduced activation, proliferation, and CSR (supplemental Figure 10). Together, these findings highlight the role of CD137 in proper differentiation and function of B cells as previously reported.¹³

CD137 is an appealing target for immunotherapy, both for autoimmunity and malignancies. It functions as an immune suppressor, enhancing Treg expansion and ameliorating T_H17 autoimmune effects.¹⁷ Conversely, CD137 is a potent immune stimulator that has been found to modulate the tumor micro-environment, enhancing T- and NK-cell cytotoxicity and their infiltration into tumors.^{18,19} CD137 agonistic monoclonal antibodies are currently in cancer immunotherapy trials, including combinations with checkpoint inhibitors to selectively activate tumor-targeting CTLs and NK cells aiming to provide a robust antitumor response.^{20,21} CD137 signaling is also used in chimeric antigen receptor T-cell immunotherapy.²² Whenever CD137 signals are enhanced, an enhanced cytotoxic response has been shown in various in vitro and in vivo models.²³⁻²⁵ As the binding of CD137 to CD137L triggers a bidirectional signaling,²⁶ loss of CD137 expression in patients may also lead to lack of CD137L function. Cd137L-deficient mice develop B-cell lymphomas.¹⁵ Consistently, 2 patients developed EBV-associated B-cell lymphomas and 1 patient displayed EBV-associated lymphoproliferation, implying that CD137 deficiency is a predisposing factor for malignant transformation. The phenotypes observed in our patients show some resemblance to that of 2 other recently reported CD137-deficient patients (supplemental Table 1).²⁷ Our findings further strengthen the role of CD137 as an appealing target for cancer immunotherapy.

Collectively, we identified novel inherited germline mutations in *TNFRSF9* that allow dissection of the essential role of this costimulatory molecule in regulating human immune homeostasis. In vitro cellular phenotypes were rescued by CD28 costimulation, possibly allowing for the development of targeted therapeutics in vivo in affected patients. CD137 deficiency should be considered in patients with dysregulated immune systems presenting with autoimmunity and autoimmune lymphoproliferative syndrome-like, common variable immune deficiency, and/or EBV-related lymphoma.

Figure 2 (continued) costimulation, respectively (**** $P < .0001$; 2-way analysis of variance [ANOVA]). (C) Representative surface expression of CD25 on T cells as measured by flow cytometry 4 days poststimulation in patient 2 compared with an HD, demonstrating a T-cell activation defect with a compensatory effect upon CD28 costimulation. (D) Rescue of T-cell proliferation and activation via CD25 expression in patient 3 (P3) by exogenous expression of wild-type CD137. (E) Analysis of T-cell receptor γ (TRG) repertoire diversity with a tree-map representation for patients 1, 2, and 3, and age-matched healthy controls. Each colored square represents a unique clone and its size reflects its productive frequency within the repertoire. Simpson's D diversity index and Shannon's H index quantify repertoire clonality. (F) Flow cytometric expression of Tregs, displaying reduced Treg rates in patients 1 and 2 compared with an HD. (G) Top, Flow cytometric expression of CD86⁺ and CD25⁺ of CD19⁺CD3⁻ cells 1 day poststimulation with CD40L in combination with IL4 showed impaired activation in patients 2 and 3. Bottom, quantification of B-cell activation, showing significantly lower B-cell activation in patient cells compared with HDs (* $P < .05$; *** $P < .001$; 2-way ANOVA). (H) Top, class-switched IgG⁺ and IgA⁺ of CD19⁺ cells upon various stimulations, displayed impaired class switch recombination in patient 3 in response to T-cell-dependent and -independent stimuli. Bottom, Quantification of class-switched (CD27⁺IgD⁻) CD19⁺ cell rates showing significantly lower frequencies in the patients (** $P < .01$; *** $P < .001$; 2-way ANOVA). (I) Top, B-cell proliferation measured by violet proliferation dye (VPD450) 4 days poststimulation showing reduced proliferating B cells in patient 3 in response to T-cell-dependent and -independent stimuli. Bottom, quantification of CD19⁺ proliferating cells, showing decreased rates in patients (* $P < .05$; 2-way ANOVA). All error bars indicate plus or minus SEM. CDR, complementarity-determining region; CpG, cytosine guanine dinucleotide; IGH, immunoglobulin heavy; Unstim, unstimulated.

Acknowledgments

The authors thank the patients and their families for participating in the study; Raúl Jimenez-Heredia (Ludwig Boltzmann Institute for Rare and Undiagnosed Diseases [LBI-RUD]), Laurène Pfajfer (LBI-RUD), Wendy Aloo (Ludwig Maximilian University of Munich [LMU]), Carlos E. Muskus (Universidad de Antioquia [UdeA]), and Laura Naranjo (UdeA) for excellent technical assistance; Kemal Deniz (Erciyes University), Burcu S. Gorkem (Erciyes University), and Julio C. Orrego (UdeA); and James R. Lupski, Richard A. Gibbs, and Zeynep H. Coban-Akdemir for sequencing through the Baylor-Hopkins Center for Mendelian Genomics.

This work was supported by the European Research Council (ERC; Consolidator grant 820074 "iDysChart" [K.B.] and an ERC Advanced grant [C.K.]), the Jeffrey Modell Foundation (JMF; R.S.), the Care for Rare Foundation, the German Research Foundation (Gottfried-Wilhelm-Leibniz Program, CRC1054 [C.K.]), and the Else Kröner-Fresenius-Stiftung (Forschungskolleg Rare Diseases of the Immune System [C.K.]). I.S. was supported by the Care for Rare Foundation and has been a scholar of the Else Kröner-Fresenius-Stiftung. M. Thian was supported by a Cell Communication in Health and Disease (CCHD; Medical University of Vienna) doctoral fellowship and a DOC fellowship (25225) of the Austrian Academy of Sciences. A.G.D. was supported by a Deutscher Akademischer Austauschdienst/German Academic Exchange Service (DAAD) Fellowship (Thematic Program on Rare Diseases and Personalized Therapies). The Baylor-Hopkins Center for Mendelian Genomics was supported by the National Institutes of Health, National Human Genome Research Institute/National Heart, Lung, and Blood Institute grant UM1HG006542.

Authorship

Contribution: I.S. and M. Thian designed, performed, and analyzed experiments for all patients; D.M. and A.K. performed transfection of CD137 in patient cells; A.L. and A.J.S. performed and analyzed immune and genetic experiments on P2; Y.N.L. performed TCR repertoire sequencing and analysis; N.G., T. Stauber, F.G., E.U., G.S., J.M.J., E.O., O.A., T.P., M.K., A.O., C.M.T.-V., and J.L.F. provided patient samples and interpreted clinical, pathology, and/or imaging data; M.R. conducted and analyzed next-generation sequencing of P1 and P2; D.M., T.M., M.J.K., and F.H. helped supervise the study and gave intellectual input; J.D. performed variant filtering, Sanger validation, and identified the CD137 mutation in P3; R.C. conducted immunophenotyping in patients' PBMCs; A.G.D., T. Shahin, E.A., and M. Tatematsu provided technical and experimental help; C.M.-J., I.K.C., and J.S.O. conducted and analyzed next-generation sequencing of P4; K.B., C.K., and R.S. conceptualized,

initiated, and supervised the study; and I.S., M. Thian, R.S., C.K., and K.B. wrote the manuscript, which was reviewed and approved by all authors.

Conflict-of-interest disclosure: The authors declare no competing financial interests.

The current affiliation for D.M. is Becton Dickinson Life Sciences, Korneo, Hungary.

ORCID profiles: M. Thian, 0000-0002-3016-0430; E.U., 0000-0002-2691-4826; A.K., 0000-0002-7020-7256; M.K., 0000-0003-2015-3541; M. Tatematsu, 0000-0002-6995-5521; C.M.-J., 0000-0001-6846-0140; I.K.C., 0000-0001-5684-5457; J.L.F., 0000-0001-5664-6415; F.H., 0000-0001-9644-2003; K.B., 0000-0001-8387-9185.

Correspondence: Kaan Boztug, St. Anna Children's Cancer Research Institute (CCRI) and Ludwig Boltzmann Institute for Rare and Undiagnosed Diseases, Zimmermannplatz 10, 1090 Vienna, Austria; e-mail: kaan.boztug@ccri.at; Christoph Klein, Dr. von Hauner Children's Hospital, University Hospital, Ludwig Maximilian University Munich, Lindwurmstr. 4, 80337 Munich, Germany; e-mail: christoph.klein@med.uni-muenchen.de; and Raz Somech, Pediatric Department A and Immunology Service, Jeffrey Modell Foundation Center, Edmond and Lily Safra Children's Hospital, Sheba Medical Center, Sackler Faculty of Medicine, Tel Aviv University, Tel HaShomer, Israel; e-mail: raz.somech@sheba.health.gov.il.

Footnotes

Submitted 17 March 2019; accepted 2 September 2019. Prepublished online as *Blood* First Edition paper, 9 September 2019; DOI 10.1182/blood.2019000644.

*I.S. and M. Thian contributed equally.

†R.S., C.K., and K.B. contributed equally.

For original data, please contact kaan.boztug@rud.lbg.ac.at.

The online version of this article contains a data supplement.

The publication costs of this article were defrayed in part by page charge payment. Therefore, and solely to indicate this fact, this article is hereby marked "advertisement" in accordance with 18 USC section 1734.

REFERENCES

1. Ward-Kavanagh LK, Lin WW, Šedý JR, Ware CF. The TNF receptor superfamily in co-stimulating and co-inhibitory responses. *Immunity*. 2016;44(5):1005-1019.
2. Tangye SG, Palendira U, Edwards ES. Human immunity against EBV—lessons from the clinic. *J Exp Med*. 2017;214(2):269-283.
3. Taylor GS, Long HM, Brooks JM, Rickinson AB, Hislop AD. The immunology of Epstein-Barr virus-induced disease. *Annu Rev Immunol*. 2015;33:787-821.
4. Law AJ, Kleinman JE, Weinberger DR, Weickert CS. Disease-associated intronic variants in the ErbB4 gene are related to altered ErbB4 splice-variant expression in the brain in schizophrenia. *Hum Mol Genet*. 2007;16(2):129-141.
5. Ho WT, Pang WL, Chong SM, et al. Expression of CD137 on Hodgkin and Reed-Sternberg cells inhibits T-cell activation by eliminating CD137 ligand expression. *Cancer Res*. 2013;73(2):652-661.
6. Raj A, Rifkin SA, Andersen E, van Oudenaarden A. Variability in gene expression underlies incomplete penetrance. *Nature*. 2010;463(7283):913-918.
7. Schwab C, Gabrysich A, Olbrich P, et al. Phenotype, penetrance, and treatment of 133 cytotoxic T-lymphocyte antigen 4-insufficient subjects. *J Allergy Clin Immunol*. 2018;142(6):1932-1946.
8. Kwon BS, Hurtado JC, Lee ZH, et al. Immune responses in 4-1BB (CD137)-deficient mice. *J Immunol*. 2002;168(11):5483-5490.
9. Vinay DS, Choi JH, Kim JD, Choi BK, Kwon BS. Role of endogenous 4-1BB in the development of systemic lupus erythematosus. *Immunology*. 2007;122(3):394-400.
10. Wang C, Lin GH, McPherson AJ, Watts TH. Immune regulation by 4-1BB and 4-1BBL: complexities and challenges. *Immunol Rev*. 2009;229(1):192-215.
11. Kim J, Kim W, Kim HJ, et al. Host CD25+CD4+Foxp3+ regulatory T cells primed by anti-CD137 mAbs inhibit graft-versus-host disease. *Biol Blood Marrow Transplant*. 2012;18(1):44-54.
12. Gruda R, Brown ACN, Grabovsky V, et al. Loss of kindlin-3 alters the threshold for NK cell activation in human leukocyte adhesion deficiency-III. *Blood*. 2012;120(19):3915-3924.
13. Zhang X, Voskens CJ, Sallin M, et al. CD137 promotes proliferation and survival of human B cells. *J Immunol*. 2010;184(2):787-795.
14. Pauly S, Broll K, Wittmann M, Giegerich G, Schwarz H. CD137 is expressed by follicular dendritic cells and costimulates B lymphocyte activation in germinal centers. *J Leukoc Biol*. 2002;72(1):35-42.
15. Middendorp S, Xiao Y, Song JY, et al. Mice deficient for CD137 ligand are predisposed to develop germinal center-derived B-cell lymphoma. *Blood*. 2009;114(11):2280-2289.
16. Lee E-A, Kim J-E, Seo JH, et al. 4-1BB (CD137) signals depend upon CD28 signals in alloimmune responses. *Exp Mol Med*. 2006;38(6):606-615.

17. Kim YH, Choi BK, Shin SM, et al. 4-1BB triggering ameliorates experimental autoimmune encephalomyelitis by modulating the balance between Th17 and regulatory T cells. *J Immunol*. 2011;187(3):1120-1128.
18. Palazon A, Teijeira A, Martinez-Forero I, et al. Agonist anti-CD137 mAb act on tumor endothelial cells to enhance recruitment of activated T lymphocytes. *Cancer Res*. 2011;71(3):801-811.
19. Vinay DS, Kwon BS. Immunotherapy of cancer with 4-1BB. *Mol Cancer Ther*. 2012;11(5):1062-1070.
20. Sznol M, Hodi FS, Margolin K, et al. Phase I study of BMS-663513, a fully human anti-CD137 agonist monoclonal antibody, in patients (pts) with advanced cancer (CA) [abstract]. *J Clin Oncol*. 2008;26(suppl 15). Abstract 3007.
21. Segal NH, Gopal AK, Bhatia S, et al. A phase 1 study of PF-05082566 (anti-4-1BB) in patients with advanced cancer [abstract]. *J Clin Oncol*. 2014;32(suppl 15). Abstract 3007.
22. Song DG, Ye Q, Carpenito C, et al. In vivo persistence, tumor localization, and antitumor activity of CAR-engineered T cells is enhanced by costimulatory signaling through CD137 (4-1BB). *Cancer Res*. 2011;71(13):4617-4627.
23. Imai C, Mihara K, Andreansky M, et al. Chimeric receptors with 4-1BB signaling capacity provoke potent cytotoxicity against acute lymphoblastic leukemia. *Leukemia*. 2004;18(4):676-684.
24. Schonfeld K, Sahm C, Zhang C, et al. Selective inhibition of tumor growth by clonal NK cells expressing an ErbB2/HER2-specific chimeric antigen receptor. *Mol Ther*. 2015;23(2):330-338.
25. Schuster SJ, Svoboda J, Chong EA, et al. Chimeric antigen receptor T cells in refractory B-cell lymphomas. *N Engl J Med*. 2017;377(26):2545-2554.
26. Langstein J, Michel J, Fritsche J, Kreutz M, Andreesen R, Schwarz H. CD137 (ILA/4-1BB), a member of the TNF receptor family, induces monocyte activation via bidirectional signaling. *J Immunol*. 1998;160(5):2488-2494.
27. Alosaimi M, Hoenig M, Jaber F, et al. Immunodeficiency and EBV induced lymphoproliferation caused by 4-1BB deficiency. *J Allergy Clin Immunol*. 2019;144(2):574-583.e5.

**CD137 deficiency causes immune dysregulation with predisposition to
lymphomagenesis**

Supplementary Appendix

Table of Contents

Supplementary Patient Clinical Histories

Supplementary Materials and Methods

Supplementary References

Supplementary Tables and Figures

Supplementary Patient Clinical Histories

Patient 1 (All-1, Fig. 1A) was born to consanguineous Turkish parents, presented with Burkitt's lymphoma (Fig. 1B) at 2 years of age. A lobulated mass in the small intestine was observed (Fig. 1B). Subsequent imaging demonstrated renal and hepatic metastases (Fig. 1B, Fig. S1A), and a lesion in the right para-spinal area infiltrating the adjacent para-vertebral muscle (Fig. S1A). The patient was treated according to the NHL BFM 2000 treatment regimen, including cytoreductive prophase treatment with cyclophosphamide, dexamethasone, and intravenous methotrexate (block AA, BB and CC). Rituximab treatment was initiated due to CD20 positivity. A reduction in tumor size was observed and the patient is currently in remission at the age of 3 years. He also suffered from recurrent ear infections, hepatosplenomegaly and hypogammaglobulinemia (Tables 1 and S1). The patient has a 7-year old sibling (All-2, Fig. 1A) without obvious clinical phenotype and no family history of immunodeficiency.

Patient 2 (BII-1, Fig. 1A) was born to consanguineous Palestinian parents. He first presented with recurrent episodes of pneumonia (Fig. S1B) during the first 3 years of life. Bi-lateral ground glass opacities indicative of a chronic lung disease were subsequently demonstrated (Fig. S1C). He displayed autoimmune lymphoproliferative syndrome (ALPS)-like disease manifestations at the age of 6 years. Hepatosplenomegaly (Fig. S1D) and lymphadenopathy (Fig. S1E, S1F, S1G) were noted in physical examination and signs of autoimmunity including autoimmune hemolytic anemia (AIHA) and immune thrombocytopenic purpura (ITP) along with positive anti-nuclear antibodies (ANA) were detected (Tables 1 and S1). An Epstein-Barr virus (EBV)-related lymphoproliferative disorder with a monoclonal T-cell population was demonstrated in lymph node pathology (Fig. S1H) which was EBER positive (Fig. S1I). The patient was treated with sirolimus and glucocorticoids which he responded well to. Cellcept therapy has recently been initiated due to persistence of

autoimmune features (i.e. AIHA, ITP, ANA positivity) upon tapering of glucocorticoid treatment. Co-trimoxazole antibiotic prophylaxis is routinely administered as well. The patient has two siblings (BII-2, Fig. 1A) without overt clinical symptoms and no family history of immunodeficiency.

Patient 3 (CII-2, Fig. 1A), a boy born to consanguineous Turkish parents, manifested with herpes labialis and a lower respiratory tract infection at the age of six years. Hepatosplenomegaly (Fig. S1J) and lymphadenopathy were found during physical examination. Episodes of pneumonia, recurrent tonsillitis, otitis media and chronic suppurative otitis media were noted since the age of eight years (Table 1). Additional features included atopic dermatitis and xerosis. Laboratory evaluation revealed a positive direct Coombs test and hypergammaglobulinemia (Table S1), necessitating IVIG substitution therapy. At ten years of age, the patient was evaluated due to diffuse lymphadenopathy (bilateral cervical, submandibular and axillary nodes). An infectious etiology was ruled out. Submandibular lymph node biopsy exhibited large, prominent, multinucleated Reed-Sternberg cells (Fig. 1B) with EBER-positive lymph node histopathology (Fig. 1C). Immunohistochemistry showed weak CD20 staining and positive CD30 staining. Non-malignant nodular splenic lesions were observed, associated with lymphoproliferation. A diagnosis of Hodgkin lymphoma, stage 1, was established and the patient was treated according to GPOH-HD 95 therapy protocol, including two cycles of chemotherapy with adriamycin, vincristine, etoposide and prednisone. He is currently in remission. He is treated with immunoglobulin substitution and amoxicillin prophylaxis (Table 1). The patient has one sibling who is currently 14 years old (CII-1, Fig. 1A). She experienced recurrent tonsillitis until the age of ten years. Immunoglobulin levels were slightly elevated. Other than that, the patient has no remarkable family history of immunodeficiency.

Patient 4 (DII-2, Fig. 1A), a 33 year old male was born to non-consanguineous Colombian parents, presented with recurrent otitis media and sinusitis since the age of

eight. Between the age of 20-22 years, five episodes of pneumonia were documented. Laboratory workup revealed decreased serum IgG, IgM and IgA (Table S1) and no detectable IgG serum antibodies against rubella. The presumptive diagnosis of CVID was established and IVIG replacement therapy was initiated (Table 1). During the following 3 years, the patient was hospitalized with granulomatous pleuropneumonia, while *H. pylori* erythematous gastritis and chronic sinusitis (Fig. S1K) were noted. The patient has one healthy 32 year old sibling (DII-1, Fig. 1A). She suffered from recurrent infections during childhood. No family history of immunodeficiency is otherwise known.

Supplementary Materials and Methods

Study Subjects

All procedures were performed upon informed consent and assent from patients, first-degree relatives, and healthy donor controls in accordance with the ethical standards of the institutional and/or national research committees and with the current update of the Declaration of Helsinki.

Genetic Analysis

Whole-exome sequencing was performed to determine the underlying genetic defect in *TNFRSF9* in all four patients. Genomic DNA was isolated from whole blood of patients and their first-degree relatives for generation of whole-exome libraries using the SureSelect XT Human All Exon V5+UTR or V6+UTR kit (Agilent Technologies, USA). Barcoded libraries were sequenced on a NextSeq 500 platform (Illumina, USA) with an average coverage depth of 100x. Bioinformatics analysis and subsequent filtering identified rare sequence variants. *TNFRSF9/CD137* mutations were confirmed by Sanger sequencing.

In silico analysis of the exon 2: c.100+1G>A substitution was performed with the bioinformatics tools NetGene2 (<http://www.cbs.dtu.dk/services/NetGene2/>) and

Fruitfly (http://www.fruitfly.org/seq_tools/splice.html). These tools predicted that the mutation affected the donor splice site at the end of exon 2. Moreover, multiple alignments of DNA sequences of *CD137* orthologous from several species show that exon2: c.100 +1G is a highly conserved region. We used the SIFT, PolyPhen-2 and CADD algorithms to assess these *in silico*¹.

Expansion of T cells

Patient or control blood was subjected to a Ficoll density gradient centrifugation, after which peripheral blood mononuclear cells (PBMCs) were collected from the interface. T cells were expanded by stimulation of the PBMCs with irradiated feeder cells (PBMCs from healthy donors), PHA (1µg/ml) and IL-2 (100U/mL) in RPMI medium containing 5% human serum. Cell lines were tested negative for mycoplasma by PCR using VenorGeM Mycoplasma Detection Kit (MP0025, Sigma-Aldrich).

Flow Cytometry

For analysis of cell surface markers, PBMCs were used as starting material or 100 µl of whole blood in EDTA was lysed using RBC Lysis Buffer (eBioscience). Cells were washed twice in FACS buffer (PBS with 5% FBS), and resuspended in 100 µl of FACS buffer with antibodies for 30 min on ice. Cells were washed twice in FACS buffer, resuspended in 300 µl of FACS buffer.

Western Blot

Whole cell lysates were prepared from control- and patient-derived expanded T cells or B-LCLs, loaded on 10% polyacrylamide TRIS-HEPES-SDS gel and separated by SDS-PAGE. Proteins were transferred to polyvinylidene difluoride (PVDF) membrane using iBlot system (Invitrogen). Blots were probed overnight with 1:1000 dilution of specific antibodies, and 1:8000 dilution of anti-HSP90α/β (Santa

Cruz) as a loading control. Bands were revealed using Amersham ECL Select Western Blotting Detection Reagent (GE Healthcare).

T- and B-cell stimulation

PBMCs were labeled with either CellTrace Violet Cell Proliferation dye VPD450 (ThermoFisher) or CFSE 5 μ M (ThermoFischer), washed with PBS with 10% FCS in a ratio of 1:1. Labeled PBMCs were stimulated with anti-CD3-coupled beads (Bio-anti-CD3, OKT3 from eBioscience coupled with anti-Biotin MACSiBeads from Miltenyi Biotec) at a ratio of 10:1 with and without 1 μ g ml⁻¹ soluble anti-CD28 (CD28.2, eBioscience) or anti-CD3 with anti-CD137, 10 μ g/ml (R&D Systems) or CD137L, 20 ng/ml (R&D Systems) and stained for cell surface markers. For blocking experiments of CD137 in T cells, a neutralizing anti-CD137 monoclonal antibody (BBK-2 clone, Invitrogen) was added at increasing concentrations (1-2 μ g/mL) or mouse IgG1, kappa isotype control P3.6.2.8.1 (Invitrogen) to anti-CD3-coupled beads and stained for cell surface markers. For B-cell proliferation assays PBMCs were stimulated with CpG ODN 2006, 50nM (ODN7909, Invivogen), or CD40 ligand 200ng/ml (R&D Systems) in combination with rhIL4 100 ng/ml, rhIL21 20ng/ml (R&D Systems) or anti-IgM 20 μ g/ml (Southern Biotech). For sorting of CD3 T cells and naïve B cells, PBMCs were stained for CD3, CD19, CD27 and IgD: PE-CY7 anti-CD3 (Beckman Coulter), PerCP/Cy5.5 anti-CD19 (HIB19, Biolegend), BV480 anti-IgD (IA6-2, BD), PE anti-CD27 (L128, BD), and afterwards sorted by FACS for CD3⁺, CD19⁺CD27⁻IgD⁺ or CD19⁺CD27⁺ populations, respectively. Sorted PBMCs were then labeled with either CellTrace Violet Cell Proliferation dye VPD450 (ThermoFisher) or CFSE, stimulated as mentioned above, and re-stained for cell surface markers.

Flow cytometry-based CTL cytotoxicity test

Assays to quantify the cytotoxic activity of CTLs were done by stimulating PBMCs with 30Gy irradiated autologous B-LCLs at 5:1 ratio in complete RPMI (Gibco)

with 10ng/mL IL-7 (Peprotech) for 14 days. At day 7, 100U/mL IL-2 (Peprotech) was added. Two rounds of stimulation were performed every 14th day. CD8⁺ T cells were sorted with MagniSort Human CD8⁺ T-cell Enrichment Kit according to manufacturer's instructions. Autologous EBV B-LCLs were stained with VPD450 (ThermoFisher) and used as targets. CD8⁺ T cells were incubated for 4 hours at different ratios of effector and target cells. Cytotoxicity was evaluated by flow cytometry gating on CD19⁺ and VPD450⁺ cells.

Flow cytometry-based CTL and NK-cell degranulation test

NK- and CTL degranulation was assessed by CD107a surface staining without (medium-cultured cells) and 3 hours after stimulation with K562 cells at a ratio of 1:1 as previously described². The erythroleukemic cell line K562 (ATCC, CCL-243) was used as a target cell line. NK cells were cultured in medium containing 600U/ml IL-2 (Novartis) for 48 h to assess degranulation of activated NK cells. CTL (cytotoxic T lymphoblasts) degranulation was evaluated in T-lymphoblasts 48 h after stimulation with 1.25 mg/ml 1- phytohemagglutinin-L (PHA-L, Sigma) and 200U/ml IL-2 (Novartis). CTL degranulation was calculated by the difference in median fluorescence intensity of CD107a of CTLs stimulated with CD3/CD28-coated microbeads (ThermoFisher Scientific) at a ratio of 1:10 for 3 h and medium cultured cells.

Flow cytometry and antibodies

For immunophenotyping the following antibodies were used: BV480 anti-CD45 (clone HI30, BD), APC-Fire 780 anti-CD3 (SK7, Biolegend), BUV395 anti-CD4 (RPAT4, BD), BUV496 anti-CD8 (RPAT8, BD), APC anti-CD45RA (BUV737, BD), BB515 anti-CD45RO (UCHL1, BD), APC anti-CD127 (A019D5, Biolegend), PE anti-CD25 (M-A251, BD), APC R-700 anti-CD27 (M-T271, BD), BB700 anti-CD28 (L293, BD), BV711 anti-HLA-DR (L243, Biolegend), BV421 anti-CCR7 (G043H7, Biolegend), BV786 anti-

CCR6 (11A9, BD), PE-CF594, anti-CXCR3 (1C6, BD), BV650 anti-CD38 (HB-7, Biolegend), BUV395 anti-CD19 (SJ25C1, BD), PE-Cy7 anti-CD20 (2H7, BD), BB515 anti-IgD (IA6-2, BD), BV421 anti-IgM (G20-127, BD), APC anti-CD38 (HB7, BD), BUV737 anti-CD21 (B-Ly4, BD), BV786 anti-CD27 (L128, BD), PE anti-CD10 (HI10a, BD), BUV496 anti-CD3 (UCHT-1, BD), BUV737 anti-CD8 (SK1, BD), PE-CF594 anti-CD56 (NCAM16.2, BD), BB515 anti-CD57 (NK-1, BD), BB700 anti-CD15 (M5E2, BD), APC anti-CD16 (3G8, Biolegend), HLA-DR anti-BV711 (L243, Biolegend), BV785 anti-CD123 (6H6, BD), BV421 anti-CD11c (B-ly6, Biolegend), PE anti TCR g-d (5A6.E9, Life Tech), APC-R700 anti-TCR a-b, (IP26, Biolegend), PE-Cy7 anti-CD33 (P67.6, BD), and BV711 anti-CXCR5 (J2252D4, Biolegend).

CD137 and CD137L expression in T cells was measured upon 48 hour stimulation of PBMCs with anti-CD3 and anti-CD28. Cells were stained with PacB anti-CD3 (clone SK7, biolegend), BV711 anti-CD4 (SK3, BD), APC-Fire 750 anti-CD8 (RPA-T8, Biolegend), PE anti-CD25 (M-A251, BD), APC anti-CD137 (4B4-1, BD) or APC anti-CD137L (5F4, Biolegend). Expression in B cells was measured upon 24 hour stimulation of PBMCs with anti-IgM in combination with CD40L (RnD). PBMCs were stained with PacB anti-CD3 (clone SK7, Biolegend), PerCP/Cy5.5 anti-CD19 (HIB19, Biolegend), BV421 anti-CD86 (FUN-1, BD), CD25 (M-A251, BD), APC anti-CD137 (4B4-1, BD). Expression in activated NK cells was measured upon 48 hours stimulation of PBMCs with IL-2 600U/ml (Novartis). PBMCs were stained with FITC anti-CD56 (NCAM16.2, BD), PacB anti-CD3 (SK7, Biolegend), APC anti-CD137 (4B4-1, BD).

Proliferative responses were measured by labeling PBMCs with 2.5 mM carboxyfluorescein diacetate succinimidyl ester (CFSE, ThermoFisher), 7-aminoactinomycin D (7-AAD, 2.5 mg/ml, BD), PacB-anti-CD3 (clone SK7, biolegend), PE-anti-CD25 (M-A251, BD), APC-Fire 750 anti-CD8 (RPA-T8, Biolegend)) and BV711 anti-CD4 (SK3, BD) 4 days after stimulation. Class-switch recombination and plasmablast numbers were measured 4 days after stimulation. PBMCs were stained with BUV395 anti-CD3 (clone SK7, BD), PerCP/Cy5.5 anti-CD19 (HIB19, Biolegend),

BV421 anti-IgD (IA6-2, BD), PE anti-CD27 (L128, BD), BUV661 anti-CD38 (HIT2, BD). Degranulation of NK cells and CTLs (cytotoxic T lymphocytes) was determined by surface staining with PacB-anti-CD3 (clone SK7, 1:100), APC-H7-anti-CD8 (SK1, 1:100), PE-Dazz-anti-CD56 (NCAM16.2, BD), FITC anti-CD56 (NCAM16.2, BD), and PE-anti-CD107a (H4A3, 1:50). T-cell signaling was performed in T cell blasts. PBMCs were stimulated with 5 ng/ml phorbol 12-myristate 13-acetate (PMA) and 1 μ M ionomycin (Sigma-Aldrich) and expanded with IL-2 (100U/ml) for 9 days. T-lymphoblasts were stimulated by cross-linking of anti-CD3 (UCHT1) 2.5 μ g/ml and/or 10 μ g/ml anti-CD28 (CD28.2) with 10 μ g/ml goat anti-mouse IgG all from BD for the indicated time. Cells were fixed and permeabilized with fixation and permeabilization kit from Molecular Probes in 90% methanol. The permeabilized cells were stained with the following intracellular antibodies detecting: ERK1/2 phosphorylated at T202 and Y204 (A647 anti-pERK1/2, BD), NF κ B P65 phosphorylated at S529 (A647 anti-NF κ B P65, BD), AKT phosphorylated at S473 (A488 anti-pAKT, (M85-61, BD)), isotype control (A488 mouse IgG κ 1 isotype control, BD).

TCR Repertoire and Analysis

Cell surface marker expression of peripheral blood mononuclear cells (PBMCs) was analyzed by immunofluorescent staining with monoclonal antibodies and flow cytometry (Epics V; Coulter Electronics, Hialeah, FL). Signal joint T-cell receptor excision circles (sjTREC) copy numbers were determined by employing quantitative real-time PCR (qRT-PCR) of genomic DNA (gDNA, 0.5 μ g) extracted from whole blood of our patients. Surface expression of individual T cell receptor V β (TCR-V β) gene families was assessed using a set of 24 V β -specific fluorochrome-labeled monoclonal antibodies (Beckman Coulter, USA) and flow cytometry. Next-generation sequencing (NGS) T-cell receptor (TCR) libraries were generated from gDNA of patients and controls using primers for conserved regions of V and J genes in the *TRG* (T-cell receptor gamma) locus according to the manufacturer's protocol (Lymphotrack,

Invivoscribe Technologies, Carlsbad, CA). Quantified libraries were pooled and sequenced using Mi-Seq Illumina technology (Illumina, USA). FASTA files from the filtered sequences were submitted to the IMGT HighV-QUEST webserver (<http://www.imgt.org>), filtered for productive sequences (no stop codons or frameshifts), and analyzed. Repertoire diversity was calculated using Shannon's H diversity index and Simpson's D index of unevenness.

Shannon's H index: $H' = -\sum_{i=1}^R p_i \ln p_i$

Simpson's D index of unevenness: $\lambda = \sum_{i=1} p_i^2$

Retroviral Construction and Transfection Protocol

N-terminally tagged CD137 was generated using retroviral pfMIG 3981 (IRES-GFP) vector. For the reconstitution experiments constructs with either wild-type CD137 or empty vector (GFP only) were used. Before electroporation of the Patient 3 and healthy donor PBMCs, retroviral vector was digested with Xba I enzyme to generate 3 kb DNA fragment containing CD137-IRES-GFP gene sequences. Digested DNA was purified using QIAquick PCR purification kit (Qiagen) according to manufacturer instructions. Patient 3 and healthy donor PBMCs were electroporated with 2 μ g of the digested DNA mixture using Amaxa Human T cell Nucleofector Kit (Lonza), program V-024, according to manufacturer instructions. Transfection efficiency was assessed by GFP expression 24 hours after electroporation.

Statistical Analysis

Statistical evaluation of experimental data was performed using Prism version 6 (GraphPad Software, USA). Probability (*P*) values < 0.05 were considered statistically

significant. *P* values and statistical tests are indicated in figure legends, where applicable.

Supplementary References

1. Adzhubei I, Jordan DM, Sunyaev SR. Predicting Functional Effect of Human Missense Mutations Using PolyPhen-2. *Current protocols in human genetics / editorial board, Jonathan L Haines [et al]*. 2013 Jan;0 7:Unit7 20.
2. Bryceson YT, Pende D, Maul-Pavicic A, Gilmour KC, Ufheil H, Vraetz T, et al. A prospective evaluation of degranulation assays in the rapid diagnosis of familial hemophagocytic syndromes. *Blood*. 2012 Mar 22;119(12):2754-63.

Table S1. Clinical and genetic manifestations of CD137-deficient patients

Patients	P1	P2	P3	P4	*Pa	*Pb
Mutation	c.1_545+1716del	NM_001561.5: c.452C>T; p.Thr151Met	NM_001561.5: c.101 -1G>A	NM_001561.5: c.100 +1G>A	NM_001561.5: c.325G>A p.Gly109Ser	NM_001561.5: c.325G>A p.Gly109Ser
Initial clinical manifestation	abdominal distention	recurrent respiratory infections	lower respiratory tract infection	recurrent infections from childhood	sinopulmonary infections, bronchiectasis, pneumococcal septicemia	recurrent sinopulmonary infections, generalized lymphadenopathy, EBV viremia
Age of initial Clinical manifestation	2 years	4 years	6 years	8 years	3 years	6 years
Consanguinity	parents are 1st degree cousins	parents are 1st degree cousins	parents are 3rd degree cousins	no known consanguinity	parents are 1st degree cousins	parents are 1st degree cousins
Infectious complications during disease course	recurrent ear infections EBV viremia	recurrent pneumonia EBV viremia	recurrent labial herpes, recurrent tonsillitis, recurrent otitis media, recurrent pneumonia EBV viremia	recurrent ear infections, recurrent pneumonia, pleuropneumonia, chronic sinusitis EBV viremia	pneumococcal septicemia sinopulmonary infections EBV viremia	sinopulmonary infections EBV viremia
Identified Pathogens	CMV, EBV	<i>adenovirus</i> , EBV, HSV	EBV, HSV	EBV	<i>streptococcus pneumoniae</i> , EBV	EBV
Hepatosplenomegaly	+	+	+	+	splenomegaly	splenomegaly
Lymphadenopathy	-	+	+	-	+	+
Malignancy	CD20 positive Burkitt lymphoma	-	EBV-positive Hodgkin's lymphoma	-	-	EBV-positive Hodgkin's lymphoma, relapse and progression to DLBCL

Treatment of B-cell malignancies	cytoreductive prophase treatment: cyclophosphamide, dexamethasone, methotrexate (AA, BB, CC blocks), rituximab	NA	etoposide, doxorubicin, vincristine	NA	NA	5 cycles: doxorubicin, bleomycin, vincristine, etoposide, prednisone, cyclophosphamide along with rituximab; upon relapse daratumumab, bortezomib, dexamethasone and rituximab
AIHA	-	+	+	-	-	-
ITP	-	+	-	-	-	-
Other features	-	ALPS like symptoms, EBV associated lymphoproliferation	short stature	distal peptic esophagitis, erythematous gastritis	hemophagocytic lymphohistiocytosis	-
Treatment of immunodeficiency/Infections	IVIG, co-trimoxazole, fluconazole	sirolimus, cellcept, co-trimoxazole	IVIG, antibiotic prophylaxis	SCIg	IVIG, rituximab	IVIG
Outcome	responded well to chemotherapy treatment protocol and rituximab, currently stable under IVIG and antibiotic prophylaxis	well on cellcept treatment and co-trimoxazole antibiotic prophylaxis	good response to chemotherapy with clinical remission. Currently stable under IVIG and antibiotic prophylaxis	stable under SCIg replacement treatment with resolution of infections	sinopulmonary infections improved upon IVIg treatment, resolution of viremia with rituximab. Currently undergoing HSCT from a healthy HLA-matched sibling	clinical remission and resolution of viremia with chemotherapy and rituximab treatment. Respiratory tract infections improved with IVIg treatment

CMV: Cytomegalovirus. EBV: Epstein-Barr virus. HSV: Herpes simplex virus. NA: Not applicable. AIHA: Autoimmune hemolytic anemia. ITP: Immune thrombocytopenic purpura.

ALPS: Autoimmune lymphoproliferative syndrome. IVIG: Intravenous immunoglobulin. SCIg: Subcutaneous immunoglobulin. HSCT: hematopoietic stem cell transplantation.

DLBCL: diffuse large B cell lymphoma.

*Pa, Pb reported by Alosaimi et al. *J Allergy Clin Immunol*, 2019.

Table S2. Immunologic characteristics of patients with CD137 deficiency

Variable	Patient 1		Patient 2		Patient 3		Patient 4	
	Value	Reference Range						
Age of evaluation	4 years		9 years		11 years		33 years	
Absolute lymphocyte count (cells/mm ³)	3390	2340-5028	3597	1300-5000	1590	1300-3000	2680	1200-4100
<i>Lymphocyte subset</i>								
CD3+ (cells/mm ³)	1551	1239-2611	2950	700-4200	1272	1000-2000	1860	780-3000
CD4+ (cells/mm ³)	1074	870-2144	1295	600-2100	858	500-1300	965	100-2300
CD45RO+ CCR7+ (%)	7.5	13.88-48.12	14.6	22.06-46.46	45.5	24.24-52.73	11.5	18-95
CD45RO+ CCR7- (%)	78.7	0.94-6.46	59.3	2.08-8.78	26.5	3.4-11.17	55.8	1-23
CD45RO- CCR7+ (%)	11.6	46.14-84.4	22	45.56-75.28	24.5	39.72-69.59	27	16-100
CD45RO- CCR7- (%)	1.1	0-1.36	0.1	0-1.06	2.43	0.1-1.29	5.7	0-6.8
CD8+ (cells/mm ³)	407	472-1107	1439	200-1100	333	300-800	772	200-1200
CD45RO+ CCR7+ (%)	0.9	5.18-31.66	3.4	12.08-30.54	4.9	13.21-37.89	7.3	1-20
CD45RO+ CCR7- (%)	62.4	0.7-11.22	43.3	1.58-13.18	15.2	1.53-15.39	29.3	14-98
CD45RO- CCR7+ (%)	3.8	36.8-83.16	34.8	41.58-77.9	77.1	41.41-73.04	23.7	41.41-73.04
CD45RO- CCR7- (%)	29.7	0.84-33.02	15.3	1.7-24.62	2.79	2.01-21.65	36.2	2.01-21.65
CD3-CD16+CD56+ (cells/mm ³)	176	155-565	54	120-483	76	100-700	417	90-600
CD19+ (cells/mm ³)	846	434-1274	360	50-300	238	200-500	278	100-500
IgD+ CD27- (%)	93	73-89	94.6	67.8-89	93.7	67.8-89	95.5	58-72.1
IgD+ CD27+ (%)	2.2	5.7-14.3	2.1	5-16.2	1.83	5-16.2	1.9	13.4-21.4
IgD- CD27+ (%)	1.2	3-10.3	0.9	4-14	0.79	4-14	1.8	9.2-18.9
CD27+ CD38+ (%)	0.76	0.5-7.06	0.70	0.9-7.36	0.37	0.7-5.67	0.61	0.9-7.36

<i>Immunoglobulins</i>								
IgG (mg/dL)	413	701-1157	1599	540-1550	2290	824-1300	550	968-2514
IgM (mg/dL)	105	42-80	714	40-240	267	44-142	33.6	103-397
IgA (mg/dL)	68.7	34-108	49	52-274	130	71-161	31	103-397
IgE (IU/mL)	26.4	2-199	0	0-200	7.77	<100	173	116-551
<i>Complement</i>								
C3(mg/dL)	N/A		68.9	90-180	105	90-180	N/A	
C4(mg/dL)	N/A		72.4	10-40	9.3	10-40	N/A	
<i>T-cell repertoire</i>								
αβ+ (%)	94		79		83		95.3	
γδ+ (%)	2	4.94-17.98	2	6.92-19.84	1.1	8.1-20.76	3.5	
TRECs	N/A		800	>400	N/A		N/A	
<i>Auto-immune workup</i>								
Positive auto-antibodies			ANA positive (1:180)		d. Coombs positive			
<i>EBV/CMV status</i>								
EBV DNA Viral Load (PCR)	652 copies/ml		7.1 X10⁵ copies/ml		9.1 X10⁴ IU/ml		610 Geq/ml	
CMV DNA Viral Load (PCR)	82 copies/ml		negative		NA		negative	
EBV Serology	NA		EBNA-1 (IgG): positive		*EBNA-1 (IgG): positive *VCA (IgM): negative *VCA (IgG): positive		NA	

CMV Serology	NA	anti-CMV (IgG): negative	*anti-CMV (IgM): 2.44 (>1.1 U/ml) *anti-CMV (IgG): positive avidity = 0.837 positive	NA
Common vaccine serologies				
Rubella Serology	&anti-rubella (IgG): 101.3 IU/ml (positive)	MMRV serology (IgG): positive	anti-rubella (IgG): 59.3 IU/ml (positive)	*anti-rubella (IgG): 0.94 uL/mL (negative) Sister: anti-rubella (IgG): 15.2 uL/mL (positive)
Varicella Serology	&anti-VZV (IgG): 1141 IU/ml (positive)		NA	NA
Hepatitis Serology	&anti-HBs (IgG): 201.4 uL/ml (positive)	anti-HAV (IgG): positive anti-HBs (IgG): negative	NA	NA
Tetanus Serology	&anti-tetanus (IgG): 2.8 U/ml (positive)	NA	anti-tetanus (IgG): 2.8 U/ml (positive)	NA

Listed are reference ranges or laboratory values for the patient's age group. Abnormal values in **bold**.

CMV Cytomegalovirus; EBNA Epstein Barr Nuclear Antigen; EBV Epstein Barr Virus; HAV Hepatitis A virus; HBV Hepatitis B virus; MMRV Measles, Mumps, Rubella, Varicella; NA Not Applicable; VCA Viral-Capsid Antigen; VZV Varicella Zoster Virus.

*Prior to IVIg / SCIg replacement therapy; &On IVIg replacement therapy

Table S3. Summary of homozygous autosomal recessive mutations in patients

Patient	Gene	Chromosome	Position	Reference	Variant in patient	Mutation type	Protein variant in patient
1	<i>ZXDB</i>	X	57620724	T	A	MISSENSE	p.Val748Asp
1	<i>TNFRSF9</i>	1	7995072-8000054	NA	NA	DELETION	NA
1	<i>PARK7</i>	1	8022845-8031023	NA	NA	DELETION	NA
2	<i>XIST</i>	X	73048904	A	G	SPLICE REGION	NA
2	<i>AFF2</i>	X	148048444	C	T	MISSENSE	p.Thr1013Met
2	<i>TNFRSF9</i>	1	7995165	C	T	MISSENSE	p.Thr151Met
2	<i>METTL18</i>	1	169763046	C	A	SPLICE REGION	NA
2	<i>GPC1</i>	2	241375361	GGCT	G	DELETION	p.Leu11del
2	<i>DNAH5</i>	5	13794053	G	A	MISSENSE	p.Gly2668Arg
2	<i>CD36</i>	7	80293747	A	G	MISSENSE	p.Tyr212Cys
3	<i>ASB12</i>	X	63445095	C	G	MISSENSE	p.Ala146Pro
3	<i>TNFRSF9</i>	1	7998889	C	T	SPLICE SITE ACCEPTOR	NA
3	<i>HS6ST1</i>	2	129075797	A	C	MISSENSE	p.Val114Gly
3	<i>IRX4</i>	5	1880839	C	T	MISSENSE	p.Arg136Lys
3	<i>ZNF808</i>	19	53058034	C	T	MISSENSE	p.Pro622Leu
4	<i>TNFRSF9</i>	1	799954	G	A	SPLICE SITE DONOR	NA

Inclusion criteria:

CADD more than 15

SIFT deleterious

Polyphen probably_damaging

Table S4. Predicted impact scores of *CD137* variants

Patient	Mutation	Chromosome	Position	PolyPhenCat	SIFTcat	CADD
1	c.1_545+1716del	1	7995072-8000054	NA	NA	NA
2	c.452C>T	1	7995165	Probably_damaging	Deleterious	24.9
3	c.101 -1G>A	1	7998889	NA	NA	27
4	c.100 +1G>A	1	799954	NA	NA	25

Supplementary Figures legends

Figure S1. Clinical features, radiology, pathology, T cell clonality. (A) Coronal T2-HASTE image (Patient 1) demonstrating multiple hypointense metastatic renal cortical masses (black arrows). A mass lesion is observed on the right paraspinal area infiltrating the adjacent paravertebral muscle (red arrow). (B) Chest CT scan demonstrating consolidation in the anterior aspect of the right middle lobe (RML), nodular opacity in the lingula and posterior mediastinal adenopathy (Patient 2). (C) Coronal reconstructions of a follow-up CT four months later demonstrating ground glass opacities in both lungs (Patient 2). (D) Splenomegaly (Patient 2) shown in coronal reconstruction of CT scan. (E) CT scan of the upper neck showing cervical lymphadenopathy (Patient 2). (F) Contrast enhanced computerized tomography (CT) demonstrating mediastinal and axillary lymphadenopathy (Patient 2). (G) Coronal reconstruction of Positron Emission Tomography showing increased uptake in the cervical, axillary and mediastinal lymph nodes. An infiltrate in the right middle lobe (RML) is demonstrated. (H) TCR-gamma spectratyping of lymph node biopsy (Patient 2) revealing two dominant peaks, supporting the presence of a monoclonal T-cell population. (I) In situ hybridization for EBV-encoded small RNAs (EBER) displaying numerous positive cells (Patient 2). Sections used are from right inguinal lymph node tissue. (J) Abdominal CT scan (Patient 3) demonstrating hepatomegaly. (K) MR demonstrating chronic sinusitis in Patient 4 with obstruction in Lt. sinus.

Figure S2. Genetic analysis. Sanger sequencing chromatograms confirming the WES findings in Family B, Family C and Family D. For Family A, WES reads in Patient 1 are compared to a healthy control showing no NGS coverage for several exons of *TNFRSF9* and *PARK7*.

Figure S3. *TNFRSF9* sequence homology in species. *TNFRSF9* sequence alignment showing the conservation of amino acid threonine at position 151 across eight species (red frame). The variant in Patient 2 (p.Thr151Met) is stated.

Figure S4. Effect of variants in the patients. (A) (upper left) Amplified gDNA utilizing forward and reverse primers to amplify exon 6 in *TNFRSF9* for Family A and controls, depicting the genomic deletion in patient 1 (AII-1) and brother (AII-2). Full length cDNA of Patient 3 (CII-2) (upper middle panel) and Patient 4 and sister (DII-1) (upper right panel) were amplified and loaded on agarose gels, depicting smaller sized bands. * and ** in middle panel depicts two aberrantly spliced transcripts. (B) Schematic illustration showing the consequences for the splice site variants in Patient 3 and Patient 4. cDNA sequencing results revealed a skipping of exon 2 in Patient 4, and a skipping of exons 3 and 6 for Patient 3. (C) Chromatograms of Sanger sequencing of the PCR product marked * and ** in figure A showing skipping of exon 3 and exons 3 and 6 in P3.

Figure S5. CD137 expressions. Flow-cytometric expression of CD137 in unstimulated and anti-CD3/CD28 stimulated T-cells for patients, siblings and healthy donors (HDs) are shown.

Figure S6. (A) Peripheral blood B-cell immunophenotyping: Memory (CD19⁺CD20⁺CD27⁺), class-switched (CD19⁺CD20⁺CD27⁺IgD⁻) and transitional B-cell (CD19⁺CD38⁺IgM⁺) frequencies are compared in patients and siblings, measured by flow-cytometry. (B) Peripheral blood T-cell immunophenotyping: Follicular helper T-cell (T_{FH}) frequencies are shown in patients and siblings, measured by flow-cytometry.

Figure S7. CD137 and CD137L inhibition in T-cell function. (A) Effect of CD137 blockade on proliferation of T-cells in healthy donors (HDs). Anti-CD137 monoclonal neutralizing antibody (BBK-2 clone) or isotype control was added to anti-CD3 stimulation at increasing concentrations showing a dose dependent inhibition of T-cell proliferation (as

measured by VPD450 dilution). Error bars indicate \pm SEM. (B) T-cell activation (CD25 expression): Flow-cytometric expression of CD25⁺ is depicted in patients and HDs upon 96 hour stimulation with anti-CD3, anti-CD3+CD137L and anti-CD3+CD28. (C) Restoration of T-cell activation upon CD137 expression. CD137 expression, CD25 T-cell activation and rate of proliferated T cells (stimulated with anti-CD3) upon exogenous expression of wild-type CD137 are shown in Patient 3. (D) *TNFSF9* mRNA expression (top panel) and CD137L surface expression (bottom panel) was measured in unstimulated and anti-CD3+anti-CD28 stimulated T-cells. *HPRT* was used as a control.

Figure S8. Cytotoxicity, degranulation and T cell receptor mediated signaling. (A) EBV-specific CTL cytotoxicity measured by the percentage of specific lysis of autologous EBV B-LCL target cells by their respective CD8⁺ T-cells at different effector to target ratios. Patient CTL cytotoxicity showed significant reduction compared to HDs (* *P* value<0.05, Two-way ANOVA). (B) CTL degranulation (CD107a) was measured in stimulated CD8⁺ T-cells by flow cytometry. (C) NK-cell degranulation in patients and HDs is compared in unstimulated and stimulated PBMCs, measured by flow-cytometry. (D) Immunoblotting showing expression of I κ B α , phospho-p65, total p65, phospho-AKT and total AKT upon anti-CD3+CD28 stimulation in expanded T cells. HSP90 was used as a loading control. Intracellular phospho-AKT and NF- κ B1 phospho-p65 levels in unstimulated and stimulated T-cell blasts, measured by flow cytometry. (E) MAPK signaling is shown measured by immunoblotting. Immunoblotting expression of total ERK1/2 and phospho-ERK1/2 upon anti-CD3+CD28 stimulation in expanded T-cells. HSP90 was used as a loading control. Intracellular phospho-ERK levels in unstimulated and stimulated peripheral CD4⁺ and CD8⁺ T-cells is depicted, measured by flow cytometry.

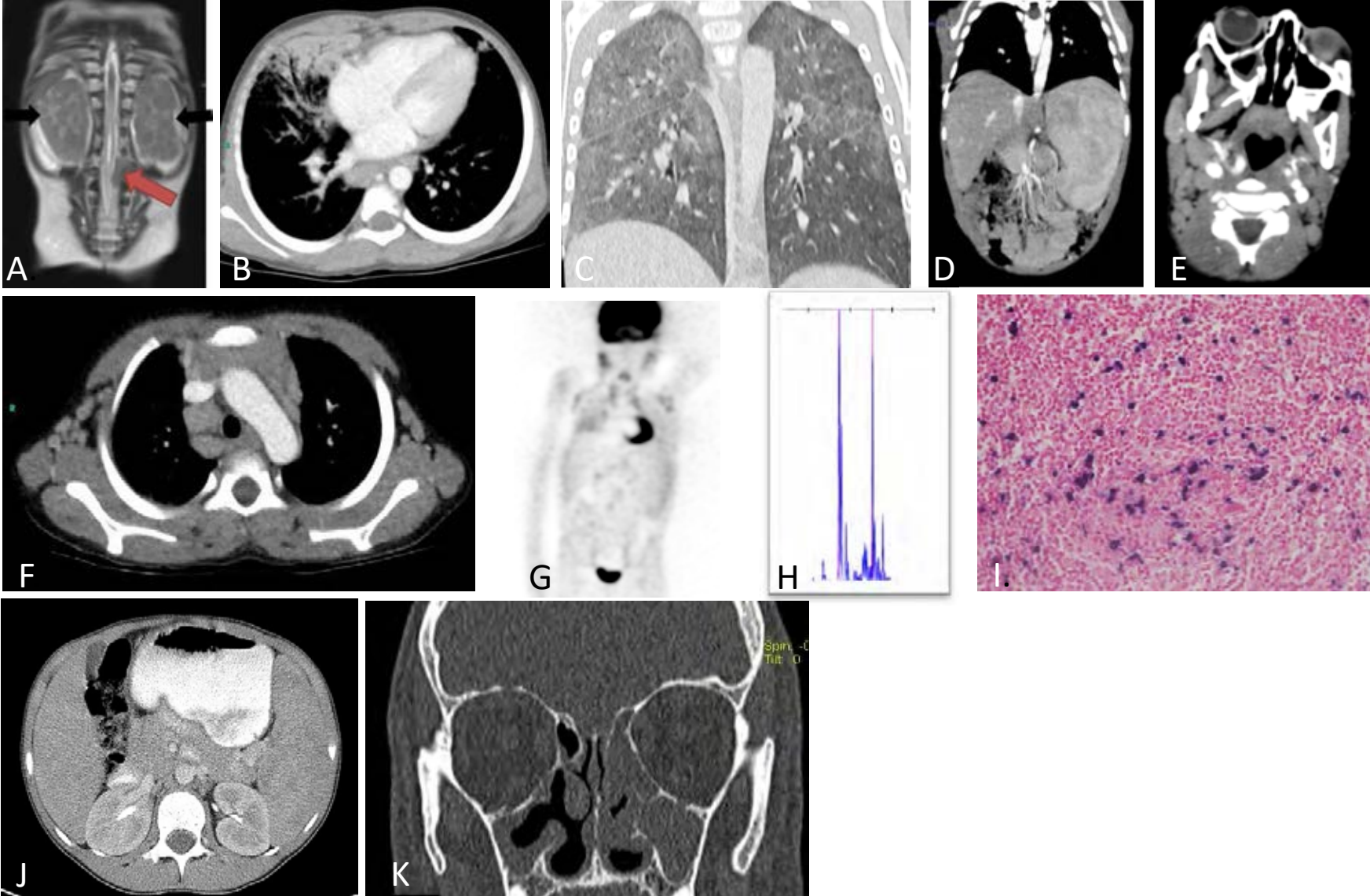
Figure S9. *In vitro* plasmablast differentiation. (A) Plasmablast (CD3⁻CD19⁺CD27⁺CD38⁺) frequencies are shown in unstimulated PBMCs and upon 96 hour stimulation with CpG,

CD40L+IL4 and CD40L+IL21, showing a significant difference between HDs and Patients. (* P value<0.05, ** P value<0.01, **** P value<0.0001, Two-way ANOVA). (B) CD137L expression in CD19⁺ B-cells upon CpG stimulation measured by flow cytometry, showing expression of CD137L in both HD and Patient 3 stimulated cells.

Figure S10. Naïve B-cell function. Naïve B-cells (CD19⁺CD3⁻IgD⁺CD27⁻) were sorted and B-cell functions were assessed in our patients. (A) CD86⁺ B-cell activation was measured 1 day post-stimulation with CpG, showing reduced B-cell activation in P3 and P4. (B) naïve B-cell proliferation measured by violet proliferation dye (VPD450) 5 days post-stimulation showing reduced rate of proliferating B-cells in P3 and P4 in response to T-cell dependent (CD40L + IL21) and independent (CpG) stimuli. (C) Class switch recombination in sorted naïve B-cells. Gating of class switched IgG⁺ and IgA⁺ of sorted naïve B-cells upon CD40L + IL21 and CpG stimuli, depicted reduced CSR in P3 and P4. (D) Reduced memory B cells rates in P2 and P4 upon CpG stimulation of sorted naïve B-cells.

Supplementary Figure 1

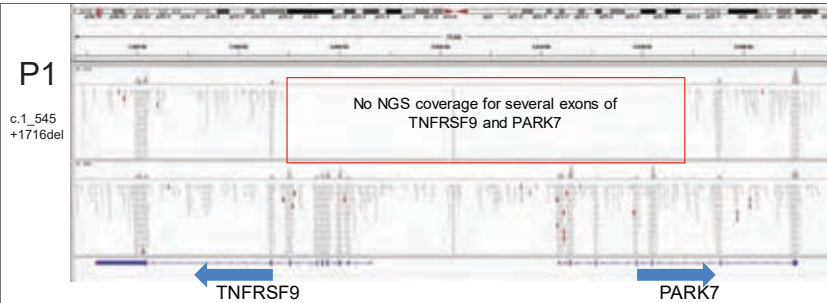
Clinical Features, radiology, pathology, T-cell clonality



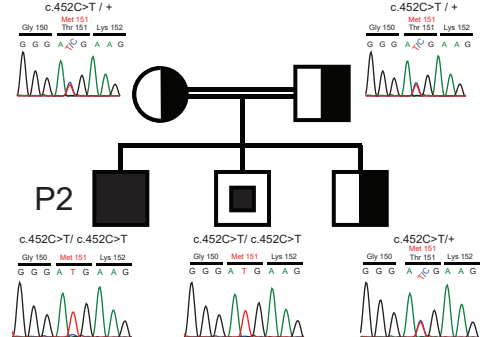
Supplementary Figure 2

Genetic analysis

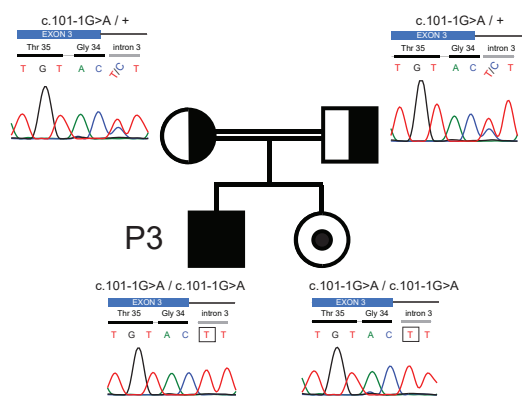
Family A



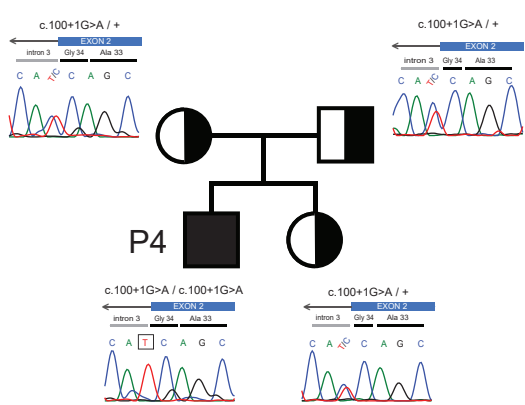
Family B



Family C



Family D



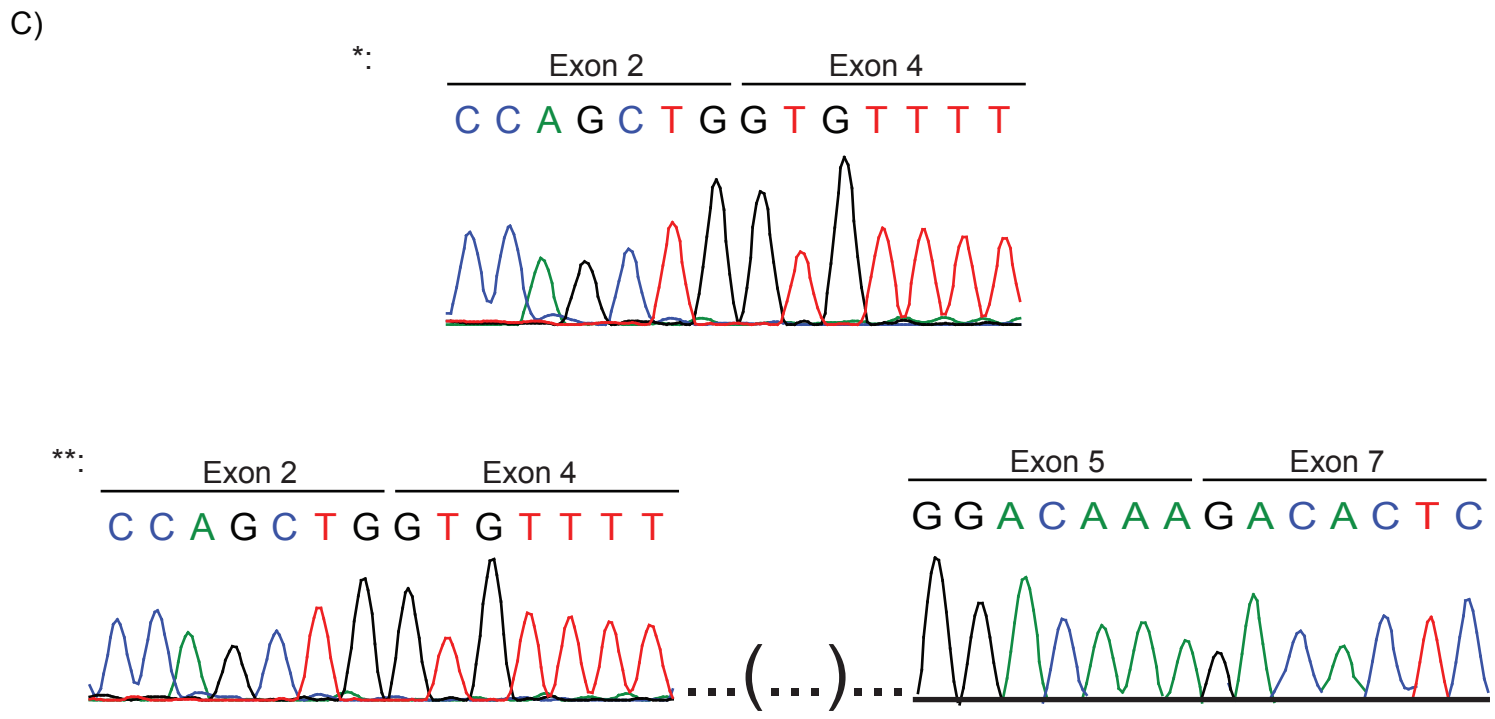
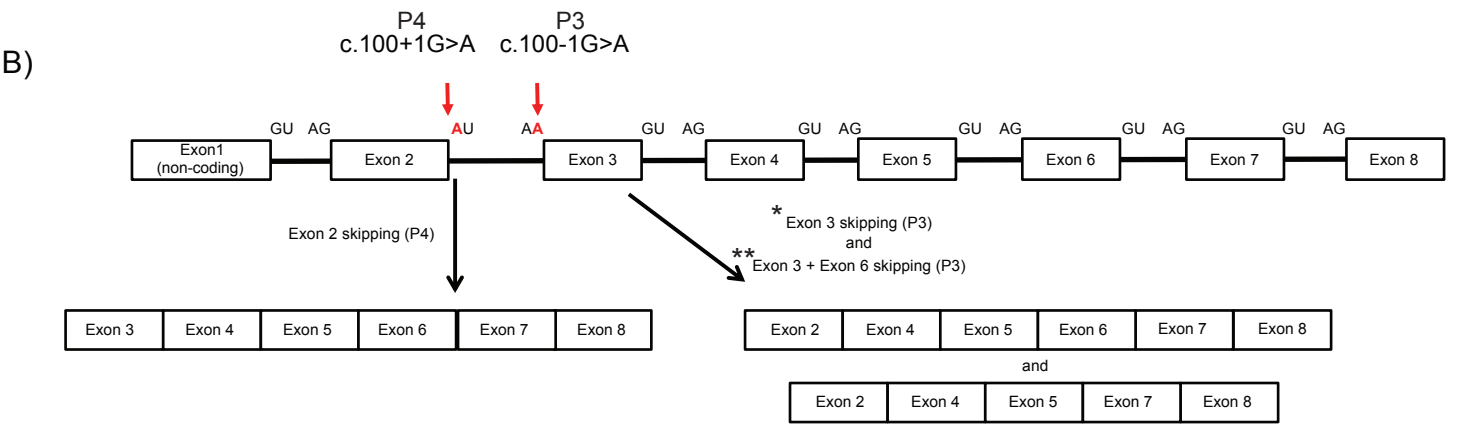
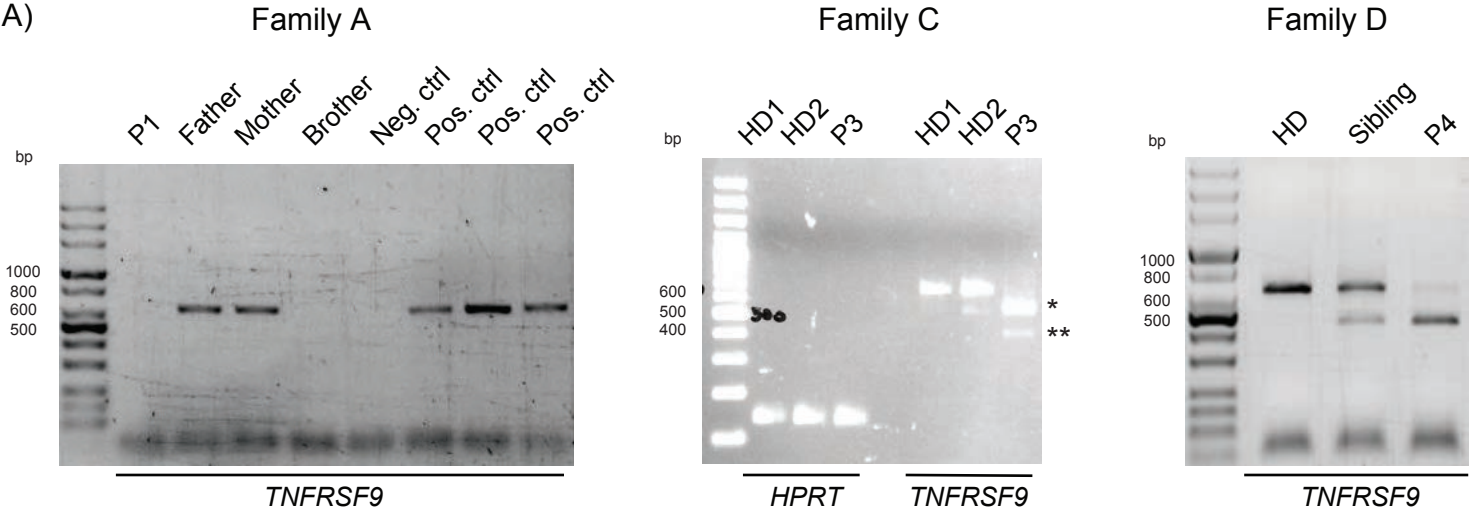
Supplementary Figure 3

TNFRSF9 sequence homology in species

p.Thr151Met

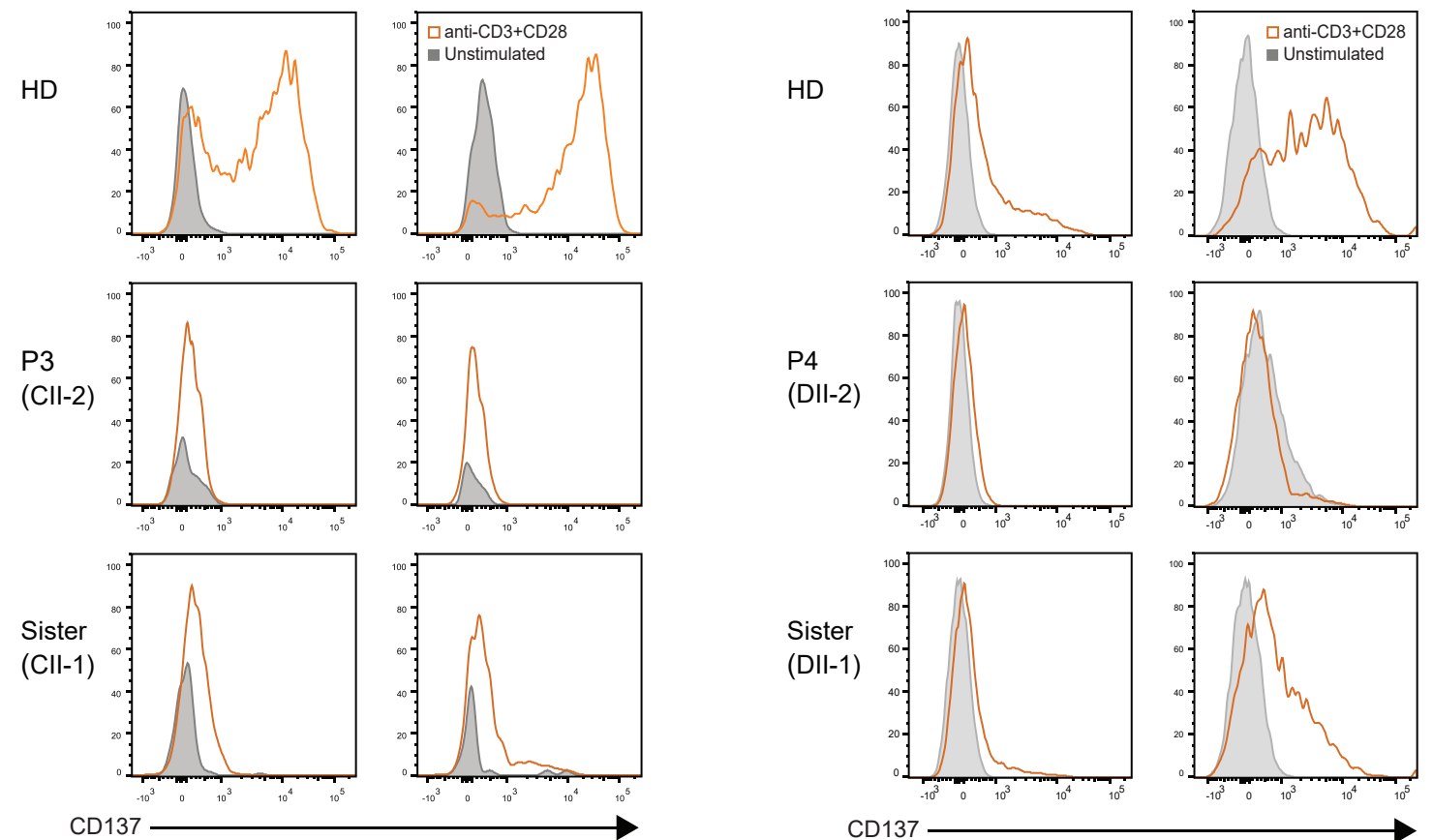
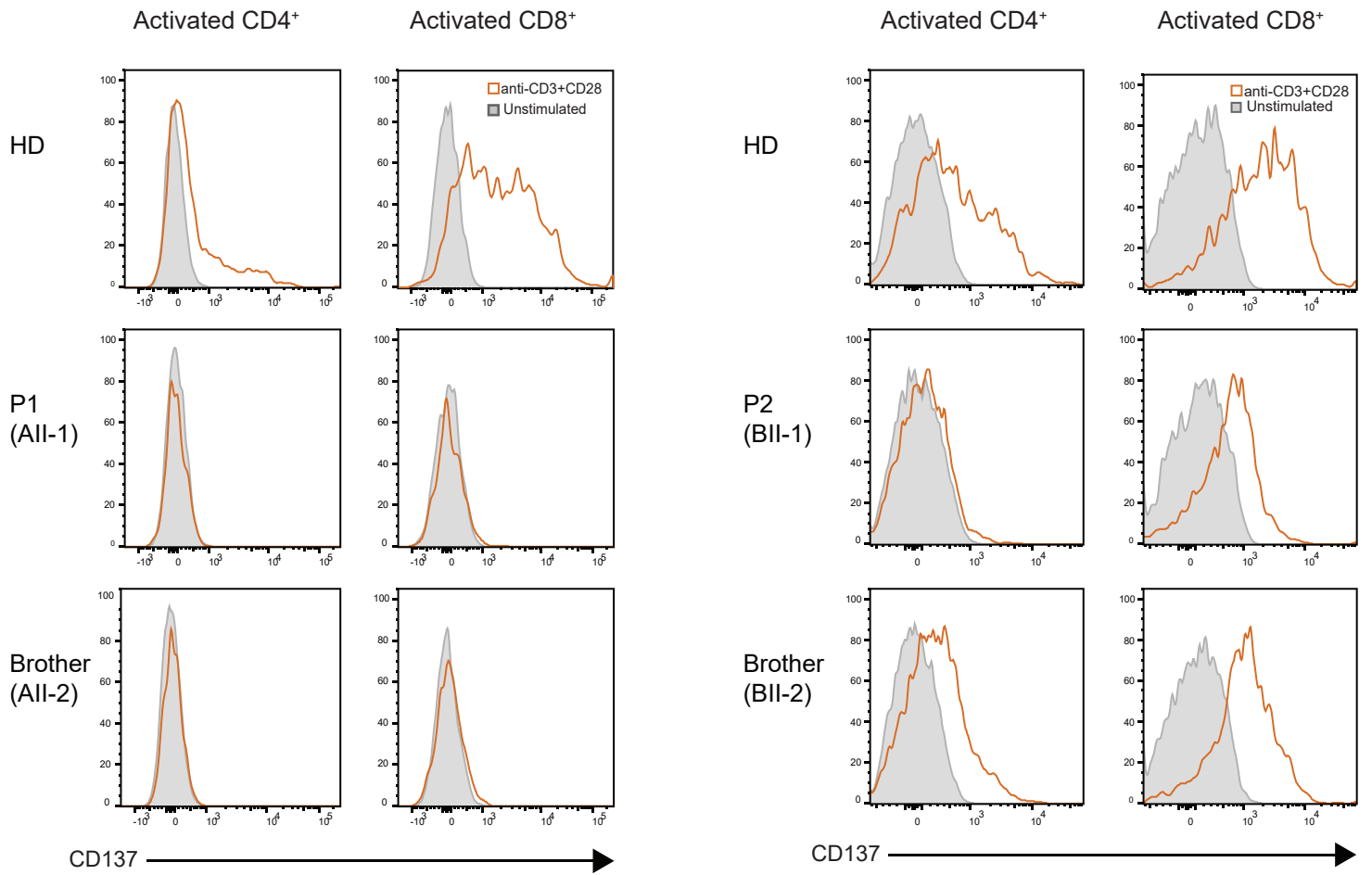
hs (human)	LTKK GCKDC CFGTENDQK-RGIC RPWT NCSLDGKSVLVNGT KERD VVCGPSPAD---LSPGAS-SVT--- 173
mm (mouse)	LTKQ GCKTCS LGTFENDQNGTGVCR PWT NCSLDGRSVLKTGT TEK DVVC GPPVVS---FSPSTT-ISV--- 173
bt (cattle)	LTNEGCKDC SF GTENDQE-HGIC RPWT DCSLNGKAVLVNGT KESD VVCGPPSSD---FSPGAS-STI--- 172
gg (chicken)	KTGSGC QACRY GTENDQP-DG SCR NWTVCS--ENQVLEPGTAT KDV VCKPSSDN---PTLATT-LPT--- 171
tg (zebra finch)	RTRNGC QACRY GTENDQP-NG SCR NWTMCS--GNQVLEPGT PA RDVICKDASVN---FTSVTT-IPT--- 182
am (alligator)	LIGTG CETCP WGTENNQS-DG FCK RWTKCS--GDEV LKQ GTSTSDVICSHMSG S ---LAPPAS---T--- 171
xl (clawed frog)	IREQ KCTDC PSGTEKPGG-ES KCR PWKICPI-GVKV VL NGT RTS DVICGDAVSHTTEPT-STTSNRVTQR 189
dr (zebra fish)	PKGRV CGQC PE GKES DKI-H STC REWTK SS CPDGYKL KK GNLTS D STCIPPP-----SSS-VRT--- 184

Supplementary Figure 4
Effects of variants in the patients



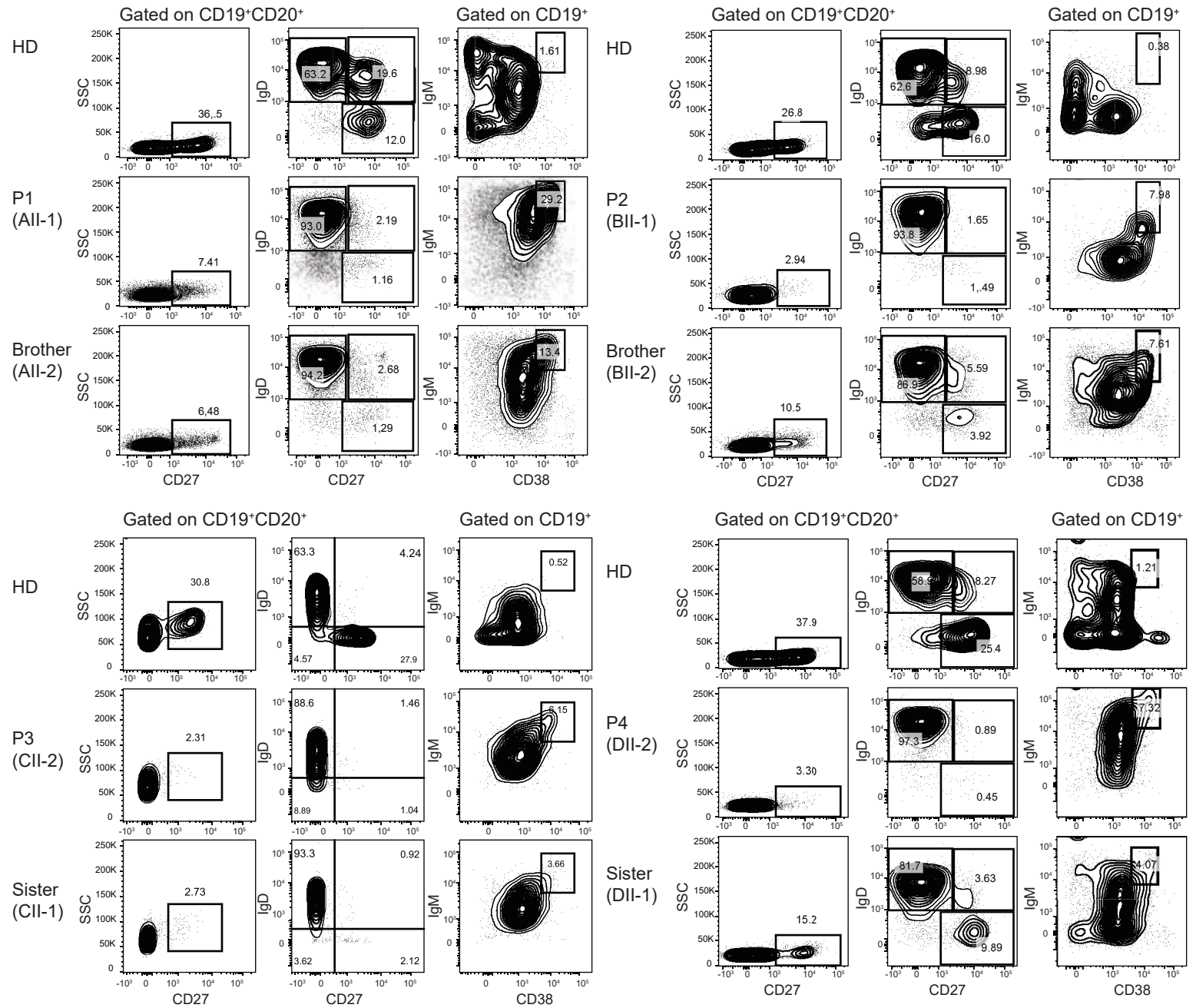
Supplementary Figure 5

CD137 expression



Supplementary Figure 6a

Peripheral blood B-cell immunophenotyping

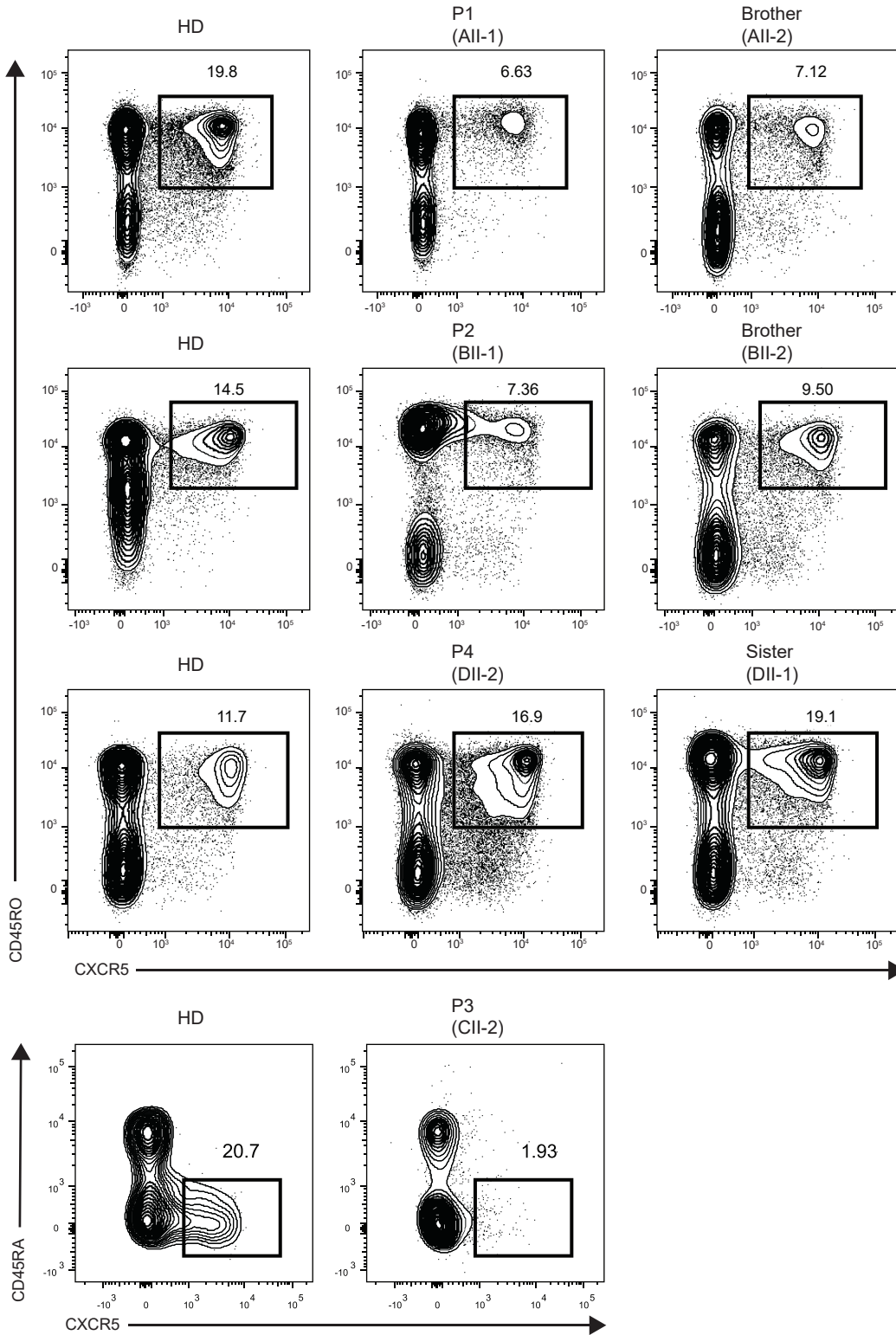


Supplementary Figure 6b

Peripheral blood T-cell immunophenotyping

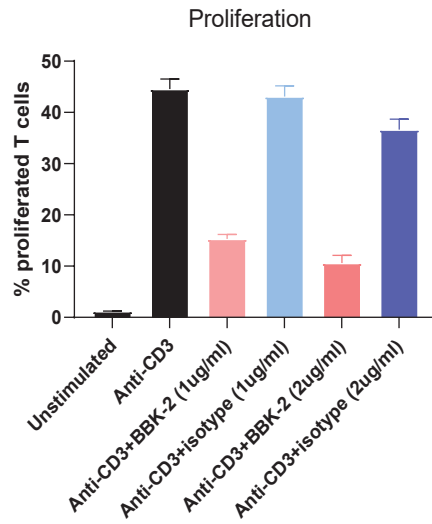
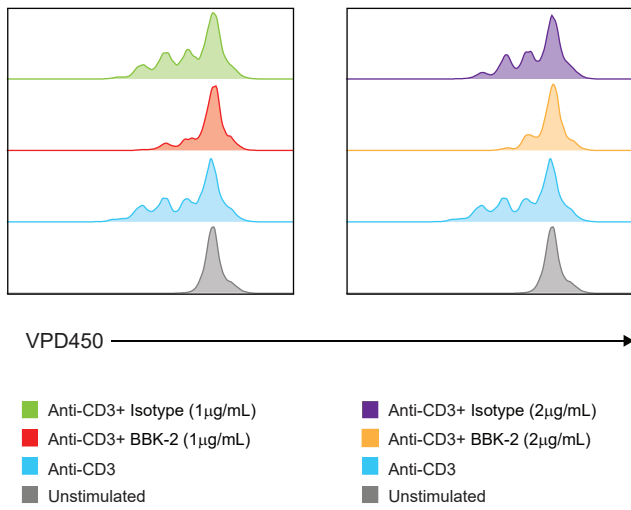
Follicular helper T-cells (T_{FH})

Gated on $CD3^+CD4^+$

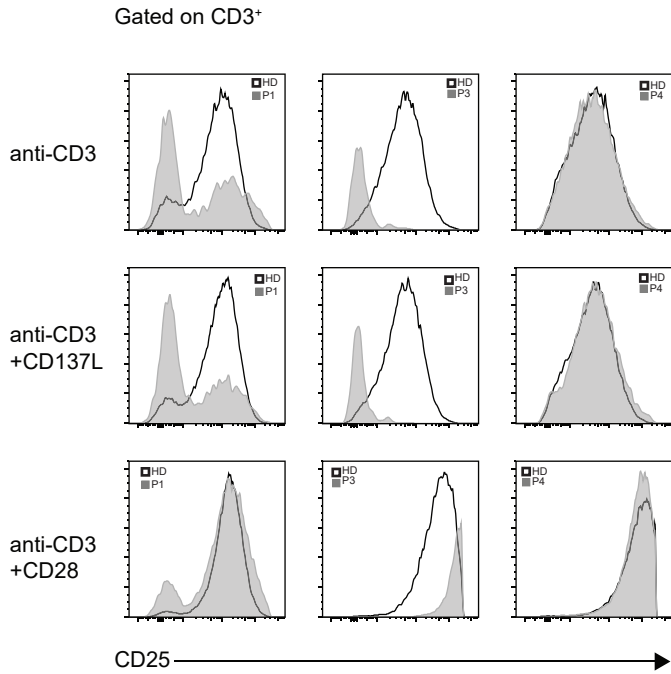


Supplementary Figure 7

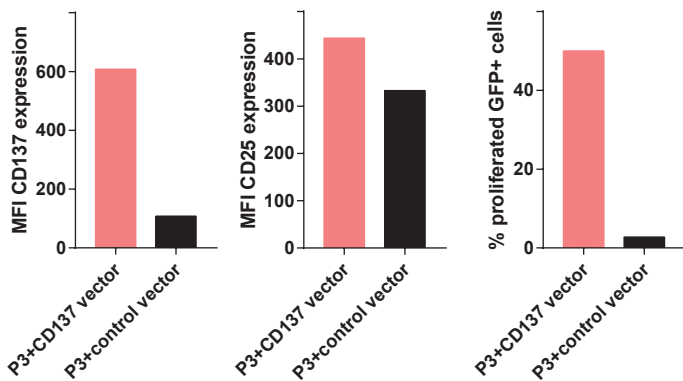
A Blocking CD137 in HD T-cells



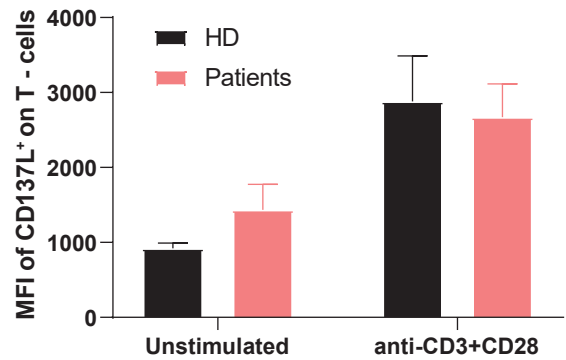
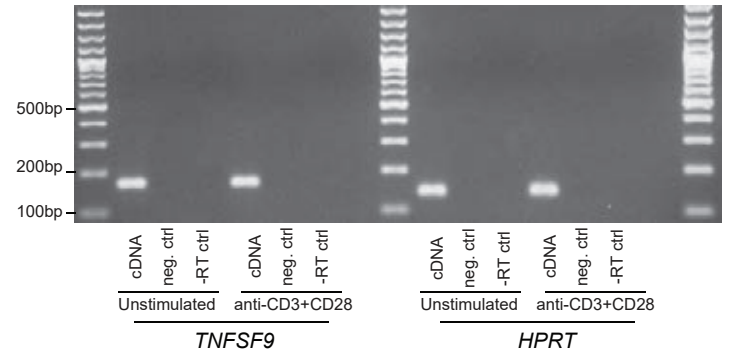
B T-cell activation (CD25 expression)



C Reconstitution of CD137 upon stimulation with anti-CD3 alone



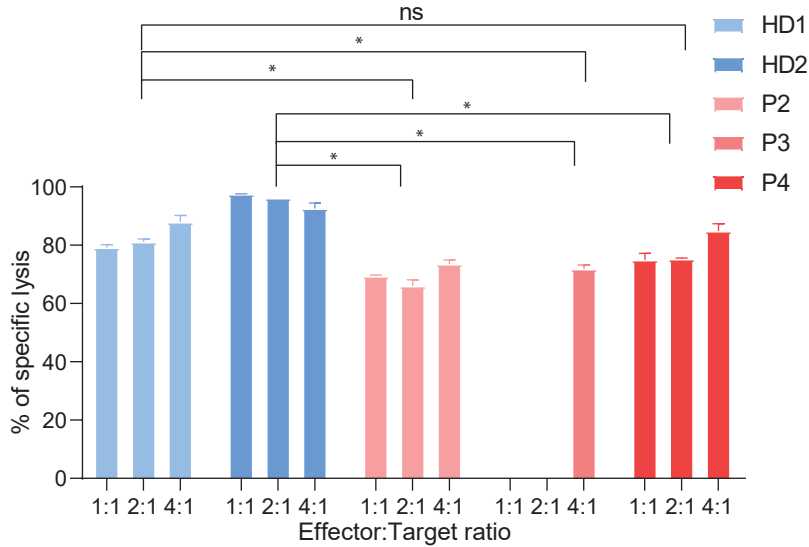
D TNFSF9 and CD137L expression in T-cells



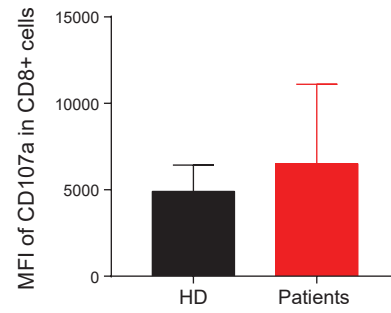
Supplementary Figure 8

CTL cytotoxicity, NK-cell degranulation and T-cell receptor mediated signaling

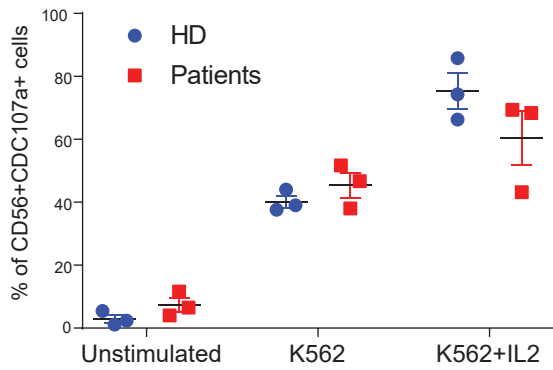
A CTL cytotoxicity



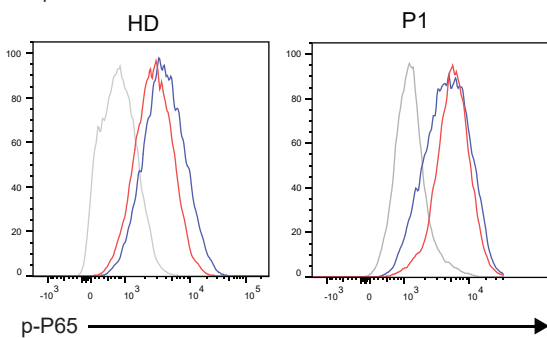
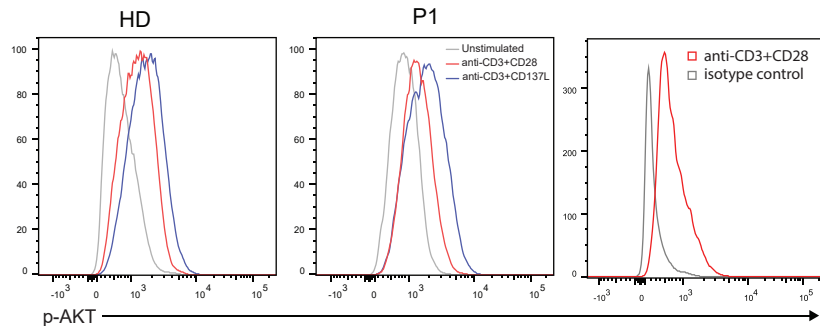
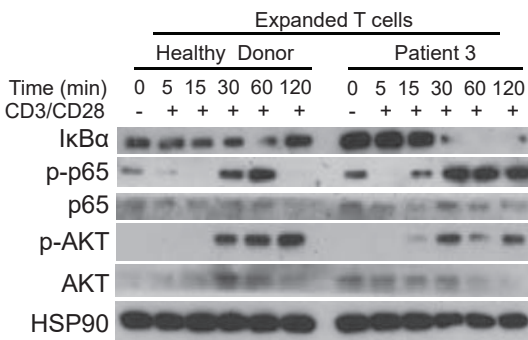
B CTL degranulation



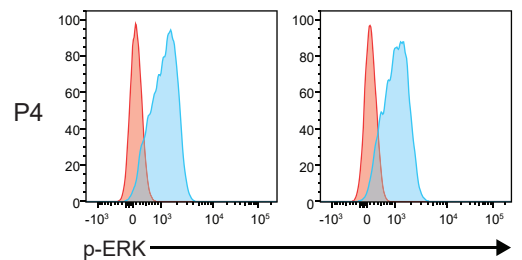
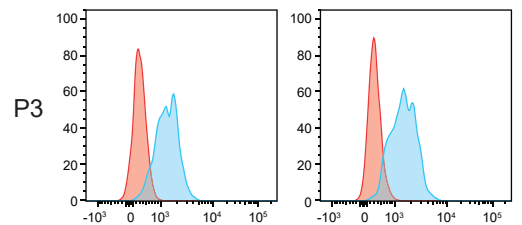
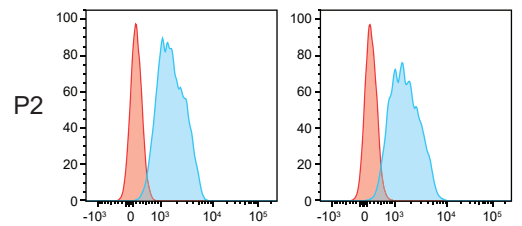
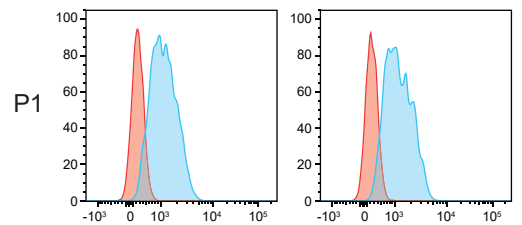
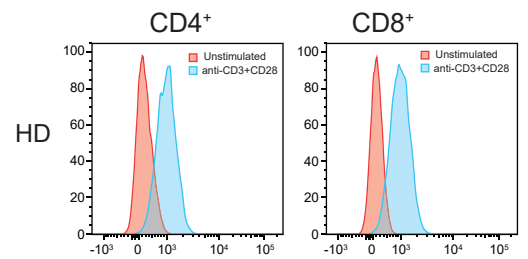
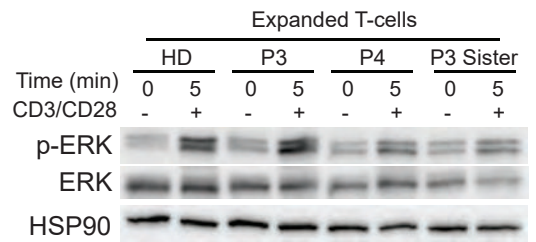
C NK-cell degranulation



D NF- κ B1 and PI3K/AKT signaling in T-cells

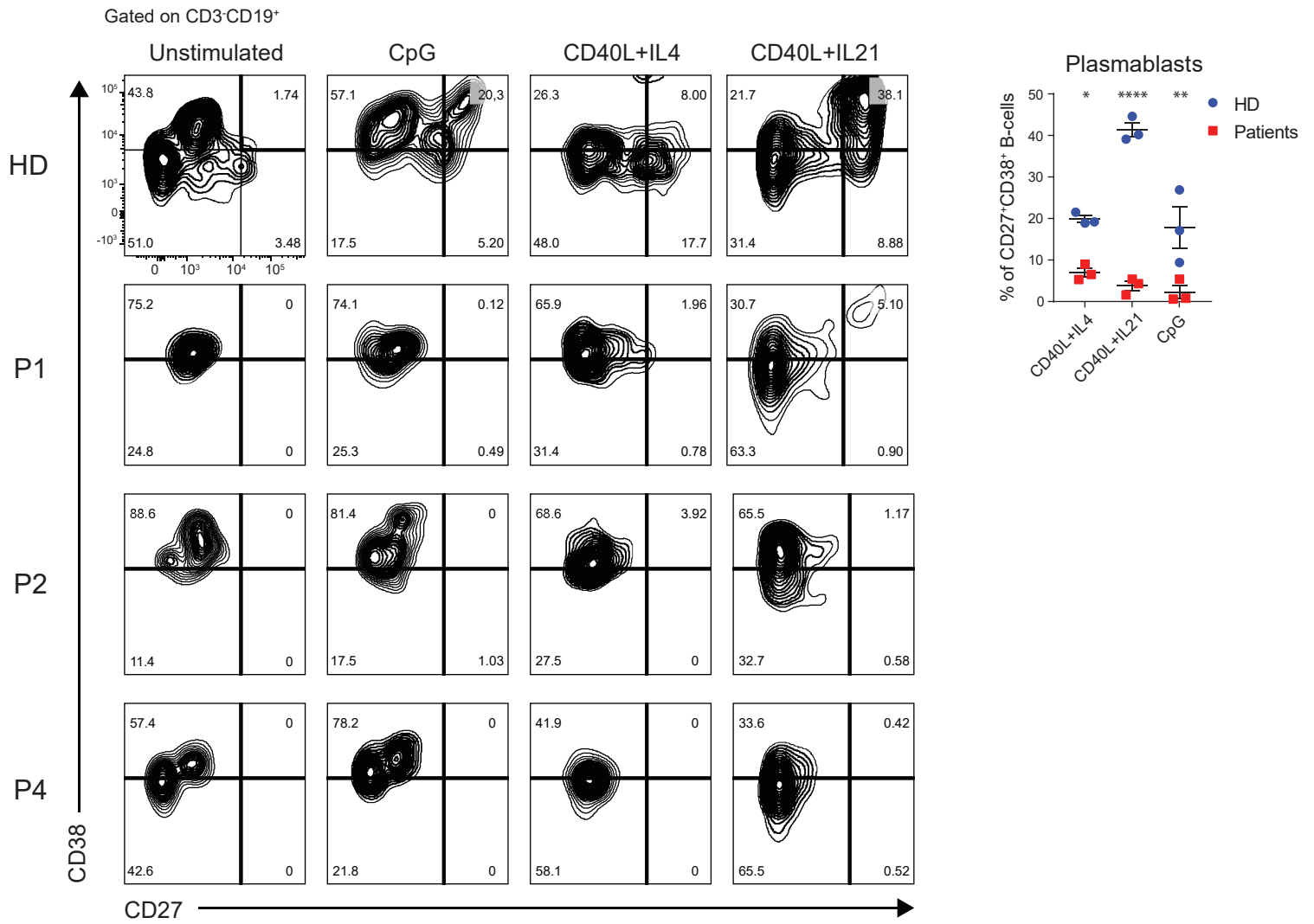


E MAPK signaling in T-cells

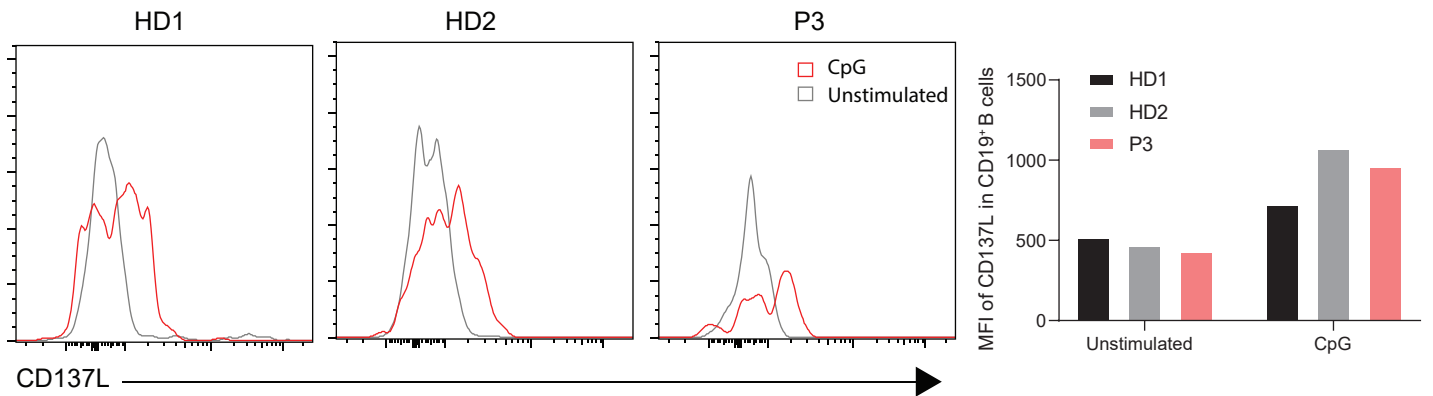


Supplementary Figure 9

A *In vitro* plasmablast differentiation

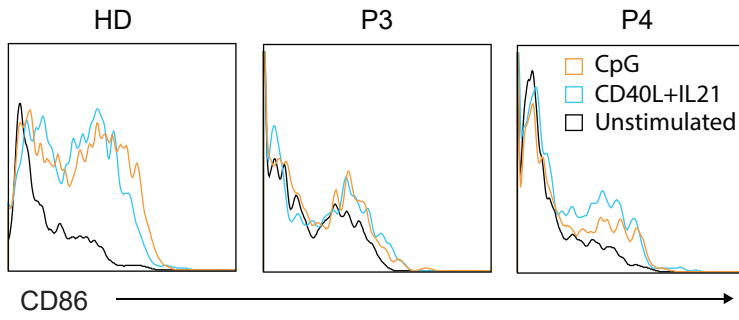


B CD137L expression on CD19⁺ B-cells

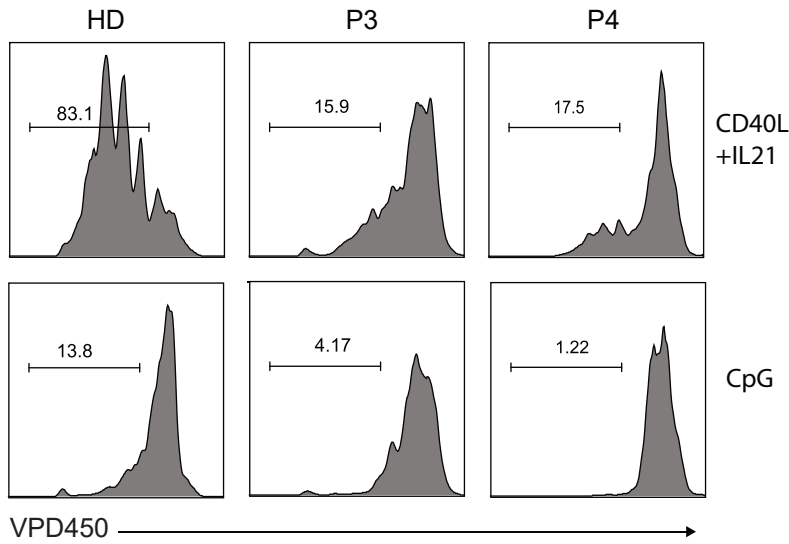


Supplementary Figure 10

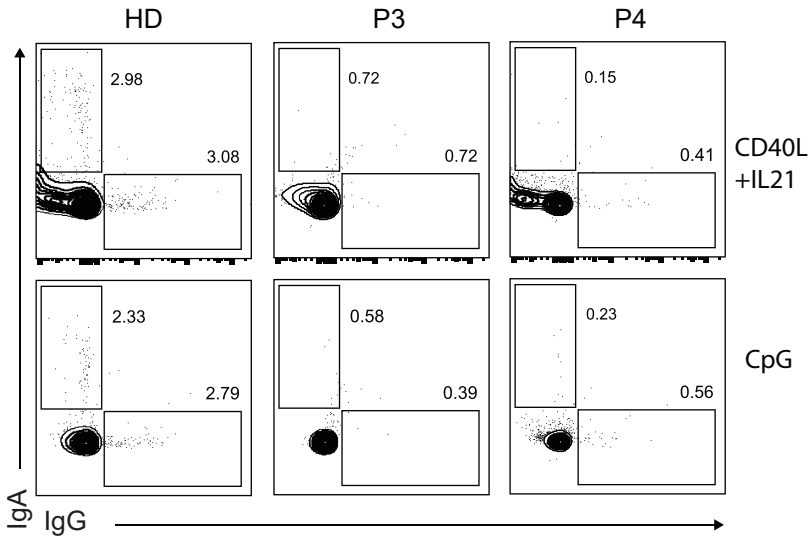
A CD86 cell surface expression in sorted naive B-cell



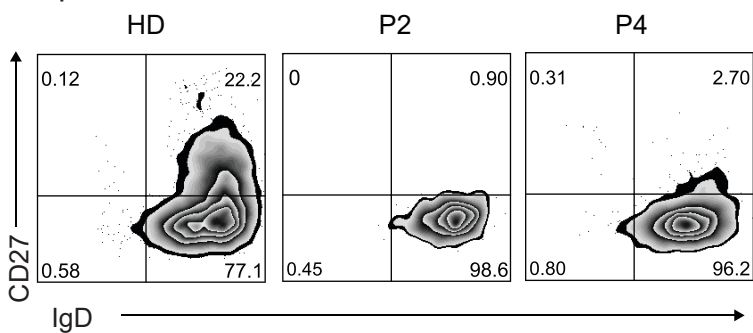
B Sorted naive B-cell proliferation



C Class switch recombination in sorted naive B-cells



D CpG stimulation in sorted naive B-cells



3.2. Germline biallelic *PIK3CG* mutations in a multifaceted immunodeficiency with immune dysregulation

Marini Thian¹⁻⁴, Birgit Hoeger¹⁻³, Anton Kamnev¹, Fiona Poyer⁵, Sevgi Köstel Bal¹⁻³, Michael Caldera³, Raúl Jiménez-Heredia¹⁻³, Jakob Huemer¹⁻³, Winfried F. Pickl⁶, Miriam Groß⁷, Stephan Ehl⁷, Carrie L. Lucas⁸, Jörg Menche³, Caroline Hutter^{2,5}, Andishe Attarbaschi⁵, Loïc Dupré^{1,9} and Kaan Boztug¹⁻⁵

¹Ludwig Boltzmann Institute for Rare and Undiagnosed Diseases, Vienna, Austria. ²St. Anna Children's Cancer Research Institute (CCRI), Vienna, Austria. ³CeMM Research Center for Molecular Medicine of the Austrian Academy of Sciences, Vienna, Austria. ⁴Department of Pediatrics and Adolescent Medicine, Medical University of Vienna, Vienna, Austria. ⁵St. Anna Children's Hospital, Department of Pediatrics and Adolescent Medicine, Medical University of Vienna, Vienna, Austria. ⁶Institute of Immunology, Center for Pathophysiology, Infectiology and Immunology, Medical University of Vienna, Vienna, Austria. ⁷Institute for Immunodeficiency, Center for Chronic Immunodeficiency (CCI), Medical Center - University of Freiburg, Faculty of Medicine, University of Freiburg, Freiburg, Germany. ⁸Department of Immunobiology, Yale University School of Medicine, New Haven, CT, USA. ⁹Center for Pathophysiology of Toulouse Purpan, INSERM UMR1043, CNRS UMR5282, Paul Sabatier University, Toulouse, France.

Germline biallelic *PIK3CG* mutations in a multifaceted immunodeficiency with immune dysregulation

The PI3K-AKT-mTOR signaling axis is a critical molecular pathway in humans, regulating multiple cellular processes.¹ Phosphatidylinositol-3-kinases (PI3K) represent key signaling hubs for signal propagation, driving cell activation, cell polarization and morphological adaptations. Studies on PI3K in human disease have highlighted PI3K-gamma (PI3K γ) as an appealing drug target for treatment of human disorders.² Murine PI3K γ studies showed its importance in regulating innate immune functions and development³⁻⁴ and activation of T cells,⁵ revealing its role in controlling inflammation.⁴ However, its role in the human immune system and diseases remains to be investigated.

Here we investigated a 14-year old female index patient, born to non-consanguineous healthy Austrian parents, who was hospitalized with severe hypotonia and prolonged fever. She had neither lymphadenopathy nor hepatosplenomegaly, and no infectious agent was found. Initial laboratory findings showed a mild thrombocytopenia, hypertriglyceridemia, increased lactate dehydrogenase (LDH) and markedly elevated ferritin (Table 1 and Figure 1A), prompting work up for hemophagocytic lymphohistiocytosis (HLH). Hemophagocytosis was indeed visible in the bone marrow aspirate (Figure 1B). Soluble CD25 was mildly elevated at 2204 U mL⁻¹ (Table 1) but below the levels typically seen in HLH.⁶ NK-cell activity as measured by CD107a expression upon stimulation was in the low normal range in the initial diagnostic (Table 1). The presence of fever, hypertriglyceridemia, hyperferritinemia and hemophagocytosis, did not allow the diagnosis of HLH, but gave evidence of macrophage activation in the context of a hyperferritinemic inflammatory syndrome (Table 1).⁶ We initiated treatment with dexamethasone, leading to clinical improvement and normalization of LDH and ferritin levels. Tapering of dexamethasone resulted in clinical deterioration and rise in ferritin (Figure 1A), and was accompanied by the development of autoimmune neutropenia as documented by HNA-1b antibodies. As the disease was distinct from classical HLH,⁶ we decided to treat the patient with recombinant human anti-IL-1 β (Anakinra, 100 mg twice daily) in combination with dexamethasone, rather than using the etoposide-based HLH-94 protocol. We discontinued dexamethasone treatment after eight weeks and, one month later, reduced the Anakinra dose to a maintenance dose of 100 mg daily. The patient has remained clinically stable and is currently receiving Anakinra (decreased to 60 mg once daily) without any inflammatory manifestations. Immunological characterization of patient peripheral blood in the asymptomatic phase after ceasing dexamethasone revealed reduced absolute natural killer (NK)-cell counts and low frequency of monocytes, and slightly low absolute lymphocyte counts (Table 1).

To explore a potential genetic etiology of the disease, we performed whole exome sequencing on patient DNA. We identified compound heterozygous variants in *PIK3CG* encoding for p110 γ , the catalytic subunit of the PI3K γ complex. Variants were validated by Sanger sequencing and both parents were identified as heterozygous carriers, each for one of the two variants (Figure 1C). The patient inherited a variant within the adaptor binding domain of p110 γ (c.145C>A, p.R49S) and (c.3254A>G, p.N1085S) near the end of the kinase

domain (Figure 1D). Both variants are rare or absent in ExAC and gnomAD databases (*Online Supplementary Table S1*), and affect evolutionarily conserved residues (*Online Supplementary Figure S1A*). Probability of loss-of-function tolerance was unlikely, CADD and PolyPhen-2 scoring suggested the variants as probably pathogenic/damaging (*Online Supplementary Table S1*). We assessed the expression of mutated p110 γ in T cells derived from patient peripheral blood mononuclear cells (PBMC), and found comparable expression levels in the patient, mother, and healthy donors (HD) (Figure 1E).

To investigate whether the identified *PIK3CG* mutations potentially cause the HLH-like disease due to defects in PI3K γ -dependent mechanisms, we first studied patient-derived NK- and T-cell functions. Diminished NK-cell function is part of the diagnostic criteria for HLH.⁶ *Pik3cg*^{-/-} mice display reduced NK-cell numbers, defective NK-cell development and, consequently, decreased cytotoxicity.³ We also observed reduced frequency, absolute counts and degranulation of patient NK cells compared to cells derived from the mother and HD (Table 1 and *Online Supplementary Figure S1B and C*). The impaired NK-cell compartment may have contributed to the observed clinical HLH-like phenotype.³

We further hypothesized that a defect in PI3K γ signaling would affect TCR-driven activation of T cells.⁷ Patient T-cell subsets were comparable to HD (*Online Supplementary Table S2*). However, we observed functional defects in patient T cells, particularly a poor activation and proliferation in response to anti-CD3 or combined anti-CD3/CD28 stimulation (Figure 2A and B and *Online Supplementary Figure S1D*). As expected, TCR-dependent T-cell activation was impaired in *PIK3CG*-mutated T cells. In contrast, patient T-cell proliferation was intact upon stimulation with phytohemagglutinin P (PHA) (Figure 2A and *Online Supplementary Figure S1D*) which can be explained due to the bypassing of TCR/PI3K γ -dependent activation mechanisms. To prove the causative role of mutated *PIK3CG* for the observed phenotypes, we performed a gene-rescue experiment on primary patient cells using GFP-labeled wild-type p110 γ and showed that the T-cell activation defect could be restored (Figure 2C). Additionally, we utilized the PI3K γ inhibitor IPI-549 to prove the causative role of PI3K γ loss-of-function for the observed phenotypes. T-cell activation and proliferation defects upon TCR stimulation were phenocopied by the addition of IPI-549 to HD cells (Figure 2D and E). Furthermore, we examined PI3K/AKT signaling and found mildly decreased AKT phosphorylation in patient cells upon stimulation (Figure 2F and *Online Supplementary Figure S1E*), similar to a recently reported patient with *PIK3CG* mutations.⁸ To prove causality in an independent cellular system, we created Jurkat *PIK3CG* knockout (KO) cells (*Online Supplementary Figure S1F*) and found decreased activation as measured by CD69 upregulation upon anti-CD3 stimulation (Figure 2G), and reduced AKT phosphorylation at the Ser473 phosphorylation site (Figure 2H and *Online Supplementary Figure S1F and G*). These data mimic the phenotypes observed in patient T cells. Furthermore, upon reconstitution with wild-type p110 γ , CD69 was upregulated on the surface of Jurkat *PIK3CG* KO cells (*Online Supplementary Figure S1H*). By contrast, upon reconstitution of mutant N1085S or R49S, no upregulation of CD69 was observed compared to empty vector (*Online Supplementary Figure S1H*), showing loss-of-function mechanisms for both individual variants. Altogether, the T-cell stimulation defects observed in *PIK3CG*-mutated patient cells recapitulate reports on *Pik3 γ* ^{-/-} murine T cells.^{5,7}

For the development of familial HLH, absence of the cytotoxic activity of cytotoxic T cells (CTL) plays a central role. The level of surface CD107a/LAMP1 was normal on patient CTL upon stimulation (*Online Supplementary Figure S4I*). Furthermore, consistent with

murine studies suggesting that PTEN activity, counteracting PI3K function, is required to maintain Treg cell stability and homeostasis,⁹ we observed a slightly increased frequency of CD4⁺CD127^{dim}FOXP3⁺CD25⁺T_{reg} cells in the peripheral blood of the patient (*Online Supplementary*

Table 1. Patient's immunological features.

Features	Initial presentation (July 2018)	After ceasing dexamethasone (Dec 2018)	After reducing Anakinra (June 2019)
Hb (g/dL)	12.3 (12.3-16)	12.6 (12.3-16)	13.1 (12.3-16)
Absolute lymphocytes (x10 ⁹ /L)	0.95 (1.1-4.5)	1.07 (1.1-4.5)	0.95 (1.1-4.5)
Absolute neutrophils (x10 ⁹ /L)	3.48 (1.9-8.0)	1.95 (1.9-8.0)	1.05 (1.9-8.0)
Absolute monocytes (x10 ⁹ /L)	0.24 (0.15-1.4)	0.15 (0.15-1.4)	0.15 (0.15-1.4)
CD3 ⁺ CD16 ⁺ CD14 ⁺ monocytes (%)	NA	7.59 (24.1-11.8)	NA
Absolute thrombocytes (x10 ⁹ /L)	119 (140-400)	334 (140-400)	296 (140-400)
Absolute CD3 ⁺ T cells (x10 ⁹ /L)	0.71 (0.75-2.51)	0.99 (0.75-2.51)	0.75 (0.75-2.51)
Absolute CD4 ⁺ T cells (x10 ⁹ /L)	0.37 (0.43-1.69)	0.53 (0.43-1.69)	0.43 (0.43-1.69)
Absolute CD8 ⁺ T cells (x10 ⁹ /L)	0.3 (0.22-1.21)	0.4 (0.22-1.21)	0.28 (0.22-1.21)
Absolute CD56 ⁺ CD3 ⁻ NK cells (x10 ⁹ /L)	0.06 (0.12 - 0.60)	0.06 (0.12 - 0.60)	0.07 (0.12 - 0.60)
Absolute CD19 ⁺ B cells (x10 ⁹ /L)	0.13 (0.12-0.64)	0.09 (0.12-0.64)	0.08 (0.12-0.64)
HLH determinants [criteria for familial HLH]			
Ferritin (ng/mL) [>500]	13898 (7-150)	33 (7-150)	22 (7-150)
Fibrinogen (mg/dL) [<150]	242 (150-450)	236 (150-450)	NA
Triglycerides (mg/dL) [>265]	265 (0-150)	41 (0-150)	NA
NK-cell degranulation [#] [low/absent]	10.64 (>10)	NA	NA
sCD25 (U/mL) [>2400]	2204 (158-623)	1320 (158-623)	NA
IgG (g/L)	11 (4.9-16.1)	6.16 (6-16)	NA
IgM (g/L)	1.27 (0.5-1.9)	0.28 (0.5-1.9)	NA
IgA (g/L)	0.98 (0.4-2.0)	0.27 (0.8-2.8)	NA
HiB IgG (µg/mL)	8.15	1.46	NA
Diphtheria IgG (IU/mL)	0.15	0.05	NA
Tetanus IgG (IU/mL)	1.25	0.25	NA

Reference ranges are indicated in round brackets. Values out of reference ranges are indicated in bold. Criteria ranges for familial HLH⁶ are indicated in squared brackets. Hb: hemoglobin; HiB: *Haemophilus influenzae* B antibody; HLH: hemophagocytic lymphohistiocytosis; Ig: immunoglobulin; NA: not applicable; sCD25: soluble CD25; [#]%CD107⁺ cells, according to the standard diagnostic measurement conducted at the Centre for Chronic Immunodeficiency, University of Freiburg, Freiburg, Germany.

Figure S1J). In comparison to T cells which activate *via* PI3K γ and PI3K δ , B cells predominantly respond *via* PI3K δ . This was corroborated by impaired B-cell development compared to rather intact T-cell populations in *PIK3CD* and *PIK3R1* loss-of-function patients.¹⁰ By contrast, *PIK3CG*-mutated patient-derived B cells showed intact proliferation and class switch recombination upon stimulation (Online Supplementary Figure S1K and L), supporting data obtained in *Pik3cg*^{-/-} mice.⁵

Since PI3K γ is highly expressed in myeloid cells, we hypothesized that loss-of-function mutations in human PI3K γ may compromise the function of these cells, thereby potentially contributing to the inflammatory features reported in the patient. Indeed, the observation that the patient responded well to anti-IL-1 β (Anakinra) therapy (Figure 1A) supports the notion that defects in the PI3K pathway in innate immune cells may underlie the inflammatory presentation. Preclinical studies have shown that PI3K γ blockade leads to reprogramming of macrophages, resulting in increased production of pro-inflammatory cytokines.¹¹ PI3K γ activation results in the PIP₃-dependent activation of Rac and, subsequently, Arp2/3-dependent actin-cytoskeleton remodeling driving cell polarization, morphology and phagocytosis.¹² We hypothesized that

PIK3CG-mutated patient cells would display abnormalities in innate cell morphology and function. We therefore differentiated freshly-isolated monocytes of patient, mother and HD to macrophages, which showed comparable expression of macrophage differentiation markers (Online Supplementary Figure S2A), implying normal differentiation. Upon stimulation, the number of adhered cells per image was similar across all groups (Online Supplementary Figure S2B). However, patient monocyte-derived macrophages displayed dramatic reduction in cell area and total amount of F-actin per cell, as compared to HD cells (Figure 2I-K). Moreover, cells from the mother displayed an intermediate phenotype, possibly linked to her heterozygous carrier status for one of the *PIK3CG* mutations. Altogether, these data indicate that PI3K γ deficiency is associated with a defect in actin-driven macrophage spreading upon stimulation. We also observed diminished phagocytosis in patient-derived monocytes and neutrophils (Figure 2L). Patient neutrophils showed a pronounced apoptotic population after isolation (Online Supplementary Figure S2C). Loss of mitochondrial membrane potential in neutrophils is an early marker for commitment to apoptosis.¹³ Consistently, mitochondrial membrane potential of patient neutrophils

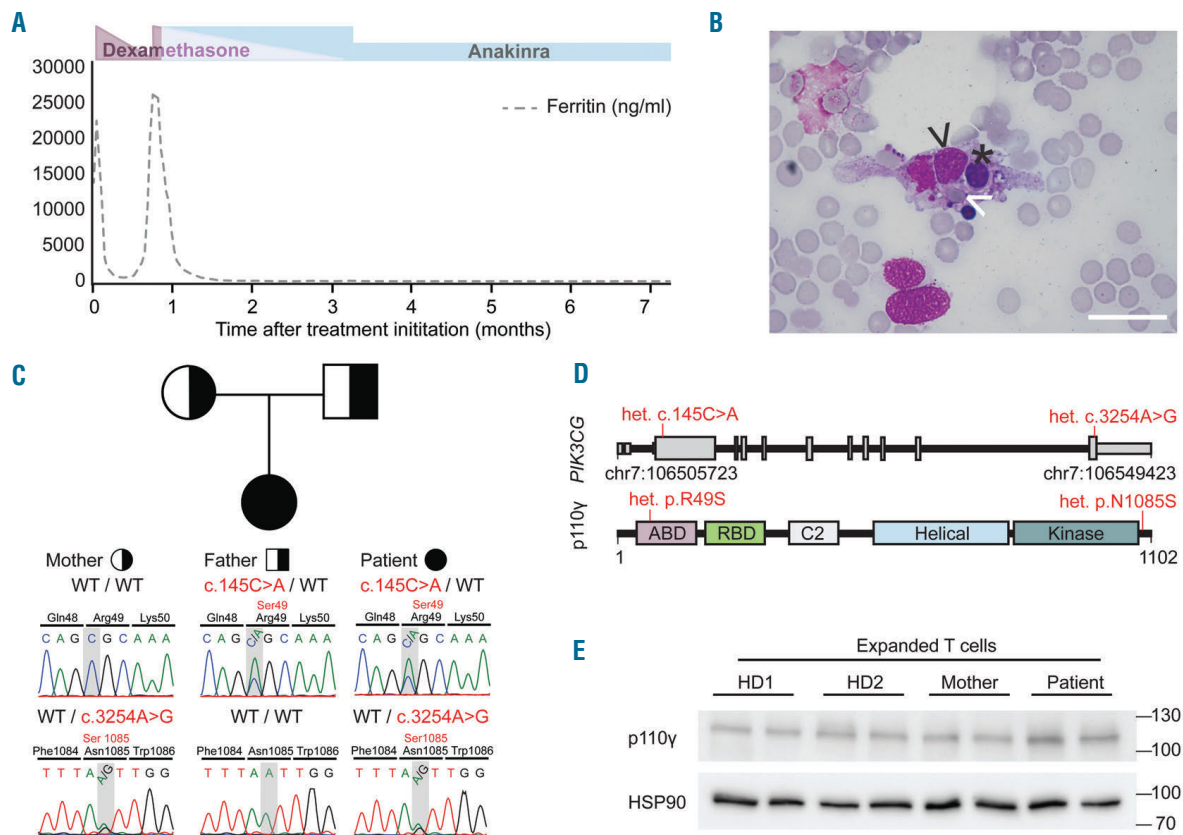


Figure 1. Compound-heterozygous *PIK3CG* mutations in a patient with systemic inflammation. (A) Patient response to dexamethasone treatment (purple) as evidenced by the decrease of ferritin in the patient's peripheral blood. Disease relapsed upon initial withdrawal of dexamethasone, as evidenced by increased ferritin levels. Reinitiation of dexamethasone normalized ferritin levels, and treatment with Anakinra (blue) was initiated and well-tolerated. Treatment was initiated at 14 years of age, and ferritin was monitored over seven months. Colored bars indicate drug dosage. (B) Patient bone marrow biopsy showing engulfment of erythroblast (black asterisk) and mature erythrocyte (white arrow) by a macrophage. The nucleus is indicated by the black arrow. Scale bar: 25 μ m. (C) Compound-heterozygous *PIK3CG* base pair substitutions in the index patient (filled symbol) segregate with parents. Sanger sequencing confirmed presence of a heterozygous variant in each parent (half-filled symbols). (D) Schematic representation of chromosomal position (top) and protein domains (bottom) of the identified *PIK3CG*/p110 γ mutations, introducing two distinct missense mutations within the adaptor-binding domain (ABD) and near the kinase domain of the protein. RBD: Ras-binding domain; het: heterozygous. (E) Expression of p110 γ protein in expanded T cells of the patient, compared with cells of mother and two healthy donors (HD). HSP90 was used as a housekeeping loading control.

was compromised (*Online Supplementary Figure S2D*). However, patient neutrophils displayed a normal oxidative burst upon stimulation (*Online Supplementary Figure S2E*). Studies in mice outlined the importance of PI3K γ in neutrophils.¹⁴ However, in a transwell migration assay,

patient neutrophils were able to migrate normally (*Online Supplementary Figure S2F*). Since PI3K δ works synergistically with PI3K γ in neutrophil migration, PI3K δ may compensate for migration processes in human neutrophils. Collectively, we report deficiency of human

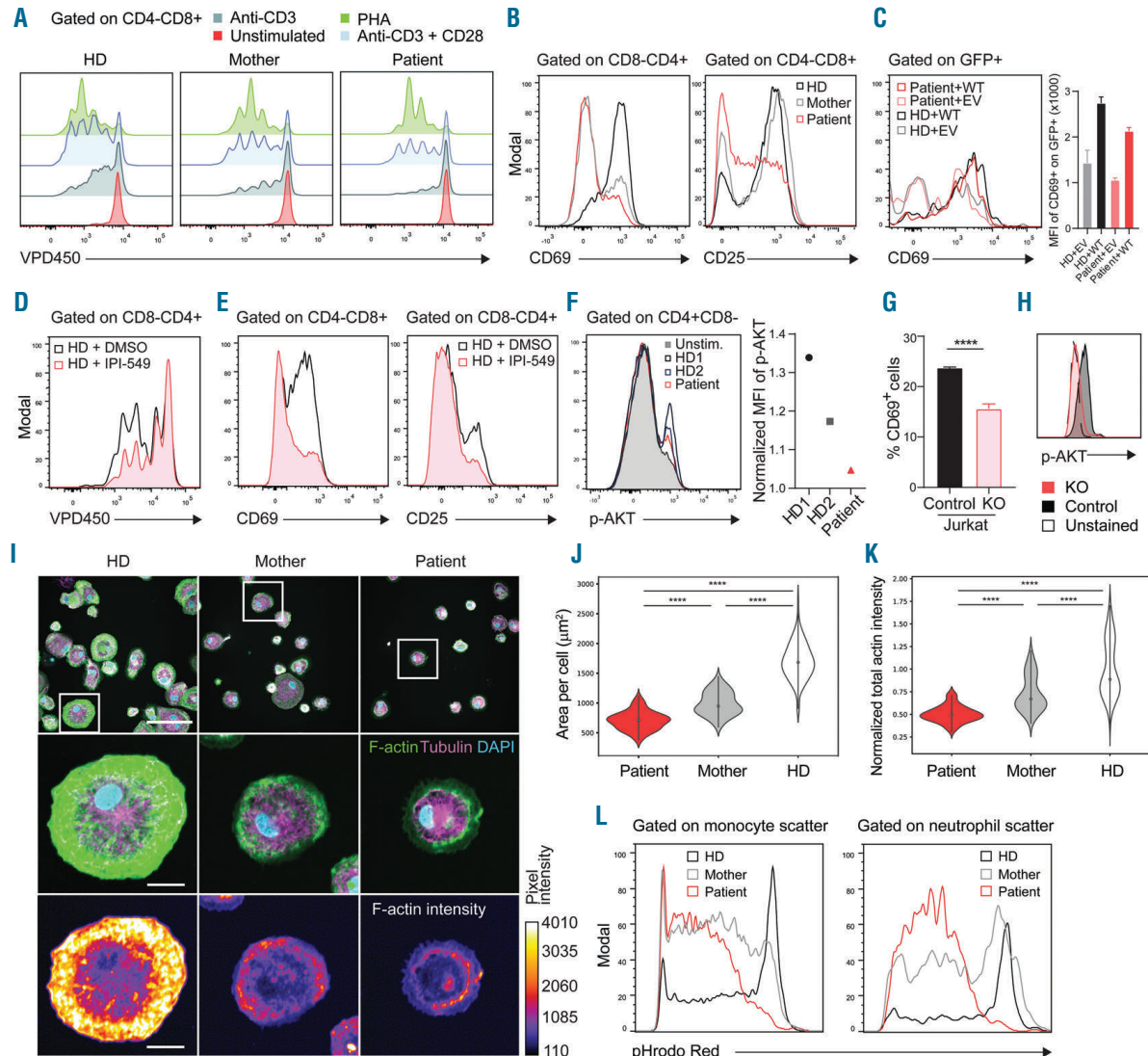


Figure 2. PI3KCG mutations affect adaptive and innate immune functions. (A) Reduced proliferative capacity of patient-derived T cells upon stimulation with anti-CD3 antibody or combined anti-CD3/CD28 antibody. Phytohemagglutinin P (PHA) stimulation was not impaired, in agreement with TCR/PI3K-independent T-cell activation. Cells were stained with violet proliferation dye (VPD450), and dye dilutions were monitored three days post stimulation. (B) Impaired activation of patient T cells. Peripheral blood mononuclear cells (PBMC) were isolated and stained for the appearance of activation markers, one day (left, CD69 upregulation) or three days (right, CD25 upregulation) after stimulation with anti-CD3/CD28. Cells were gated on lymphocytes and CD8 $^{+}$ CD4 $^{+}$ (left) or CD4 $^{+}$ CD8 $^{+}$ (right) populations. (C) Rescue of T-cell activation via CD69 expression on day 2 post stimulation with anti-CD3 in patient cells by exogenous expression of wild-type (WT) PI3KCG or empty vector (EV). Gated on GFP $^{+}$ transfected cells (left). Mean fluorescence intensity (MFI) of CD69 expression on GFP $^{+}$ transfected cells (right). (D) PI3K γ inhibition by IPI-549 phenocopies T-cell proliferation defects. Cells were stimulated with anti-CD3/CD28 and monitored for VPD450 dye dilution as in (A). (E) Addition of PI3K γ inhibitor IPI-549 (1 μ M) phenocopies the T-cell activation defect, compared to DMSO control. Cells were stimulated as in (B) and gated on CD4 $^{+}$ CD8 $^{+}$ (left) or CD8 $^{+}$ CD4 $^{+}$ (right) lymphocytes. (F) Impaired activation of AKT signaling in PI3KCG-mutated patient PBMC, gated on CD4 $^{+}$ CD8 $^{+}$ T cells. PBMC were stimulated with anti-CD3/CD28 for 15 minutes. (Left) Phospho-AKT signal was reduced in patient cells compared to healthy donors (HD). (Right) Normalization to unstimulated control. (G) Decreased activation of PI3KCG knockout (KO) Jurkat cells compared to Renilla KO control upon anti-CD3 stimulation. **** P <0.0001, two-way ANOVA. (H) Reduced MFI of AKT Ser473 phosphorylation in PI3KCG KO Jurkat cells compared to Renilla KO control and unstained control. (I) Representative immunostaining images of 40 \times magnification after 5 hours incubation with PMA/ionomycin in HD, mother and patient monocyte-derived macrophages. Images show reduced cell spreading and total F-actin intensity in patient macrophages upon stimulation. Scale bars: 100 μ m (top), 20 μ m (middle, bottom). The lookup table (bottom right) indicates a color code for pixel values. (J) Patient macrophages show lack of cell spreading as indicated by significantly smaller cell area compared to mother and HD cells. **** P <0.0001, Mann-Whitney U test. (K) Reduced total F-actin intensity of patient macrophages compared to mother and HD cells. **** P <0.0001, Mann-Whitney U test. (L) Reduced phagocytosis ability of patient-derived monocytes (left) and neutrophils (right). Whole-blood samples were incubated with pHrodo Red *E. coli* and phagocytosed bacteria were evaluated by flow cytometry. Populations were gated based on forward/side scatter characteristics of monocytes and neutrophils, respectively. All error bars indicate \pm standard error of mean.

p110 γ underlying a previously unknown inborn error of immunity with HLH-like systemic inflammation and aberrant immune cell function. Intriguingly, despite compromised functions of both innate and adaptive immune cells, so far the patient has not experienced serious infections as compared to a patient recently reported with PIK3CG mutations.⁸ Larger patient cohorts and longer follow up will thus be necessary to unravel the full clinical spectrum of the disease.

Marini Thian,^{1,2,3,4} Birgit Hoeger,^{1,2,3} Anton Kamnev,¹ Fiona Poyer,⁵ Sevgi Köstel Bal,^{1,2,3} Michael Caldera,⁵ Raúl Jiménez-Heredia,^{1,2,3} Jakob Huemer,^{1,2,3} Winfried F. Pickel,⁶ Miriam Groß,⁷ Stephan Ehl,⁷ Carrie L. Lucas,⁸ Jörg Menche,³ Caroline Hutter,^{2,5} Andishe Attarbaschi,⁵ Loïc Dupré^{1,9} and Kaan Boztug^{1,2,3,4,5}

¹Ludwig Boltzmann Institute for Rare and Undiagnosed Diseases, Vienna, Austria; ²St. Anna Children's Cancer Research Institute (CCRI), Vienna, Austria; ³CeMM Research Center for Molecular Medicine of the Austrian Academy of Sciences, Vienna, Austria; ⁴Department of Pediatrics and Adolescent Medicine, Medical University of Vienna, Vienna, Austria; ⁵St. Anna Children's Hospital, Department of Pediatrics and Adolescent Medicine, Medical University of Vienna, Vienna, Austria; ⁶Institute of Immunology, Center for Pathophysiology, Infectiology and Immunology, Medical University of Vienna, Vienna, Austria; ⁷Institute for Immunodeficiency, Center for Chronic Immunodeficiency (CCI), Medical Center - University of Freiburg, Faculty of Medicine, University of Freiburg, Freiburg, Germany; ⁸Department of Immunobiology, Yale University School of Medicine, New Haven, CT, USA and ⁹Center for Pathophysiology of Toulouse Purpan, INSERM UMR1043, CNRS UMR5282, Paul Sabatier University, Toulouse, France

Funding: this work was funded by the European Research Council (ERC Consolidator Grant 820074 to KB) and the Vienna Science and Technology Fund (WWTF-LS16-060 to KB and LD). MT was supported by the Cell Communication in Health and Disease programme (CCHD, Medical University of Vienna) and a DOC fellowship of the Austrian Academy of Sciences (ÖAW 25225). BH was supported by the Austrian Science Fund FWF Hertha Firnberg program (T934-B30). SE and MG were supported by the Deutsche Forschungsgemeinschaft SFB1160 (TPA01).

Acknowledgments: the authors thank the patient and her family for participating in this study. We thank Javier Rey-Barroso (Institute of Pharmacology and Structural Biology of Toulouse) for the excellent technical advice. We thank the Superti-Furga laboratory, especially

Felix Kartnig (CeMM), for technical assistance and access to the microscope. We thank Ana Krolo (LBI-RUD), Yolla German (LBI-RUD & Center for Pathophysiology of Toulouse Purpan), Arno Rottal and Ulrike Körmöcz (Institute of Immunology, Medical University of Vienna) for technical assistance.

Correspondence: KAAN BOZTUG - kaan.boztug@ccri.at

doi:10.3324/haematol.2019.231399

References

1. Fruman DA, Chiu H, Hopkins BD, et al. The PI3K Pathway in Human Disease. *Cell*. 2017;170(4):605-635.
2. Janku F, Yap TA, Meric-Bernstam F. Targeting the PI3K pathway in cancer: are we making headway? *Nat Rev Clin Oncol*. 2018;15:273-291.
3. Tassi I, Cella M, Gilfillan S, et al. p110 γ and p110 δ Phosphoinositide 3-Kinase Signaling Pathways Synergize to Control Development and Functions of Murine NK Cells. *Immunity*. 2007;27(2):214-227.
4. Kaneda MM, Messer KS, Ralainirina N, et al. PI3K γ is a molecular switch that controls immune suppression. *Nature*. 2016; 539(7629):437-442.
5. Sasaki T, Irie-Sasaki J, Jones RG, et al. Function of PI3K γ in Thymocyte Development, T Cell Activation, and Neutrophil Migration. *Science*. 2000;287(5455):1040-1046.
6. Henter J-I, Home A, Arico M, et al. HLH-2004: Diagnostic and therapeutic guidelines for hemophagocytic lymphohistiocytosis. *Pediatr Blood Cancer*. 2007;48(2):124-131.
7. Alcázar I, Marques M, Kumar A, et al. Phosphoinositide 3-kinase γ participates in T cell receptor-induced T cell activation. *J Exp Med*. 2007;204(12):2977-2987.
8. Takeda AJ, Maher TJ, Zhang Y, et al. Human PI3K γ deficiency and its microbiota-dependent mouse model reveal immunodeficiency and tissue immunopathology. *Nat Commun*. 2019;10:4364-4376.
9. Huynh A, DuPage M, Priyadharshini B, et al. The phosphatase PTEN-mediated control of PI-3 kinase in Tregs cells maintains homeostasis and lineage stability. *Nat Immunol*. 2015;16(2):188-196.
10. Nunes-Santos C, Uzel G, Rosenzweig SD. PI3K pathway defects leading to immunodeficiency and immune dysregulation. *J Allergy Clin Immunol*. 2019;143(5):1676-1687.
11. De Henau O, Rausch M, Winkler D, et al. Therapy by targeting PI3K γ in myeloid cells. *Nature*. 2016;539(7629):443-447.
12. Hawkins PT, Stephens LR. PI3K signalling in inflammation. *Biochim Biophys Acta*. 2015;1851(6):882-897.
13. Fossati G, Moulding DA, Spiller DG, et al. The mitochondrial network of human neutrophils: role in chemotaxis, phagocytosis, respiratory burst activation, and commitment to apoptosis. *J Immunol*. 2003;170(4):1964-1972.
14. Hirsch E, Katanaev VL, Garlanda C, et al. Central Role for G Protein-Coupled Phosphoinositide 3-Kinase γ in Inflammation. *Science*. 2000;287(5455):1049-1054.

Supplementary Materials for

Germline biallelic *PIK3CG* mutations in a multifaceted immunodeficiency with immune dysregulation

Marini Thian^{1,2,3,4}, Birgit Hoeger^{1,2,3}, Anton Kamnev¹, Fiona Poyer⁵, Sevgi Köstel Bal^{1,2,3}, Michael Caldera³, Raúl Jiménez-Heredia^{1,2,3}, Jakob Huemer^{1,2,3}, Winfried F. Pickl⁶, Miriam Groß⁷, Stephan Ehl⁷, Carrie L. Lucas⁸, Jörg Menche³, Caroline Hutter^{2,5}, Andishe Attarbaschi⁵, Loïc Dupré^{1,9} and Kaan Boztug^{1,2,3,4,5}

¹Ludwig Boltzmann Institute for Rare and Undiagnosed Diseases, Vienna, Austria.

²St. Anna Children's Cancer Research Institute (CCRI), Vienna, Austria.

³CeMM Research Center for Molecular Medicine of the Austrian Academy of Sciences, Vienna, Austria.

⁴Department of Pediatrics and Adolescent Medicine, Medical University of Vienna, Vienna, Austria.

⁵St. Anna Children's Hospital, Department of Pediatrics and Adolescent Medicine, Medical University of Vienna, Vienna, Austria.

⁶Institute of Immunology, Center for Pathophysiology, Infectiology and Immunology, Medical University of Vienna, Vienna, Austria.

⁷Institute for Immunodeficiency, Center for Chronic Immunodeficiency (CCI), Medical Center - University of Freiburg, Faculty of Medicine, University of Freiburg, Freiburg, Germany.

⁸Department of Immunobiology, Yale University School of Medicine, New Haven, CT, USA.

⁹Center for Pathophysiology of Toulouse Purpan, INSERM UMR1043, CNRS UMR5282, Paul Sabatier University, Toulouse, France.

Corresponding author:

Kaan Boztug, MD

St. Anna Children's Cancer Research Institute (CCRI) and Ludwig Boltzmann Institute for Rare and Undiagnosed Diseases

Zimmermannplatz 10, Vienna, Austria

kaan.boztug@ccri.at

MATERIALS AND METHODS

Whole Exome Sequencing and analysis

Whole exome sequencing was performed using a TruSeq Rapid Exome kit as well as the Illumina HiSeq3000/4000 system and the cBot cluster generation instruments as previously described,^{1,2} with minor changes. Briefly, reads were aligned to the human genome version 19 by means of the Burrows-Wheeler Aligner (BWA). VEP was used for annotating single nucleotide variants (SNVs) and insertions/deletions lists. The obtained list was then filtered according to the presence of variants with a minor allele frequency (MAF) >0.01 in 1,000 Genomes, gnomAD, and dbSNP build 149. After further filtering steps for nonsense, missense, and splice-site variants using VCF.Filter software,³ an internal database was used to filter for recurrent variants. Moreover, variants were prioritized using tools, such as SIFT, Polyphen-2 and the combined annotation dependent depletion (CADD) score,^{4,5} that predict the deleteriousness of a present variant.

Sanger sequencing

Sanger sequencing was used to validate the two variants found in *PIK3CG*:

variant 1, ENST00000359195.3:c.145C>A, p.Arg49Ser; and variant 2, ENST00000359195.3:c.3254A>G, p.Asn1085Ser, in the affected patient and her family members. This was done by designing specific primers for the two variants.

For variant 1,

Fw1: 5'- CATGTACGCCGCCTATACCT -3',

Rv1: 5'- TACCACTGCCCCCTTCTTCTG -3';

and for variant 2,

Fw2: 5'- TCCTGTTCTCCATGATGCTG-3',

Rv2: 5'- AACCAATCAGCAATGCCAACA-3'.

Cell Culture

Human PBMCs were isolated by Ficoll-Paque PLUS (GE Healthcare) density gradient centrifugation, washed twice in PBS, and resuspended in complete RPMI-1640 media (Gibco) containing 10 % heat-inactivated FBS, 1 % penicillin and streptomycin (Invitrogen) and 1 % HEPES buffer solution 1 M (Invitrogen). CTL and NK cell degranulation was assessed by CD107a surface staining for 3 h in presence or absence of dynabeads human T-activator CD3/CD28 (Thermo Fisher Scientific) stimulation or K562 target cells respectively. The erythroleukemic cell line K562 (ATCC, CCL-243) was used as target cell line. NK cells were cultured in complete RPMI-1640 media with or without 600 U mL⁻¹ IL-2 (Peprotech) for 48h to assess NK degranulation of activated or non-activated NK cells respectively. Proliferative response was measured by labeling PBMCs with 1 mM Violet Proliferation Dye 450 (BD Biosciences) according to manufacturer's instructions. For T-cell activation and proliferation assay, PBMCs were stimulated with 2 µg mL⁻¹ anti-CD3 (OKT3, Thermo Fisher Scientific) or with 1 µg mL⁻¹ anti-CD28 (Thermo Fisher Scientific) or 5 µg mL⁻¹ PHA (Sigma-Aldrich) for 1-3 days. PI3Kγ inhibitor IPI-549 was used at 1µM. For B cell proliferation and class switch recombination assays, PBMCs were stimulated with 200 ng mL⁻¹ CD40 ligand (R&D Systems) and 100 ng mL⁻¹ rhIL4 (R&D Systems) for 5 days. For T-cell expansion, PBMCs were stimulated with feeder cells (gamma-irradiated PBMCs) and 1 µg mL⁻¹ PHA (Sigma-Aldrich) with 100 U mL⁻¹ IL-2 (Peprotech) for 14 days. Expanded T cells were starved by serum deprivation 2 h prior to 200 ng mL⁻¹ SDF1 (Peprotech) stimulation. Jurkat E6-1 cells were cultured in complete RPMI-1640 media and stimulated with 2 µg mL⁻¹ anti-CD3 (OKT3). Reconstitution with GFP-labeled wild-type *PIK3CG* or empty vector GFP control was performed on a NEPA21 electroporator (Nepagene), according to manufacturer's recommendations, with a poring pulse of 175 V for 5 ms.

Monocyte isolation and differentiation

Primary monocytes were isolated from PBMCs using human Pan Monocyte Isolation Kit (Miltenyi Biotec) according to manufacturer's instructions. To generate human monocyte-derived macrophages, isolated primary monocytes were cultured in complete RPMI-1640 medium (Gibco) with 50 ng mL⁻¹ recombinant human M-CSF (Peprotech) for 7 days. Surface markers for human macrophages such as CD163, CD206 were used to stain human monocyte-derived macrophages by flow cytometry. For morphology imaging, human monocyte-derived macrophages were plated on 384-well-plate (PerkinElmer) and stimulated with 250 ng mL⁻¹ PMA (Sigma-Aldrich) and 1 µg mL⁻¹ ionomycin (Sigma-Aldrich) for 5 h.

Microscopy and image analysis

Following incubation, cells were fixed with 3% Formalin (Pierce) in growth media for 15 min at 37 °C and incubated 15 min at 37 °C in permeabilization buffer (eBioscience) supplemented with 2% heat inactivated FBS (HyClone). Cells were stained first with anti- α -Tubulin antibodies (1:200, Sigma-Aldrich) for 1 h at RT followed by overnight staining at 4 °C with Phalloidin-Alexa488 (1:500; Thermo Fisher Scientific), DAPI (5 µg/ml, Thermo Fisher Scientific) and AF-555 secondary antibody conjugates (1:1000, Invitrogen). Finally, cells were washed and stored in PBS at 4 °C. Stained cells were imaged using PerkinElmer Opera Phenix high content screening system equipped with 20x (0.4NA) and 40x (1.1NA, water immersion) lenses, confocal unit (Yokogawa CSU-X) and solid state laser illumination (405nm, 488nm, 561nm, 640nm). Each plate was imaged twice: first with 20x lens to image all cells in each well (25x 1080x1080 pxl fields of view (FOV) per well; 640 nm/pxl resolution), followed by imaging with 40x lens to collect high-resolution images of cell footprint (9x 1080x1080 pxl FOV per well; 320 nm/pxl resolution; 3x Z stacks with dZ = 0.5 µm near the coverslip surface). All subsequent measurements were performed using the 20x dataset. 40x datasets were used to create representative images. Quantification of cell area and total amount of F-actin per cell

were done using CellProfiler software and custom written pipeline. Resulting measurements were then further processed using custom written Python scripts. Analysis of significance between donor groups was done using Mann–Whitney *U* test and Bonferroni correction for multiple comparisons.

Flow cytometry

Immunophenotyping was performed on a BD LSR-Fortessa. PBMC staining of surface markers was performed for 30 minutes at 4°C in the dark. The fixation/permeabilization kit for intracellular antigens or transcription factors (Affymetrix, eBioscience) were used for intracellular markers. Frozen PBMCs from patient and healthy donor controls were thawed and allowed to recover for four hours at 37°C in complete media (RPMI-1640 with 10% FBS). Following extracellular staining, cells were stimulated for 15 minutes at 37°C with Dynabeads© Human T activator CD3/CD28 (ThermoFisher) and IL2 (100 IU/mL). Cells were then immediately fixed for 10 minutes at 37°C, washed and permeabilized for 35 minutes on ice. Cells were then stained with p-AKT-PE for 1 hour at room temperature, washed again and resuspended in FACS buffer for flow cytometry analysis. All analyses were performed using FlowJo X (TreeStar Inc.) and Prism 8.0 (GraphPad Software). The following antibodies were used for flow cytometry: From Beckman Coulter: CD16-FITC (clone 3G8), CD4-PECy7 (SFC112T4D11), CD56-PE (N901), CD56-PECy5 (N901); from eBioscience, Affymetrix: CD4-PerCPCy5.5 (RPA-T4), CD19-PerCPCy5.5 (HIB19), CD69-APC (FN50), FOXP3-APC (236A/E7); from BD Biosciences: CD19-PECy7 (SJ25C1), CD14-PECy5 (61D3), CD16-PECy7 (3G8), CD25-PE (M-A251), CD25-BV605 (2A3), CD27-V450 (M-T271), CD3-APC-H7 (SK7), CD4-BV605 (RPA-T4), CD45RA-AF700 (HI100), CD56-V450 (B159), CD8-V450 (RPA-T8), IgD-FITC (IA6-2), anti-AKT-PE (pS473); from Biolegend: CD163-BV605 (GHI/61), CD206-PE (MMR); from Miltenyi Biotec: IgA-PE (IS11-8E10); IgG-APC (IS11-3B2.2.3).

Immunoblotting

Whole cell lysates were prepared from control- and patient-derived expanded T cells, loaded on 10% acrylamide gel, separated by SDS-PAGE and transferred to a polyvinylidene difluoride membrane (Bio-Rad). Membranes were incubated with 5% BSA in Tris-buffered saline with 0.5% Tween (TBS-T) and were probed overnight with 1:1000 dilution of anti-p110 γ (4252) or anti-phospho-AKT Ser473 (D9E) or anti-AKT (pan, 40D4) from Cell Signaling, and 1:8000 dilution of anti-HSP90 α/β (Santa Cruz) as a loading control. Bands were revealed using Amersham ECL Select Western Blotting Detection Reagent (GE Healthcare).

Generation of CRISPR/Cas9-edited Jurkat cell lines

sgRNAs targeting *PIK3CG* were designed using the GPP Web portal (<https://portals.broadinstitute.org/gpp/public/analysis-tools/sgna-design>) and cloned into a lentiCRISPRv2 using FastDigest Esp3I (Thermo Fisher Scientific) and standard molecular cloning. Lentivirus was generated from transfection of Lenti-X 293T cells (Takara Bio) with Polyfect (Qiagen) using the lentiviral envelope and packing vectors pMD2.g and psPAX2. Lentiviral supernatant was harvested 48 h post transfection, filtered and directly applied to Jurkat E6-1 cells. Transduction was carried out by spinfection (1 h, 37°C, 800 rcf) in presence of 8 $\mu\text{g mL}^{-1}$ Polybrene. Transduced cells were selected with 1 $\mu\text{g mL}^{-1}$ Puromycin (Sigma). Single clones were selected by limiting dilution and editing was assessed using TIDE.⁶ The utilized knockout cells showed 84.6% total editing efficiency, with 21.5% at position +2, 42.9% at position +4 and 19.5% at position -1 after Cas9 cutting site. sgRNA and primer sequences for TIDE were as follows:

For sgRNA,

Fw: caccgAAGTATGACGTCAGTTCCCA,

Rv: aaacTGGGAAGTACTGACGTCATACTTc;

and for TIDE,

Fw: TCTAGCCGTGAAGACCCAGT,

Rv: GCATAATGCTGCTTAATTTTTCAGT.

Phagocytosis assay

The phagocytic function of neutrophils and monocytes was evaluated in 100 μ L of sodium-heparinized whole blood sample to 20 μ L pHrodo Red *E. coli* (Life Technologies) for 15 minutes at 37°C according to manufacturer's instructions. Erythrocytes were lysed using reagents provided in pHrodo Red *E. coli* BioParticles Phagocytosis Kit for Flow Cytometry (Life Technologies) and analyzed using flow cytometry (PE channel). Monocytes and neutrophils were distinguished based on forward/side scatter characteristics.

Neutrophil assays

Neutrophils were isolated from whole blood by Ficoll-Paque PLUS (GE Healthcare) density gradient centrifugation. After recovering of PBMCs, the remaining fraction was sequentially pulsed with Milli-Q water and 3 M KCl for erythrocyte lysis, and neutrophils were recovered by centrifugation. Isolated neutrophils were kept in complete RPMI-1640 media, spread on a 10cm culture dish, until further use. For detection of apoptotic cells, neutrophil samples were taken at the indicated time points, replaced by Annexin-V binding buffer (BD Biosciences), and stained on ice for 5 min with propidium iodide (BD Biosciences) and Annexin-V-APC (BD Biosciences), before acquisition by flow cytometry. HD neutrophils treated at 70 °C served as positive control for gate setting. Gating was based on forward/side scatter including live and dead neutrophils. For evaluation of mitochondrial membrane potential, neutrophil fractions were washed in PBS and stained with 3.5 μ M JC-1 (Thermo Fisher Scientific) for 15 min at 37 °C. After PBS wash, samples were treated with 100 nM valinomycin in complete RPMI-1640 media. Samples were either taken immediately (0 h) or incubated for 2 h. Cells were gated on single-cell neutrophils by forward/side scatter, and final gates were set on comparing

mitochondrial J-aggregates (PE channel) with cytosolic JC-1 monomers (AlexaFluor488 channel) appearing from mitochondrial membrane leakage. For evaluation of oxidative burst capacities, neutrophils were resuspended in pre-warmed KRP-PBS buffer and placed in a 37 °C thermoshaker. At time point 0, Oxyburst green reagent (Thermo Fisher Scientific, used 1:20) was added and samples were immediately taken at the indicated time points, by pipetting into tubes prepared with ice-cold PBS. For flow cytometry acquisition, an unlabeled sample was taken for peak setting (FITC channel) within the neutrophil scatter gate. For neutrophil chemotaxis, 50,000 neutrophils were placed into the upper chambers of a 96-well transwell plate (Corning, 5 µm pore size), and left to migrate towards 5 nM fMLP or DMSO control in complete RPMI. After 20 min incubation, migrated neutrophils were counted by forward/side scatter detection, and normalized to sample controls of 50,000 neutrophils seeded into the lower compartments, respectively, to reflect total input.

Statistical Analysis

Statistical evaluation of experimental data was performed using Prism version 8 (GraphPad Software, USA). Probability (*P*) values < 0.05 were considered statistically significant. *P* values and statistical tests are indicated in figure legends, where applicable.

SUPPLEMENTARY TABLES

Table S1: Characteristics of the identified germline-encoded *PIK3CG* variants.

Gene	Position	Ref.	Obs.	Substitution	PolyPhen-2	CADD	gnomAD allele counts	ExAC allele counts	ExAC pNull
<i>PIK3CG</i>	Chr7 106545777	A	G	p.N1085S	probably damaging	23.8	---	---	4.4365 E-06
<i>PIK3CG</i>	Chr7 106508151	C	A	p.R49S	benign	22	---	hom: 0, het: 2 (117466), MAF: 1.703 E-05	4.4365 E-06

Prediction scores were calculated with PolyPhen-2 and CADD tools.^{4,5} Current genomes include 10,738 (gnomAD, <https://gnomad.broadinstitute.org/>) and 60,706 individuals (ExAC, <http://exac.broadinstitute.org/>). MAF frequencies are indicated for identified heterozygotes (accession date: May 21, 2019). Gene names are indicated in italic font. (Ref.: reference; Obs.: observed; het: heterozygous; hom: homozygous; MAF: minor allele frequency; pNull: probability of loss-of-function tolerance; ---: not reported)

Table S2: Extended immunological features of patient T-cell subsets.

Variables	Patient (Dec 2018)
CD4+ (%)	61.6 (25-48)
CD45RA+ CCR7+ (%)	45.8 (43.3-63.2)
CD45RA- CCR7+ (%)	40.5 (30.85-45.25)
CD45RA- CCR7- (%)	12.7 (4.2-16.25)
CD45RA+ CCR7- (%)	0.88 (0.1-2.1)
Variables	Patient (Dec 2018)
CD8+ (%)	12.2 (9-35)
CD45RA+ CCR7+ (%)	60.1 (37-69.35)
CD45RA- CCR7+ (%)	19.7 (14-36.85)
CD45RA- CCR7- (%)	12.2 (2.4-15.5)
CD45RA+ CCR7- (%)	7.98 (3.9-27.25)

Reference ranges are indicated in round brackets. Values out of reference ranges are indicated in bold font.

SUPPLEMENTARY REFERENCES

1. Ozen, A. *et al.* CD55 Deficiency, Early-Onset Protein-Losing Enteropathy, and Thrombosis. *New England Journal of Medicine*. 2017;377(1):52–61.
2. Salzer, E. *et al.* RASGRP1 deficiency causes immunodeficiency with impaired cytoskeletal dynamics. *Nature Immunology*. 2016;17(12):1352–1360.
3. Müller, H. *et al.* VCF.Filter: Interactive prioritization of disease-linked genetic variants from sequencing data. *Nucleic Acids Research*. 2017;45(W1):W567–W572.
4. Kircher, M. *et al.* A general framework for estimating the relative pathogenicity of human genetic variants. *Nature Genetics*. 2014;46:310.
5. Adzhubei, I. A. *et al.* A method and server for predicting damaging missense mutations. *Nature Methods*. 2010;7(4):248–9.
6. Brinkman, EK. *et al.* Easy quantitative assessment of genome editing by sequence trace decomposition. *Nucleic Acid Research*. 2014;42(22):e168.

SUPPLEMENTARY FIGURE LEGENDS

Figure S1. Additional cellular data on patient cells. **(A)** Affected amino acid stretches of p110 γ are conserved across species. **(B)** Reduced NK cell frequency in patient peripheral blood. Numerical inserts depict percentages within the final gate. **(C)** Reduced degranulation capacity in patient-derived NK cells, as compared to mother and HD, indicative of impaired cytotoxic capacities. Peripheral blood-derived NK cells were incubated for 3 h with K562 target cells (middle panel) or NK cells activated with IL2 for 48 h prior to K562 target cells (right panel), and compared according to percentages of CD107a (LAMP1) positive CD3⁻CD56⁺ cells as a proxy of degranulation ability (* $P < 0.05$, ** $P < 0.01$, Two-way ANOVA). **(D)** Quantification of proliferated CD8⁺ T cells in percentage upon stimulation with various stimuli (** $P < 0.01$, Two-way ANOVA). **(E)** Impaired activation of AKT signaling in *PIK3CG*-mutated patient cells. Patient-derived expanded T cells were stimulated with SDF-1 for the indicated time points. Phospho-AKT signal intensity was compared with total AKT signal. HSP90 was used as housekeeping loading control. **(F)** Abrogated p110 γ and reduced p-AKT expressions in *PIK3CG* knockout (KO) Jurkat cells compared to Renilla KO control Jurkat cells. GAPDH was used as a housekeeping loading control. **(G)** Reduced normalized mean fluorescence intensity (MFI) of AKT Ser473 phosphorylation in *PIK3CG* KO Jurkat cells compared to Renilla KO control (** $P < 0.01$, Mann-Whitney U test). Dotted line represents the normalization to unstained control. **(H)** Genetic rescue of CD69⁺ activation (normalized) in *PIK3CG* KO Jurkat cells using wild-type (WT) vector, empty vector (EV), mutant N1085S or mutant R49S vectors ($P = 0.1$, Mann-Whitney U test). **(I)** Intact cytotoxic capacity in patient CTLs compared to cells from mother and HDs. Cells were incubated for 3 h with CD3/CD28 stimulation and compared according to mean fluorescence intensity (MFI) of CD107a (LAMP1) on CD3⁻CD8⁺ T cell surfaces as a proxy of degranulation ability. **(J)** Increased frequency of peripheral blood CD4⁺CD127^{dim}FOXP3⁺CD25⁺ T_{reg} cells in patient, compared to mother and HD. Numerical

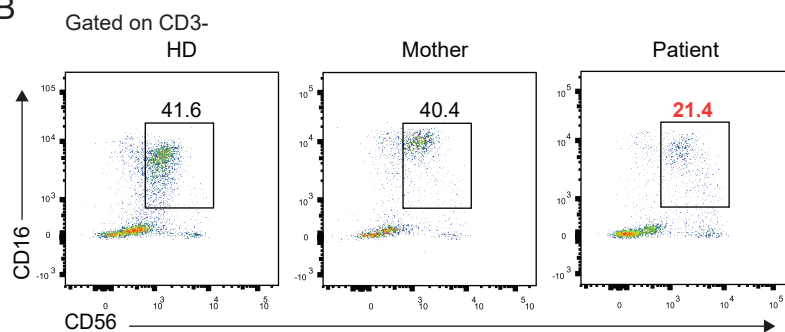
inserts depict percentages. **(K)** Patient B cells proliferate normally during 5-day stimulation with CpG or CD40L in combination with IL4 or IL21. **(L)** Class switch recombination capacity of patient B cells is intact after 5-day stimulation with CD40L with IL4.

Figure S2. Additional data on innate immune cells. **(A)** Comparable macrophage surface markers CD163 and CD206 on monocyte-derived macrophages of patient, mother and HD, after 9 days in differentiation culture. **(B)** Violin plots showing average cell number per image of patient, mother and HD. **(C)** Slightly elevated cell death in patient neutrophils. Freshly-isolated neutrophils showed a pronounced propidium iodide-positive population (top, red numerical insert). Apoptotic neutrophils persist during incubation (bottom). Numerical inserts indicate percentages. **(D)** Compromised mitochondrial membrane potential in patient neutrophils. Mitochondria were stained with JC-1 dye, membrane leakage was monitored during incubation with valinomycin. Presence of mitochondrial J-aggregates was compared with appearance of cytosolic JC-1 monomers. Patient neutrophils rapidly lose membrane integrity compared to mother and HD, as observed by the increased dye loss (red numerical insert). Numerical inserts indicate percentages. **(E)** Patient neutrophils are able to initiate oxidative burst upon Fc receptor stimulation as shown by the appearance of oxyburst green-positive cells. **(F)** Patient-derived neutrophils are able to migrate towards fMLP, compared to cells from HDs and mother.

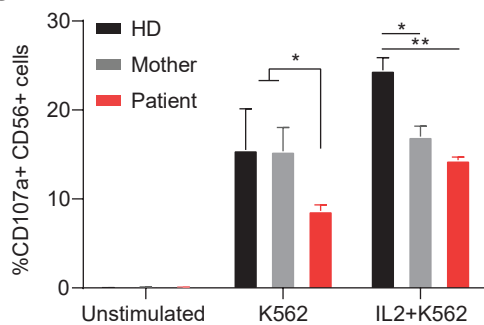
A

	het. p.R49S	
H. sapiens	ELIPIEFVLPSTQRKCKSPETALLHVAG	63
P. troglodytes	ELIPIEFVLPSTQRKCKSPETALLHVAG	63
M. musculus	ELIPIEFVLPSTQRISKTPETALLHVAG	63
X. tropicalis	EQIPIEFILPSTNRCSKVQETMLLEVAG	63
	het. p.N1085S	
H. sapiens	FLDQIEVCRDKGWTVQFNWFLHLVLGIK	1095
P. troglodytes	FLDQIEVCRDKGWTVQFNWFLHLVLGIK	1095
M. musculus	FLDQIEVCRDKGWTVQFNWFLHLVLGIK	1095
X. tropicalis	FLDQIEVCRDKGWTVQFNWFLHLVLGIK	1095

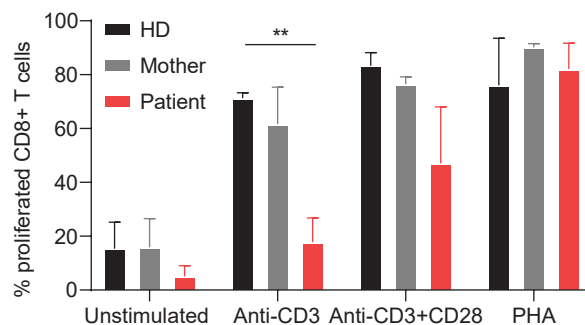
B



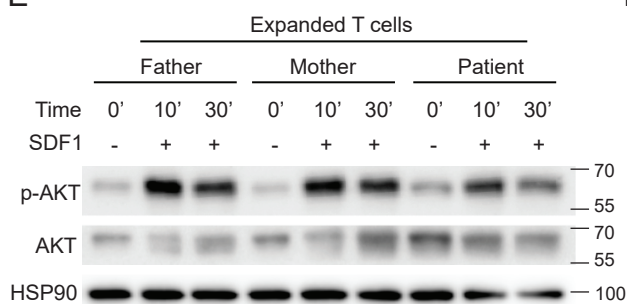
C



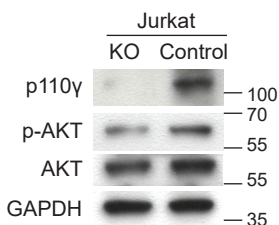
D



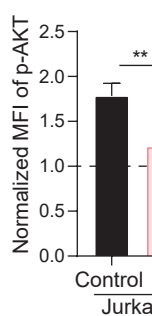
E



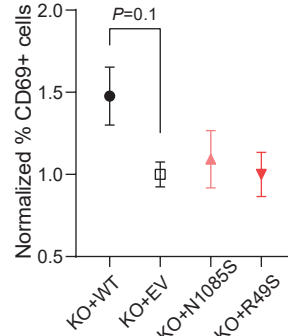
F



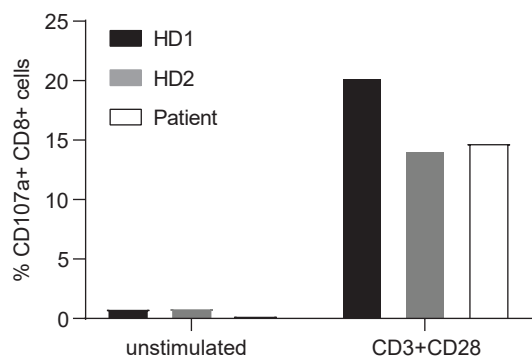
G



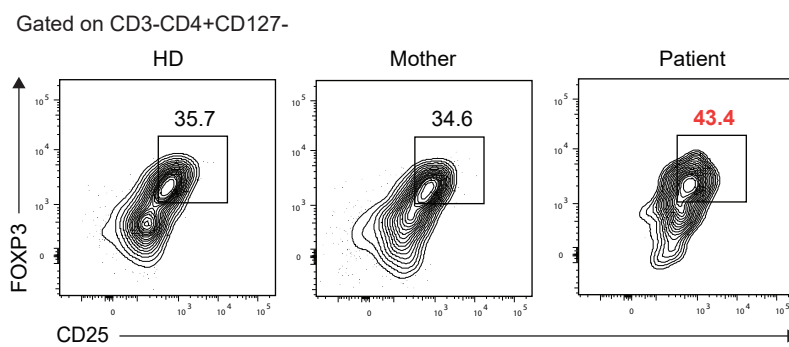
H



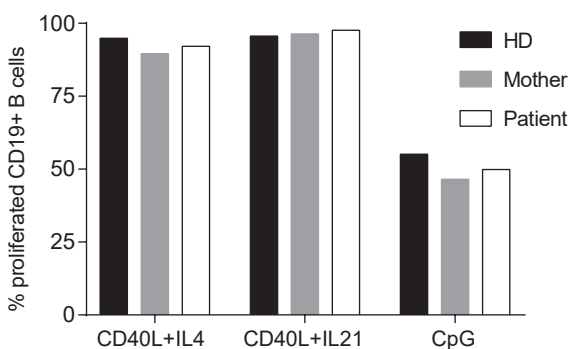
I



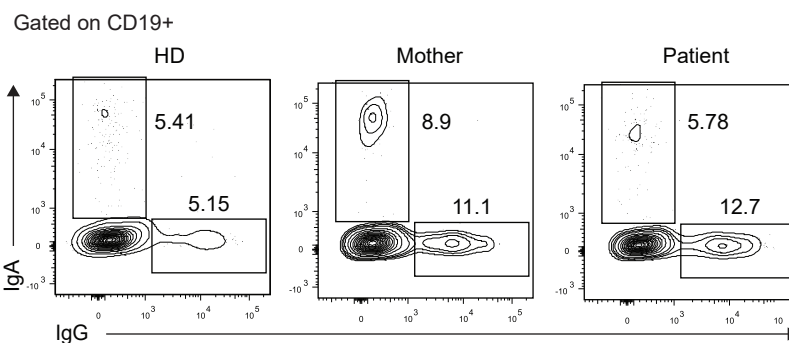
J

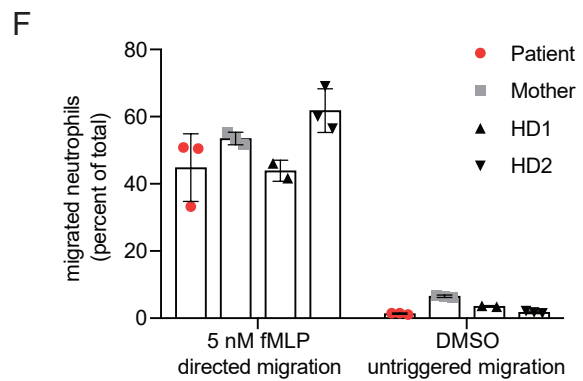
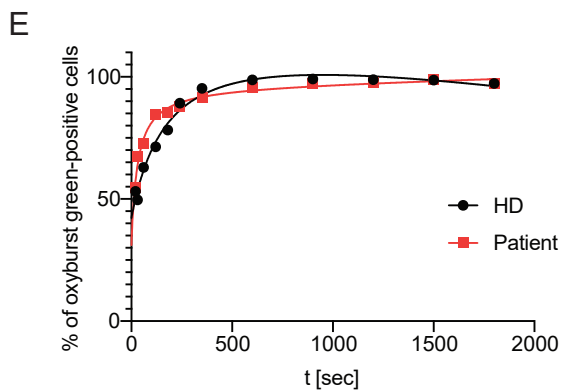
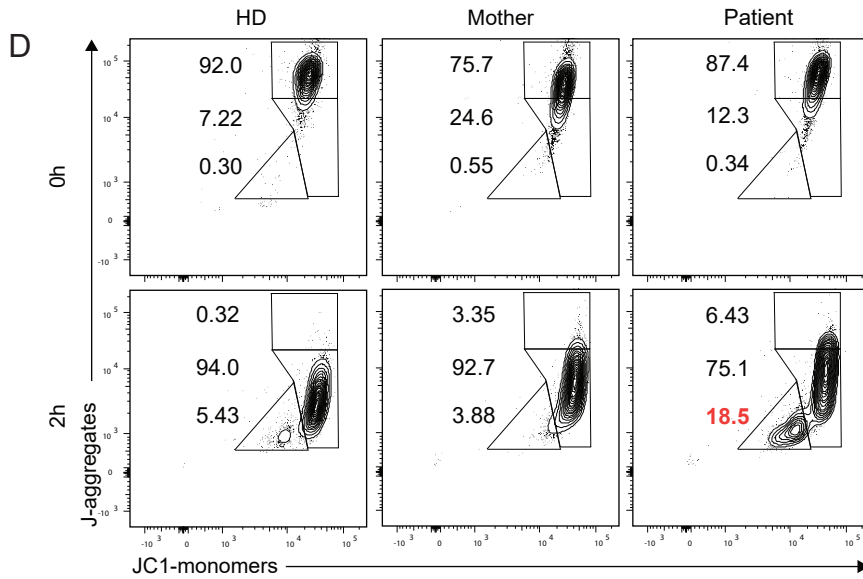
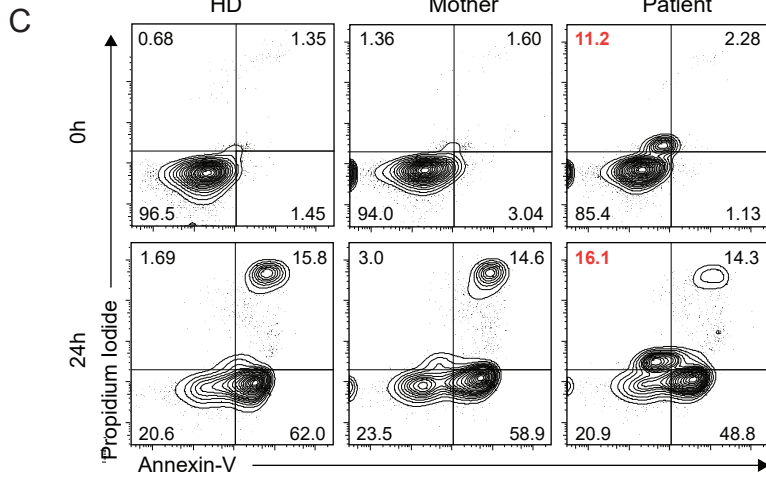
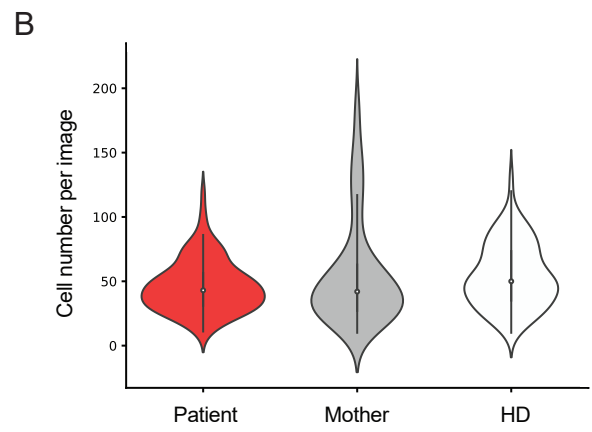
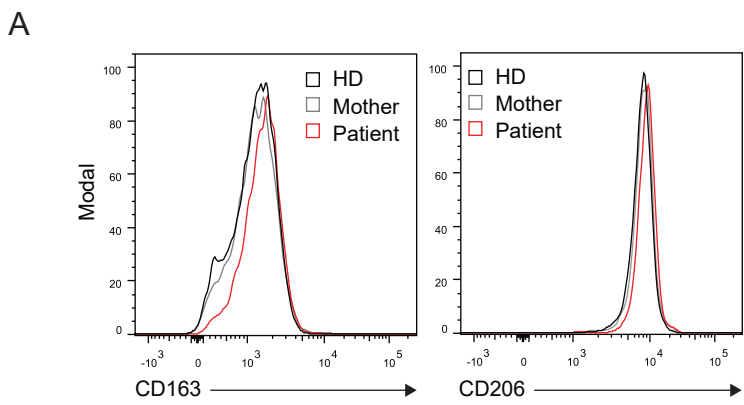


K



L





4. Discussion

In the following chapters, we will discuss each manuscript from the results section in detail. We will first understand the basic biology, followed by discussing novel findings in the context of prior knowledge from the literature.

4.1. Human CD137 deficiency and impaired EBV immunity

4.1.1. The role of CD137 in immunity

CD137 (also known as 4-1BB or TNFRSF9) is a costimulatory molecule expressed transiently by activated T cells, while its ligand (CD137L or 4-1BBL) is expressed on activated APCs such as DCs, macrophages and B cells. However, many non-immune cells also express CD137L constitutively, albeit in low amount. A bidirectional signaling exists in CD137-CD137L system (Kwon, 2015; Etxeberria et al, 2020).

Functionally, costimulation of CD137 or CD137 ligation in T cells leads to the production of IL-2 and IFN- γ as well as T-cell proliferation. It has been reported that CD137 costimulation promotes T-cell differentiation into memory and effector T cells. Furthermore, CD137 costimulation protects T cells from apoptosis and increase T-cell respiratory capacity. Signaling downstream of CD137 is mediated by TNF-receptor associated factor 1 and 2 (TRAF1 and TRAF2) to activate NF- κ B, ERK, p38 MAPK and AKT pathways. These signaling pathways induce the expression of survival genes while reducing the expression of pro-apoptotic genes (Ward-Kavanagh et al, 2016; Etxeberria et al, 2020).

CD137 has been implicated in autoimmune several disorders. Studies have shown that targeting CD137-CD137L signaling interaction resulted in reduced disease severity in multiple models of autoinflammatory and autoimmune diseases. An increase serum levels of soluble CD137 has been reported in MS and RA patients, indicating that CD137 might be a useful biomarker for disease severity, as well as a target for clinical trials. Interestingly, stimulation of CD137 signaling with an agonist monoclonal antibody (mAb) also alleviated allograft response and autoimmune disorders in preclinical models. It has been proposed that CD137 mAb induce apoptosis of pathogenic CD8⁺ T cells and induce differentiation of suppressive Tregs (Ward-Kavanagh et al, 2016). However, exactly how CD137 exerts its role in autoinflammation and autoimmunity is unclear.

Studies using tumor models showed CD137 is inducible on both CD8⁺ and CD4⁺ T cells, including Tregs. However, CD137 has a dominant role of CD137 in CD8⁺ T cells. CD137 agonists were shown to prevent CTL anergy and thereby break T-cell tolerance towards tumor antigens, restore T-cell dysfunctionality in the tumor microenvironment (TME) and increase persistence of tumor-specific CTLs (Etxeberria et al, 2020).

Owing to its strong costimulatory activity and expression on tumor-specific T cells to maintain cytotoxic function and favors survival and memory differentiation in TME, CD137 is considered an appealing target for immunotherapy. Moreover, CD137 functions to enhance Treg expansion which can be a target to selectively deplete Tregs that have higher CD137 expressions (Etxeberria et al, 2020).

CD137 agonistic mAb (Urelumab and Utolimumab) are currently in clinical trials and are also studied in combination with checkpoint inhibitors such as CTLA-4 and PD-1 inhibitors in order to selectively activate tumor targeting T- and NK-cells in order to provide a robust antitumor response. True synergistic combinations are a major aim in cancer immunotherapy which in this case, could also be achieved with bispecific antibodies containing both activities in a single moiety (Etxeberria et al, 2020).

CD137 signaling is also utilized in chimeric antigen receptor (CAR) T cell immunotherapy. A CAR usually consists of an extracellular domain that binds to a specific antigen on tumor cells, a transmembrane domain and intracellular domains which provide signals for T-cell activation to target tumor cells. The addition of the CD137 to the intracellular anti-CD3 ζ motif enhances cytotoxicity with persistent anti-tumor response in vivo (Song et al, 2011; Porter et al, 2011). To date, the only CD137-based approach approved by the Food and Drug Administration (FDA) is the CD19 targeting CAR-T cells (Tisagenlecleucel) for the treatment of B-cell pediatric lymphoblastic leukemia (Maude et al, 2018) and refractory diffuse large B-cell lymphoma (Schuster et al, 2019).

4.1.2. Human CD137 deficiency

Since its discovery, CD137 has gained significant attention and has been studied extensively (Kwon & Weissman, 1989; Schwarz et al, 1993). However, only recently, three independent studies including the work done in this thesis (chapter 3.1.) reported patients with germline mutations in *TNFRSF9* encoding for CD137 (Alosaimi et al, 2019; Somekh et al, 2019; Rodriguez et al, 2019).

For the first time, a total of 6 novel mutations in 7 patients were characterized. Alosaimi et al. identified two unrelated patients who shared the same homozygous missense mutation in *TNFRSF9*. Both patients successfully underwent hematopoietic stem cell transplantation (Wildermann et al, 2021). Activated T cells showed abolished CD137 expression in both patients and they suffered from immunodeficiency and EBV-driven lymphoproliferation, one patient additionally developed HLH and another patient developed Hodgkin's lymphoma. CD8⁺ T cell expansion, expression of IFN- γ and perforin, and cytotoxicity against allogeneic EBV-transformed B cells were significantly impaired in both patients. Moreover, patient activated CD8⁺ T cells showed defective mitochondrial function (Alosaimi et al, 2019).

In the work included in this thesis (chapter 3.1.), the author of this thesis and colleagues reported four unrelated patients with four distinct homozygous mutations in *TNFRSF9*. Interestingly, in 3 of the pedigrees, 1 healthy sibling each was also homozygous for the same *TNFRSF9* mutation, suggesting incomplete penetrance of the disease. All patients suffered from immunodeficiency and two of them additionally developed EBV-related lymphoma (Burkitt's and Hodgkin's) and one developed EBV-induced lymphoproliferation. Defects were observed in both T- and B-cell populations including activation and proliferation. Upon exogenous expression of wildtype CD137, T-cell proliferation and activation defects were restored. Additionally, we showed that defective proliferation in CD137-deficient T cells can be restored by other costimulatory molecules such as OX40 or CD28. We also showed a significant reduction in the diversity of the TCR repertoires, impaired EBV-specific CTL cytotoxicity and impaired CSR in patient B cells. The study also highlighted the previously less appreciated direct role of CD137 in activated B cells since it was more widely known that its ligand, CD137L is expressed on APCs such as B cells. Our study showed that CD137 can also be expressed in activated human B cells and may play a direct role in proper

differentiation and function of B cells. Consistently, patients showed highly reduced proportions of memory B cells, plasmablasts and T_{FH} cells (Somekh et al, 2019).

Rodriguez et al. reported a patient with homozygous LOF mutations in *PIK3CD* and *TNFRSF9*. The patient suffered from EBV-related T cell lymphoproliferative disease. The patient has a sister who is asymptomatic but shared the same homozygous mutation in *TNFRSF9*. The sister has persistently high EBV load but normal immunological parameters, except for a low proportion of memory B cells, suggesting incomplete clinical penetrance. There were defective activation and proliferation of T cells from the patient and sister. These defects were restored in T cells from the sister upon CD137 expression using lentiviral vector, as the patient eventually succumbed to fatal HLH (Rodriguez et al, 2019).

Phenotypic distinctions between individuals can often be attributed to variation in underlying genetic and environmental conditions. Interestingly, a total of 4 siblings with the same homozygous *TNFRSF9* mutations found in the patients were healthy and asymptomatic, indicating a strong incomplete clinical penetrance mode of inheritance. Further studies on other genetic variants, genetic expressions of other costimulatory molecules as well as epigenetic regulation would be important to address the phenotypic differences in these individuals even in homogeneous environments.

4.1.3. Defective EBV immunity in CD137-deficient patients

A robust immunity is crucial to defend the body against pathogens such as EBV. In individuals with impaired immune function, EBV infection may result in life-threatening diseases as discussed in chapter 1.4.2.

In the three studies of human CD137 deficiency reported so far, all patients had EBV viremia and 6 out of 7 patients developed EBV-driven diseases. These data strongly support a key role for CD137 in host immunity against EBV. A robust immune response against virus includes effective cytotoxic killing of infected cells. In this regard, Alosaimi et al. and the work presented in this thesis have independently shown that CD137-deficient patients have impaired EBV-specific CD8⁺ T cell cytotoxic killing (Alosaimi et al, 2019; Somekh et al, 2019). This suggests that a functional CD137 is essential in controlling EBV infection and its associated diseases and malignancies.

Additionally, the lack of CD137 will inevitably affect CD137-CD137L interaction, which induces a bidirectional signaling. Consistently, CD137L-deficient mice developed B-cell lymphomas (Middendorp et al, 2009). The loss of reverse signaling by CD137L on the APCs of CD137-deficient patient T cells may contribute to the observed phenotypes.

Costimulatory signaling through other TNFR superfamily members have also been identified to play a nonredundant role in EBV immunity, such as CD27 and its ligand, CD70. While CD137 is expressed upon activation in T cells, CD27 is constitutively expressed. Patients with CD27 or CD70 deficiency also suffered from EBV-associated diseases. Studies have shown that these patients have defective EBV-specific CTL cytotoxicity response (Tangye & Latour, 2020). Nonredundant functions of different human TNFR superfamily members could be clarified with studies involving patients with mutations and/or deficiencies in these molecules in the future.

Further studies on the use of CD137 agonistic mAb may be explored in CD137 deficient patients and patients with EBV-associated malignancies such as Hodgkin's lymphoma.

4.2. Human PI3K γ deficiency and immune dysregulation

4.2.1. The biology of PI3K γ

Studies on PI3K in human disease have highlighted phosphatidylinositol 3-kinase gamma (PI3K γ) as an appealing drug target for treatment of human proliferative disorders (Rückle et al, 2006; Janku et al, 2018).

PI3K γ consists of a catalytic protein (p110 γ) encoded by *PIK3CG*, and a regulatory domain (p84/p101). PI3K γ is activated by GPCRs such as chemokine receptors. Both the regulatory and catalytic subunits of PI3K γ directly bind to G-protein $\beta\gamma$ subunits upon activation. p110 γ contains a classical Ras-binding domain (RBD) which can bind RAS-GTP directly to further regulate its catalytic activity. PI3K γ belongs to class IB PI3Ks which selectively phosphorylate PIP₂ to form PIP₃, the latter serving as recruiting moiety to localize effector proteins at the plasma membrane, via interaction with their pleckstrin homology domain. Subsequently, AKT is phosphorylated and activated which in turn, phosphorylates a myriad of downstream substrates (Rommel, 2007; Fruman et al, 2017).

PI3K γ is highly expressed in various immune cells, including mast cells, macrophages, neutrophils, and eosinophils. Studies showed that PI3K γ plays fundamental roles in chemokine-dependent leukocyte chemotaxis and mast cell activation (Janku et al, 2018). PI3K γ -mutant mice showed defective neutrophil and macrophage recruitment in response to inflammatory stimuli to the sites of inflammation. Neutrophil oxidative burst, T-cell activation and DC migration were also impaired in these mice (Rommel, 2007).

The development of PI3K isoform-specific inhibitors has gained much attention in order to treat immune disorders. Treatment with PI3K γ -selective inhibitor has been shown to reduce glomerulonephritis and increase survival in a model of systemic lupus erythematosus (SLE). Moreover, PI3K γ was defined as a promising target for airway inflammatory diseases and RA (Rommel, 2007).

Preclinical studies have demonstrated that tumor-associated macrophages (TAMs) highly expressed PI3K γ which can contribute to resistance to immune-checkpoint inhibitors such as anti-CTLA4. The use of selective pharmacologic targeting PI3K γ reprogrammed TAMs from M2-like phenotype characterized by expression of IL-10

and TGF- β to M1-like phenotype which promote CTL-mediated tumor regression, increase proinflammatory cytokine production and restore tumor sensitivity to immune-checkpoint inhibitors (Fruman et al, 2017; Janku et al, 2018).

Currently, selective inhibitor of PI3K γ which is orally administered, IPI-549 is being tested in clinical trials as a monotherapy and in combination with immune-checkpoint inhibitor nivolumab in patients with different advanced-stage carcinomas or melanoma (Janku et al, 2018).

4.2.2. Human *PIK3CG* mutations

Germline mutations in several components of PI3K signaling pathway have been identified and characterized in humans leading to immunodeficiency and immune dysregulation (Nunes-Santos et al, 2019). Even though its role has been widely investigated in mouse models, germline biallelic mutations in PI3K γ complex or its components have not been described until recently.

In 2019, Takeda et al. reported the first description of germline biallelic human PI3K γ deficiency while our independent investigation was ongoing in our patient. The patient inherited compound heterozygous mutations in *PIK3CG* encoding for p110 γ . The patient had humoral defects and lymphocytic tissue infiltration. More recently, she suffered from enterocolitis and autoimmune hemolytic anemia and autoimmune cytopenia. Currently, the patient is treated with immunoglobulin replacement therapy and mycophenolate mofetil to suppress inflammation. Patient T cells showed defects in activation with increased T_H1 marker CXCR3. Inflammatory cytokines were found to be elevated in patient serum. Using PI3K γ inhibitor in THP-1 cell line and THP-1 *PIK3CG* shRNA knockdown, Takeda et al. showed an upregulation and secretion of IL-12 and IL-23, which can be restored using a GSK3 inhibitor upon stimulation. Moreover, *Pik3cg*-deficient mice also showed an upregulation and secretion of IL-12 upon stimulation (Takeda et al, 2019).

In the work presented in this thesis (chapter 3.2.), the author of this thesis and colleagues reported the second patient with novel germline compound heterozygous mutations in *PIK3CG*. The patient presented with systemic autoinflammation with HLH-like phenotype. Patient responded well to the recombinant human anti-IL-1 β (Anakinra) therapy in combination with dexamethasone. *PIK3CG* mutations caused reduced T-cell activation, proliferation and AKT signaling upon PI3K γ -dependent stimulation, and

defects were phenocopied by a PI3K γ inhibitor and in Jurkat *PIK3CG* knockout (KO) cell line. These defects were restored by exogenous expression of wildtype p110 γ in primary patient cells and Jurkat *PIK3CG* KO cell line. NK-cell numbers and degranulation capacity were moderately decreased, but not to the extent characteristic of HLH. Patient monocyte-derived macrophages showed impaired phagocytosis and decreased cell spreading and total actin intensity upon stimulation. In addition, patient-derived neutrophils showed defective phagocytosis and elevated cell death. No humoral defects such as activation, proliferation nor CSR were observed (Thian et al, 2020).

Interestingly, the two patients described with compound heterozygous loss-of-function mutations in *PIK3CG* have different clinical phenotypes, which are likely contributed by different mutations as well as external factors such infections and environmental variation. However, both patients suffered from autoinflammation and are currently treated with anti-inflammatory drugs. Therefore, future studies on patients with different *PIK3CG* mutations would be helpful to understand the precise role of PI3K γ in human immunity and its full clinical manifestations.

4.2.3. Immune dysregulation in PI3K γ -deficient patients

Different experimental systems have shown conflicting conclusions regarding inflammatory and anti-inflammatory functions of PI3K γ . In the two studies of human PI3K γ deficiency reported so far, both patients showed defects in monocytes, macrophages and T cells which resulted in inflammation with immune dysregulation. Both studies thus clarified the importance of human PI3K γ in controlling inflammation and immune regulation.

PI3K γ has been shown in mice to mediate the migration of immune cells such as neutrophils and DCs. In addition, pre-exposure of neutrophils to TNF impaired the generation of reactive oxygen species (ROS) induced by subsequent stimuli such as chemo-attractants by *Pik3cg*-deficient mice (Rommel et al, 2007). However, both studies in PI3K γ -deficient patients demonstrated normal neutrophil migration and ROS production under the conditions tested. It is therefore possible that other PI3K isoforms such as PI3K δ works synergistically with PI3K γ in neutrophil migration and ROS production and PI3K δ may compensate for the loss of PI3K γ function in human neutrophils. Despite the normal neutrophil migration and ROS production, the work included in this thesis clarified that PI3K γ plays a more important role in the survival

and function of human neutrophils (Thian et al, 2020). Therefore, the two studies provided valuable insights into the difference between human and mouse systems.

Interestingly, the patient reported by Takeda and colleagues was presented with hypogammaglobulinemia and autoimmunity. However, no defects in B cells were found in the patient reported by the author of this thesis (Thian et al, 2020) and the patient mainly suffered from autoinflammation rather than autoimmunity. It is unclear whether humoral defects seen in the patient reported by Takeda et al is intrinsically due to the mutations in *PIK3CG* or indirectly due to the impairment of T cell function. Further studies with different patients are crucial to clarify the role of human PI3K γ in humoral immunity.

Both studies also utilized selective PI3K γ inhibitor IPI-549 on healthy primary human cells which mimicked PI3K γ -deficient patient phenotype. As IPI-549 is currently in clinical trials for its use in cancer patients, it will be helpful to monitor the development of immunodeficiency and inflammation.

Collectively, the two studies highlight the pleiotropic role of human PI3K γ in regulating innate and adaptive immune responses and reveal a pivotal role in restraining inflammation. Larger patient cohorts and longer follow up will thus be necessary to unravel the full clinical spectrum of the disease.

5. Conclusion and Outlook

Altogether, the work in this thesis revealed hitherto novel roles of human CD137/ 4-1BB and PI3K γ in immune activation, function, and regulation. Our work has contributed to the genetic and molecular diagnosis of patients suffered from previously unknown diseases and therefore served to encourage better characterization of these diseases in future studies. Furthermore, our work opened avenues to the identification of better treatment options and personalized therapy for these patients.

References

- Akar HH, Patiroglu T, Hershfield M, and Van Der Burg M (2016) Combined Immunodeficiencies : Twenty Years Experience from a Single Center in Turkey. *Clin. Immunol.* 41:107–15.
- Al-samkari H, and Berliner N (2018) Hemophagocytic Lymphohistiocytosis. *Ann. Rev. Pathol. Mech. Dis.* 13:27-49.
- Alosaimi MF et al (2019) Immunodeficiency and EBV-Induced Lymphoproliferation Caused by 4-1BB Deficiency. *J. Allergy Clin. Immunol.* 144:574-583
- Bevins CL, and Salzman NH (2011) Paneth Cells, Antimicrobial Peptides and Maintenance of Intestinal Homeostasis. *Nat. Rev. Microbiol.* 9:356-368.
- Broz P, and Dixit VM (2016) Inflammasomes: mechanisms of assembly, regulation and signaling. *Nat. Rev. Immunol.* 16:407-420.
- Chen L, and Flies DB (2013) Molecular Mechanisms of T Cell Co-stimulation and Co-inhibition. *Nat. Rev. Immunol.* 13:227–42.
- Coillard A, and Segura E (2019) In Vivo Differentiation of Human Monocytes. *Front. Immunol.* 10:1–7.
- Croft M (2003) Co-Stimulatory Members of the TNFR Family: Keys to Effective T-Cell Immunity? *Nat. Rev. Immunol.* 3:609–20.
- Croft M et al (2012) TNF Superfamily in Inflammatory Disease: Translating Basic Insights. *Trends Immunol.* 33: 144–52. <http://dx.doi.org/10.1016/j.it.2011.10.004>.
- Croft M, Benedict CA, and Ware CF (2013) Clinical Targeting of the TNF and TNFR Superfamilies. *Nat. Rev. Drug Discov.* 12:147-168. <http://dx.doi.org/10.1038/nrd3930>.
- Crotty S (2019) T Follicular Helper Cell Biology: A Decade of Discovery and Diseases. *Immunity* 50:1132-48.
- Etzeberria I, Glez-Vaz J, Teijeira A, and Melero I (2020) New Emerging Targets in Cancer Immunotherapy: CD137/4-1BB Costimulatory Axis. *ESMO Open* 4:e000733. [doi:10.1136/esmoopen-2020-000733](https://doi.org/10.1136/esmoopen-2020-000733)

Fruman DA et al (2017) Review The PI3K Pathway in Human Disease. *Cell* 170: 605–35. <http://dx.doi.org/10.1016/j.cell.2017.07.029>.

Gasteiger G et al (2017) Cellular Innate Immunity: An Old Game with New Players. *J. Innate Immun.* 9:111–25.

Geginat J et al (2014) Plasticity of Human CD4 T Cell Subsets. *Front. Immunol.* 5:1–10.

George MR (2014) Hemophagocytic Lymphohistiocytosis: Review of Etiologies and Management. *J. Blood Med.* 5:69–86.

Häger M, Cowland JB, and Borregaard N (2010) Neutrophil Granules in Health and Disease. *J. Intern. Med.* 268:25–34.

Havnaer A, and Han G (2019) Autoinflammatory Disorders: A Review and Update on Pathogenesis and Treatment. *Am. J. Clin. Dermatol.* 20: 539–64.

Hawkins PT, and Stephens LR (2015) PI3K Signalling in inflammation. *Biochimica et Biophysica Acta* 1851: 882–97.

Hayden MS, and Sankar Ghosh (2012) NF- κ B, the First Quarter-Century: Remarkable Progress and Outstanding Questions. *Genes Dev.* 26: 203–34.

Hirahara K, and Nakayama T (2016) CD4⁺ T-Cell Subsets in Inflammatory Diseases: Beyond the Th1/Th2 Paradigm. *Int. Immunol.* 28: 163–71.

Hwang, J-R, Byeon Y, Kim D, and Park S-G (2020) Recent Insights of T Cell Receptor-Mediated Signaling Pathways for T Cell Activation and Development. *Exp. Mol. Med.* 52:750–61. <http://dx.doi.org/10.1038/s12276-020-0435-8>.

Janku F, Yap TA, and Meric-Bernstam F (2018) Targeting the PI3K Pathway in Cancer: Are We Making Headway? *Nat. Rev. Clin. Oncol.* 15: 273-291.

Koyasu S (2003) The Role of P13K in Immune Cells. *Nat. Immunol.* 4:313–19.

Krainer J, Siebenhandl S, and Weinhäusel A (2020) Systemic Autoinflammatory Diseases. *J. Autoimmun.* 109:1-10.

Kumar BV, Connors TJ, and Farber DL (2018) Human T Cell Development, Localization, and Function throughout Life. *Immunity* 48:202-13.

Kwon B, and Weissman SM (1989) cDNA sequences of two inducible T-cell genes. *Proc. Natl. Acad. Sci.* 86:1963-67.

Kwon B (2015) Is CD137 Ligand (CD137L) Signaling a Fine Tuner of Immune Responses? *Immune Netw.* 15:121–24.

Liu T, Zhang L, Joo D, and Sun S-C (2017) NF- κ B Signaling in inflammation. *Signal Transduct. Target Ther.* 2:e17023

Long HM, Meckiff BJ, and Taylor GS (2019) The T-Cell Response to Epstein-Barr Virus– New Tricks From an Old Dog. *Front. Immunol.* 10: 1–11.

Manning BD, and Toker A (2017) AKT/PKB Signaling: Navigating the Network. *Cell* 169:381–405.

Maude SL et al (2018) Tisagenlecleucel in Children and Young Adults with B-Cell Lymphoblastic Leukemia. *N. Engl. J. Med.* 278:439–48.

Mccusker C, and Warrington R (2011) Primary Immunodeficiency. *Allergy Asthma Clin Immunol.* 7: 1–8.

Middendorp S et al (2018) Mice Deficient for CD137 Ligand Are Predisposed to Develop Germinal Center–Derived B-Cell Lymphoma. *Blood* 114: 2280–90.

Murphy K (2012) Janeway’s Immunobiology 8th Edition. New York: Garland Science, Taylor & Francis Group, LLC.

Nemazee D (2017) Mechanisms of Central Tolerance for B Cells. *Nat. Rev. Immunol.* 17:281-94.

Nunes-santos CJ, Uzel G, and Rosenzweig SD. PI3K Pathway Defects Leading to Immunodeficiency and Immune Dysregulation. *J. Allergy Clin. Immunol.* 143: 1676–87. <https://doi.org/10.1016/j.jaci.2019.03.017>.

Oeckinghaus A, Hayden MS, and Ghosh S (2011) Crosstalk in NF- κ B Signaling Pathways. *Nat. Immunol.* 12: 695–708.

Porter DL et al (2011) Chimeric Antigen Receptor–Modified T Cells in Chronic Lymphoid Leukemia. *N. Engl. J. Med.* 365:725-33.

Raphael I, Nalawade S, Eagar TN, and Forsthuber TG (2015) T Cell Subsets and Their Signature Cytokines in Autoimmune and Inflammatory Diseases. *Cytokine* 74: 5–17.

Ratajczak W, Niedźwiedzka-rystwej P, Tokarz-deptuła B, and Deptuła W (2018) Immunological Memory Cells. *Centr. Eur. Immunol.* 43:194–203.

Revy P et al (2000) Activation-Induced Cytidine Deaminase (AID) Deficiency Causes the Autosomal Recessive Form of the Hyper-IgM Syndrome (HIGM2). *Cell* 102: 565–75.

Rodriguez R et al (2019) Concomitant PI3KCD and TNFRSF9 Deficiencies Cause Chronic Active Epstein-Barr Virus Infection of T Cells. *J. Exp. Med.* 216: 2800–18.

Rommel C, Camps M, and Ji H (2007) PI3K δ and PI3K γ : Partners in Crime in Inflammation in Rheumatoid Arthritis and Beyond? *Nat. Rev. Immunol.* 7:191–201.

Rückle T, Schwarz MK, and Rommel C (2006) PI3K γ Inhibition: Towards an ‘Aspirin of the 21st Century’? *Nat. Rev. Drug Discov.* 5:903–18.

Ruland J (2011) Return to Homeostasis: Downregulation of NF- κ B Responses. *Nat. Immunol.* 12:709–14.

Sakurai H et al (1999) I κ B Kinases Phosphorylate NF- κ B P65 Subunit on Serine 536 in the Transactivation Domain. *J. Biol. Chem.* 274:30353–56.

Sanchez-Paulete AR et al (2016) Deciphering CD137 (4-1BB) Signaling in T-Cell Costimulation for Translation into Successful Cancer Immunotherapy. *Eur. J. Immunol.* 46:513–22.

Schatz DG, and Ji Y (2011) Recombination Centres and the Orchestration of V(D)J Recombination. *Nat. Rev. Immunol.* 11:251-63.

Schroeder HW Jr, and Cavacini L (2010) Structure and function of immunoglobulins. *J. Allergy Clin. Immunol.* 125:S41-S52.

Schuster SJ et al (2019) Tisagenlecleucel in Adult Relapsed or Refractory Diffuse Large B-Cell Lymphoma. *N. Engl. J. Med.* 380:45-56.

Schwarz H, Tuckwell J, and Lotz M (1993) A Receptor Induced by Lymphocyte Activation (ILA): A New Member of the Human Nerve-Growth-Factor/ Tumor-Necrosis-Factor Receptor Family. *Gene* 134: 295–98.

Sharpe AH (2009) Mechanisms of Costimulation. *Immunol. Rev.* 229:5–11.

Shevyrev D, and Tereshchenko V (2020) Treg Heterogeneity, Function, and Homeostasis. *Front. Immunol.* 10:1–13.

Sieni E et al (2014) Familial Hemophagocytic Lymphohistiocytosis: When Rare Diseases Shed Light on Immune System Functioning. *Front. Immunol.* 5:1–19.

Smale ST (2011) Hierarchies of NF- κ B Target-Gene Regulation. *Nat. Immunol.* 12: 689–94.

Somekh I et al (2019) CD137 deficiency Causes Immune Dysregulation with Predisposition to Lymphomagenesis. *Blood* 134:1510–16.

Song D-G et al (2011) In Vivo Persistence, Tumor Localization, and Antitumor Activity of CAR-Engineered T Cells Is Enhanced by Costimulatory Signaling through CD137 (4-1BB). *Cancer Res.* 21: 4617–28.

Stockinger B, and Omenetti S (2017) The Dichotomous Nature Of T Helper 17 Cells. *Nat. Rev. Immunol.* 17: 535–44. <http://dx.doi.org/10.1038/nri.2017.50>.

Sun S-C (2012) The Noncanonical NF- κ B Pathway. *Immunol. Rev.* 246: 125–40.

Takeda AJ et al (2019) Human PI3K γ Deficiency and Its Microbiota-Dependent Mouse Model Reveal Immunodeficiency and Tissue Immunopathology. *Nat Commun.* 10:4364.

Takeuchi O, and Akira S (2010) Pattern Recognition Receptors and Inflammation. *Cell* 140: 805–20. <http://dx.doi.org/10.1016/j.cell.2010.01.022>.

Tangye SG, Ma CS, Brink R, and Deenick EK (2013) The Good, the Bad and the Ugly — TFH Cells in Human Health and Disease. *Nat. Rev. Immunol.* 13: 412–26.

Tangye SG et al (2020) Human Inborn Errors of Immunity: 2019 Update on the Classification from the International Union of Immunological Societies Expert Committee. *J. Clin. Immunol.* 40:24–64.

Tangye SG, and Sylvain L (2020) Primary Immunodeficiencies Reveal the Molecular Requirements for effective Host Defense against EBV Infection. *Blood* 135:644-655.

Taylor GS et al (2015) The Immunology of Epstein-Barr Virus – Induced Disease. *Annu. Rev. Immunol.* 33:787-821.

Thian M et al (2020) Germline biallelic PIK3CG mutations in a multifaceted immunodeficiency with immune dysregulation. *Haematologica* 105:e488.

Ward-kavanagh L, Lin WW, Sedy JR, and Ware CF (2016) The TNF Receptor Superfamily in Co-Stimulating and Co-Inhibitory Responses. *Immunity* 44:1005-19.

Wildermann C et al (2021) Successful Hematopoietic Stem Cell Transplantation in a 4-1BB Deficient Patient with EBV -Induced Lymphoproliferation. *Clin. Immunol.* 222: 2020–22.

Wu, C-Y et al (2014) The Role of Actin Reorganization in Chemotaxis and Cell. *Br. J. Pharmacol.* 171:5541–54.

Xu Z et al (2012) Immunoglobulin Class-Switch DNA Recombination: Induction, Targeting and Beyond. *Nat. Rev. Immunol.* 12:517-31.

Zhang Q, Lenardo MJ, and Baltimore D (2017) 30 Years of NF- κ B: A Blossoming of Relevance to Human Pathobiology. *Cell* 168: 37–57.

Curriculum Vitae

Marini Thian

Email: marini.ng20@gmail.com

Education

Medical University of Vienna **Sep 2016 – Present**

Doctor of Philosophy in Molecular Medicine

- Cell Communication in Health and Diseases (CCHD) Predoctoral Fellow
- Austrian Academy of Sciences (ÖAW) DOC Predoctoral Fellow

National University of Singapore (NUS) **Aug 2012 – Jun 2016**

Bachelor of Science in Life Sciences (Biomedical Sciences)

- Graduated with **Honours, Highest Distinction**
- Cumulative Average Point: **4.58** out of 5.00

Tampines Junior College (TPJC) **Jan 2010 – Dec 2011**

Singapore-Cambridge General Certificate of Education (Advanced, "A" Level)

Research Experience

Ludwig Boltzmann Institute for Rare and Undiagnosed Diseases

- **St. Anna Children's Cancer Research Institute** **Sep 2016 – Present**
- **Research Center for Molecular Medicine (CeMM)**

PhD Candidate

- Research project on the identification and characterisation of novel genetic defects in patients with immune dysregulation at Prof Kaan Boztug's lab

National University of Singapore

- **Department of Microbiology & Immunology**

Research Assistant

May 2016 – Sep 2016

- Research project on the effects of chemotherapy on $\gamma\delta$ T cells KO mice at Prof Haiyan Liu's lab

National University of Singapore

- **Department of Microbiology & Immunology**

Aug 2015 - Mar 2016

- Honours year research project on the effects of influenza A (H1N1) virus in asthmatic murine models at Prof David Michael Kemeny's lab

University of Bonn

- **Institute of Pharmacology and Toxicology**

June 2015 - July 2015

- Research study on the effects of G-Protein activation in adipocyte differentiation mouse model at Prof Alexander Pfeifer's lab

The University of Queensland

▪ *Diamantina Institute*

Dec 2014 – Jan 2015

- Research project on the relationship between the levels of IgA-coated gut microbiota and the intestinal homeostasis and diseases in mice at Prof Mark Morrison's lab

King's College London

▪ *Randall Division of Cell & Molecular Biophysics* May 2014 – Aug 2014

- Research project on the immunoglobulin class switch recombination in the nasal mucosa of allergen immunotherapy patients at Prof Hannah Gould's lab

National University of Singapore

▪ *Department of Biochemistry*

Dec 2013

- Research project to discover the effects of phosphorylation (epigenetics) on various *S. pombe* genes to the cell cycle at Dr Chen Ee Sin's lab

▪ *Special Programme in Science (SPS)*

Jan 2013 – Jun 2013

- Targeted Drug Delivery in Cancer Cells Literature Review

Publications

1. Kalinichenko A, Casoni GP*, Dupré L*, Trotta L*, Huemer J, Galgano D, German Y, Haladik B, Pazmandi J, **Thian M**, ..., and Boztug K. (2021) RhoG deficiency abrogates cytotoxicity of human lymphocytes and causes hemophagocytic lymphohistiocytosis. *Blood*. Prepublished on 29 Jan 2021: <https://doi.org/10.1182/blood.2020008738>
2. **Thian M** et al. (2020) Germline biallelic *PIK3CG* mutations in a multifaceted immunodeficiency with immune dysregulation. *Haematologica*. 105(10):e488-492. Doi:10.3324/haematol.2019.231399
3. Somekh I*, **Thian M*** et al. (2019) CD137 deficiency causes immune dysregulation with predisposition to lymphomagenesis. *Blood*. 134(18):1510-1516. Doi:10.1182/blood.2019000644
4. Spencer S*, Köstel Bal S*, Egnér W*, Lango Allen H*, Raza SI*, Ma CA, Gürel M, Zhang Y, Sun G, Sabroe RA, Greene D, Rae W, Shahin T, Kania K, Ardy RC, **Thian M**,..., and Thaventhiran JED. (2019) Loss of the interleukin-6 receptor causes immunodeficiency, atopy, and abnormal inflammatory responses. *J Exp Med*. 216(9):1986-1998. doi: 10.1084/jem.20190344.
5. van Rijn JM*, Ardy RC*, Kuloğlu Z*, Härter B*, van Haaften-Visser DY*, van der Doef HPJ, van Hoesel M, Kansu A, van Vugt AHM, **Thian M**, Kokke FTM, Krolo A, ..., and Boztug K. (2018) Intestinal failure and aberrant lipid metabolism in patients with DGAT1 deficiency. *Gastroenterology*. 155(1):130-143.e15. doi:10.1053/j.gastro.2018.03.040.

6. Lee DCP, Tay NQ, **Thian M**, Prabhu N, Furuhashi K, Kemeny DM. (2018) Prior exposure to inhaled allergen enhances anti-viral immunity and T cell priming by dendritic cells. *PLoS One*. 13:e0190063. doi: 10.1371/journal.pone.0190063.

*Equal contribution

Conference Participation

8th Annual Meeting of the International Cytokine & Interferon Society (ICIS)
Virtual Meeting, 1-4 November 2020

19th Biennial Meeting of the European Society for Immunodeficiencies (ESID)
Online Meeting, 14-17 October 2020
Poster presentation: Germline biallelic *PIK3CG* mutations in a multifaceted immunodeficiency with immune dysregulation

2nd Focused Meeting of the European Society for Immunodeficiencies (ESID)
Brussels, Belgium, 18-21 September 2019
Poster presentation: CD137 deficiency – a novel inborn error of immunity

36th Annual Meeting of the Pediatric Immunology Working Group (API)
Frauenchiemsee, Germany, 17-19 May 2019
Oral presentation: CD137 deficiency causes immune dysregulation with predisposition to lymphomagenesis

3rd Harald von Boehmer Midwinter Conference (MWC) 'Advances in Immunobiology'
Seefeld in Tirol, Austria, 19-23 January 2019
Poster presentation: Early-onset autoinflammatory disease in the context of gastrointestinal tract

14th Annual Young Scientist Association (YSA) PhD Symposium
Medical University of Vienna, Austria, 7-8 June 2018

13th Annual Young Scientist Association (YSA) PhD Symposium
Medical University of Vienna, Austria, 8-9 June 2017

34th Annual Meeting of the Pediatric Immunology Working Group (API)
Kloster Banz, Germany, 25-27 May 2017

10th Annual 'Bridging the Gap' Cell Communication in Health and Diseases (CCHD) PhD Symposium
Medical University of Vienna, Austria, 18-19 April 2017

8th Annual International Singapore Symposium of Immunology
Grand Copthorne Waterfront Hotel, Singapore, 26-27 May 2016

Memberships

Pediatric Immunology Working Group (API)	2019
Austrian Society for Allergology and Immunology (ÖGAI)	2019-2020
European Society for Immunodeficiencies (ESID) Junior	2019-2020
Young Scientist Association (YSA)	2017-2020
Singaporean Society for Immunology (SgSI)	2016

Awards and Achievements

▪ European Society for Immunodeficiencies (ESID) 2020 Registration Grant Award	Aug 2020
▪ ÖGAI Travel Awards for 3 rd Midwinter Conference (MWC) 2019	Jan 2019
▪ DOC PhD Fellowship of the Austrian Academy of Sciences (ÖAW)	Jan 2019
▪ CCHD PhD Fellowship by Medical University of Vienna	Sep 2016
▪ Science Student Overseas Exposure Fund - Alice & Peter Tan Academic Awards	Oct 2015
▪ NUS Awards for Study Abroad Enhancement Scholarship	Jul 2015
▪ German Research Foundation (DFG) Scholarship by University of Bonn	Jun 2015
▪ Dean's Honours List by the NUS Faculty of Science (Top 5%)	Jan 2015
▪ Winter Research Scholarship by the University of Queensland	Dec 2014
▪ Summer Research Studentship by King's College London	May 2014
▪ NUS Awards for Study Abroad Enhancement Scholarship	Apr 2014
▪ Competent Gavelier Communicator by Toastmasters International	Dec 2011

Leadership and Service

Indonesian Students' Association in Austria (PPI Austria)

Head of Education Department

Jan 2017 – Jan 2018

- Successfully organised and hosted the 'Joint Conference for Indonesian students' in Austria, Hungary and Czech Republic with presentations in English by over 12 Indonesian PhD and Master students

NUS Science Open House

Student Representative

May 2013

- Successfully organised and welcomed prospective NUS Science students and provided in-depth information about various Science Programmes introduced by the Faculty of Science

TPJC Gavel Club

Vice President (Membership)

Secretary

May 2010 – Jul 2011

- Successfully organised the publicity recruitment of new members and hit the highest membership of the year 2011 school-wide.
- Directed the annual Public Speaking Competition for Secondary school category

Youth Olympic Games Singapore

Information Service Officer

Aug 2010

- Zealous in serving and providing assistance to spectators
- Able to think flexibly to overcome any communication barriers with international non-English speaking spectators